ELECTROCHEMICAL MINERALIZATION OF PER- AND POLYFLUOROALKYL SUBSTANCES

by

Vivek Francis Pulikkal

A dissertation submitted to the faculty of
The University of North Carolina at Charlotte
in partial fulfillment of the requirements
for the degree of Doctor of Philosophy in
Civil Engineering

Charlotte

2021

Approved by:

_____
Dr. Mei Sun

_____
Dr. Olya Keen

_____
Dr. James Bowen

_____
Dr. James Amburgey

_____
Dr. John Stogner

ABSTRACT

VIVEK FRANCIS PULIKKAL. Electrochemical Mineralization of Per- and Polyfluoroalkyl Substances. (Under the direction of DR. MEI SUN)

Per- and polyfluoroalkyl substances (PFAS) are fluorinated organic compounds with broad applications in aqueous film-forming foams (AFFF) for firefighting, lubricants, waterproof and stain-resistant products. Perfluorooctanoic acid (PFOA), a toxic and carcinogenic PFAS, is replaced by GenX. Nevertheless, PFOA is expected to be present in the environment for an extended period after its phasing out due to its recalcitrant nature. In addition, GenX is predicted to have similar toxicity as PFOA. Various PFAS, including PFOA and GenX, have been widely detected in surface water and groundwater in the United States and worldwide. The current treatment practice for PFAS fails to provide a permanent solution and is likely to increase the risk of recontamination of surface water and groundwater.

Among various destructive methods, electrochemical mineralization, which uses electric power to transform PFAS into bicarbonate and fluoride, is a promising option. However, past studies on electrochemical mineralization of PFAS have limitations such as low PFAS mineralization and incomplete fluorine mass balance. This study focused on addressing these issues and examined the treatment performance using PFOA, GenX, and AFFF waste streams as examples.

The first task of the study was to identify the suitable anode material and achieve complete fluorine mass balance for electrochemical mineralization, using PFOA as the example compound. Boron-doped diamond (BDD) was selected as the best out of the three anode materials tested (Ebonex Plus, Ti/RuO_2, and BDD) based on its PFOA degradation efficiency and life span. In a batch study conducted at 20 mA/cm^2, more than 80% PFOA degradation and complete fluorine mass balance were achieved. In addition to screening suitable anode materials, the reactors used for

electrochemical mineralization were also continuously redesigned during the study, and multiple issues were identified and fixed to achieve the best performance.

The second task of this study was to assess the electrochemical mineralization of GenX using boron-doped diamond electrodes in two different reactor types: continuous reactors with recirculation and batch reactors. Experiments using the continuous reactors with recirculation were carried out at 10, 20, 25, and 30 mA/cm^2. Based on GenX degradation and defluorination ratio, 20 mA/cm^2 was selected as the optimum current density. At this current density, GenX degradation, defluorination ratio, and mass balance of 65%, 14%, and 70% were achieved, respectively. In batch reactor studies conducted at 20 mA/cm^2, 1M NaOH was found best for fluoride capture and methanol for organic fluorine capture.

The third task of this study was to explore the electrochemical mineralization of PFAS in simulated AFFF waste streams from firefighting practice. Batch studies on electrochemical mineralization of two AFFF solutions were conducted at 20 mA/cm^2. Utilizing the total oxidable precursor assay and targeted analysis, the degradation of perfluoroalkyl acids and their precursor was evaluated. The two tested AFFF solutions achieved 25-42% fluorine mass balance based on TOP assay and fluoride analysis.

This research serves as a guide for future electrochemical research by providing optimal reactor design and suitable analyses. Particularly, results from this study demonstrated the significance of PFAS loss in aerosol forms generated during the electrochemical process and possible solutions to avoid such loss by capturing and recirculating aerosols to achieve high PFAS degradation and complete fluorine mass balance.

ACKNOWLEDGEMENTS

First and foremost, my sincere gratitude and many thanks to my mentor, Dr. Mei Sun for her guidance and support throughout my Ph.D. journey. I am grateful for the opportunity to work with her and thank her providing a supportive research environment.

I thank Dr. Olya Keen and Dr. James Amburgey for supporting my laboratory research and for being part of my dissertation committee. I extend my gratitude to my other committee members Dr. James Bowen, Dr. John Stogner for their bright insights and suggestions that helped me improve the quality of my research work and dissertation. I thank Dr. Xiuli Lin for her support as the environmental lab manager at UNC Charlotte. I greatly appreciate Ted Brown for his help with the construction of my electrochemical reactors.

I extend my gratitude for my friends Abhisek Manikonda, Livingstone Dumenu, Rui He, Akpovona Ojaruega, Abhispa Sahu, Manohar Seetharamu, Yuling Han, Yen-Ling Liu, Heather Oakes for making my UNC Charlotte life a fun and enjoyable one. I also thank my wife, my parents, my brother, my sister-in-law and my niece for their unrelenting love and support.

I express my sincere appreciation to the North Carolina PFAS Testing Network, the Water Resources Research Institute, NC and UNC Charlotte for supporting me through scholarships and research funding.

DEDICATION

I dedicate this dissertation to my dad, Francis Pulikkal, and my wife, Visva Bharati Barua for their support, love, and encouragement throughout my Ph.D. journey.

Table of Contents

LIST OF TABLES

LIST OF FIGURES

LIST OF ABBREVIATIONS

PFAS	Per- and polyfluoroalkyl substances
AFFF	Aqueous film-forming foams
PFOA	Perfluorooctanoic acid
HFPO-DA	Hexafluoropropylene oxide-dimer acid
BDD	Boron-doped diamond
EPA	Environmental protection agency
PFOS	Perfluorooctane sulfonic acid
UCMR3	The third unregulated contaminant monitoring rule
AOP	Advanced oxidation processes
PFCA	Perfluorinated carboxylic acids
AOF	Adsorbable organic fluorine
LC-MS/MS	Liquid chromatography-tandem mass spectrometry
PFR	Plug flow reactor
DC	Direct current
PEEK	Polyether ether ketone
CNC	Computer numerical control
IC	Ion chromatography
PFAA	Perfluoroalkyl acids
ESI	Electrospray ionization
MRM	Multiple reaction monitoring
PFBA	Perfluorobutanoic acid
PFPeA	Perfluoropentanoic acid

PFBS	Perfluorobutane sulfonic acid
PFHxA	Perfluorohexanoic acid
PFPeS	Perfluoropentane sulfonic acid
PFHpA	Perfluoroheptanoic acid
PFHxS	Perfluorohexane sulfonic acid
LOQ	Limit of quantification
TOF	Total organic fluorine
TOP	Total oxidable precursor
FTS	Fluorotelomer sulfonic acid
PFNA	Perfluorononanoic acid
PFDA	Perfluorodecanoic acid

1. Introduction

1.1 Concerns over per- and polyfluoroalkyl substances

Per- and polyfluoroalkyl substances (PFAS) are a family of perfluorinated and polyfluorinated organic compounds widely used in lubricants, polyurethane production, inks, varnishes, firefighting foams, food packaging, adhesives, electroplating, textiles, and stain-resistant coating in clothing and carpets (Hu et al. 2016; ITRC 2018; Lau et al. 2007; Moody et al. 2003; Prevedouros et al. 2006; Quiñones and Snyder 2009).

Among various PFAS, perfluorooctanoic acid (PFOA) is one of the most widely used and well-studied (USEPA, 2016c) (Fig. 1.1). Its main application is its ammonium salt used as a surfactant in Teflon production (Emmett et al. 2006). PFOA is also used to synthesize fluoroacrylic esters and as aqueous film-forming foam (AFFF) in fire extinguishers, which had a market of 6.8 million liters in the US during 1985 (Giesy and Kannan 2002; Kudo and Kawashima 2003; Moody and Field 2000). PFOA owes its wide application to its hydrophobicity, lipophobicity, and thermal stability (ITRC 2018). The hydrophobicity and lipophobicity of PFOA are due to the electronegativity of fluorine atoms, which lower its surface tension (Lau et al. 2007).

However, studies have shown that PFOA is toxic and carcinogenic for both humans and animals (USEPA 2016a). Investigations on rats and mice have shown adverse health effects like suppression of immune system, birth defects, and liver and kidney damage (USEPA 2016a). PFOA accumulates in serum, kidney, and liver, with a long half-life in humans (2 to 9 years) (USEPA 2012). It is estimated that 98% of Americans have PFOA in their blood (Calafat et al. 2007; USEPA 2016b; c). Due to these concerns, the US Environmental Protection Agency (EPA) has set

a health advisory level based on lifetime exposure for the combined concentration of PFOA and perfluorooctane sulfonic acid (PFOS) at 70 ng/L (USEPA 2016d).

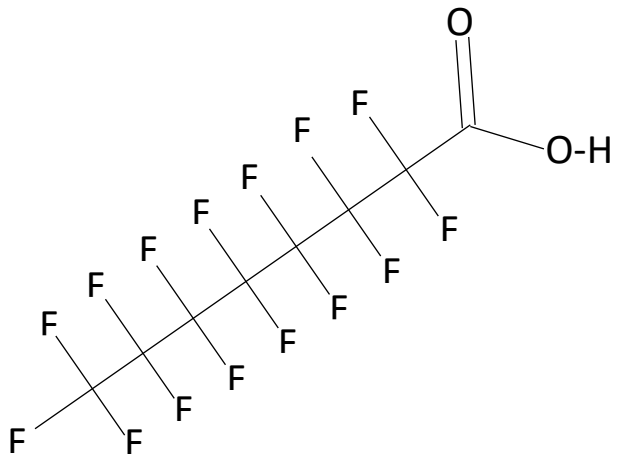

Fig. 1.1 Molecular structure of perfluorooctanoic acid

Subsequently, PFOA was completely phased out in the US by 2015, initiated per the 2010/2015 Stewardship program (USEPA 2014, 2017a). Currently in the US, PFOA is replaced by two compounds: "GenX" from DuPont, the ammonium salt of hexafluoropropylene oxide dimer acid (HFPO-DA, Fig. 1.2); and "ADONA" from 3M/Dyneon (3H-perfluoro-3-[(3-methoxy-propoxy)propanoic acid] (Sun et al. 2016a; Wang et al. 2013). These replacement PFAS are both ethers. The rationale behind using ethers as replacement PFAS is that the oxygen atom connecting the alkyl groups is expected to make the compounds more susceptible to degradation and less bioaccumulative (Strynar et al. 2015). However, recent studies have predicted GenX/ADONA with similar or higher persistence, mobility, and toxicity than PFOA (Cheng and Ng 2018; Gomis et al. 2018).

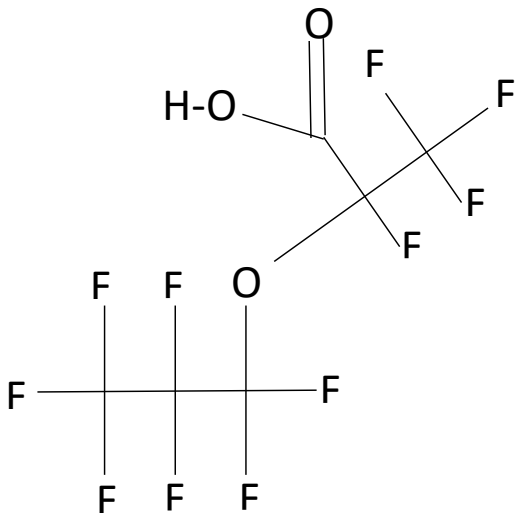

Fig. 1.2 Molecular structure of hexafluoropropylene oxide dimer acid

1.2 Detection of PFAS in drinking water sources

PFOA has a low vapor pressure of 0.525 mm Hg and an organic carbon-water partitioning coefficient (log Koc) of 2.06 (USEPA 2016c). Therefore, PFOA tends to accumulate in soils with high organic carbon (Moody et al. 2003) and particles in the atmosphere (Prevedouros et al. 2006). In addition, PFOA has a low estimated pKa of around 2.8, thus completely deprotonates in natural water environment (Prevedouros et al. 2006; USEPA 2016c) and has a high solubility of 9.5 g/L (USEPA 2017a). Thus, PFOA in natural waterbodies is present both in dissolved form and adsorbed to suspended solids. Similarly, other PFAS also tend to accumulate in surface water and groundwater due to their low vapor pressure, high solubility, and persistence (European Food Safety Authority 2008; ITRC 2018; Prevedouros et al. 2006). These properties make ingestion of contaminated drinking water one of the most critical exposure routes to PFAS (Xiao et al. 2015).

In the US, PFOA concentrations up to 4300, 6410, and 11000 ng/L have been detected in finished drinking water, groundwater, and surface water, respectively (Crone et al. 2019). The presence of

PFOA in finished drinking water points to the ineffectiveness of conventional drinking water treatments to remove PFOA. The Third Unregulated Contaminant Monitoring Rule (UCMR3), a nationwide study on the occurrence of emerging contaminants in finished drinking water by the USEPA, reported PFOA concentrations up to 349 ng/L, well above the USEPA recommendation of 70 ng/L for the combined concentration of PFOA and PFOS (USEPA 2017b). PFOA also had the highest detection frequency among all the PFAS tested in large surface water and groundwater systems (Crone et al. 2019).

In China, PFOA had the highest abundance in surface water and groundwater taken at rural and urban areas compared to other PFAS (Chen et al. 2016). PFOA has also been detected in Chinese surface waters at concentrations ranging from 0.48 to 4150 ng/L and in groundwater sources at 7-2510 ng/L (Cao et al. 2019; Chen et al. 2016; Crone et al. 2019; Wang et al. 2016; Xu et al. 2021).

In Europe, PFOA had been detected in groundwater samples tested in the Netherlands at concentrations ranging from 1 to 47000 ng/L with a mean of around 6000 ng/L (Gebbink and Leeuwen 2020; Xu et al. 2021). In surface water, PFOA has been detected in River Thames (UK), River Rhine (Germany and Netherlands), and Mälaren Lake (Sweden) at concentrations ranging from 5.56 to 11.71 ng/L, 0.86 to 20 ng/L, and 0.55 to 10 ng/L respectively. Besides Europe, PFOA had also been detected in Australian groundwater taken near the Yarra River in Melbourne, with a detection frequency of 100% and concentrations ranging from 1.7 to 74 ng/L (Hepburn et al. 2019).

Like PFOA, GenX has also been detected ubiquitously in surface water and groundwater around the world. The earliest detection of GenX was reported in the Rhine river and estuaries of the Elbe, Weser, and Ems Rivers in the North Sea along the German and Dutch coast in 2015, where a mean GenX concentration of 7 ng/L was detected in the Rhine River (Heydebreck et al. 2015). In the

US, GenX was first reported in North Carolina by a non-targeted PFAS identification study done in Cape Fear River and its tributaries (Strynar et al. 2015). A subsequent study conducted downstream of a fluorochemical manufacturing plant in the Cape Fear River found GenX concentrations up to 4500 ng/L with an average of 631 ng/L (Sun et al. 2016b). In Asia, the first GenX detection was reported in China's Xiaoqing River, with a mean concentration of 271.4 ng/L (Heydebreck et al. 2015).

Globally, the highest GenX concentration in surface water reported so far was downstream of a fluoropolymer facility in the Xiaoqing River Watershed in China in 2018 at 9350 ng/L (Song et al. 2018). Xiaoqing River has elevated PFAS concentrations due to discharges from four industrialized cities nearby. In Europe, the highest GenX concentration was detected downstream of a fluoropolymer plant in the Alz River in Germany in 2020 at up to 3600 ng/L (Joerss et al. 2020). In the US, the Cape Fear River Watershed in North Carolina topped the list with GenX concentrations up to 4500 ng/L (Sun et al. 2016b). The fact that all the surface water sites with the highest GenX concentrations in Asia, Europe, and the United States were observed downstream of fluoropolymer plants shows that fluoropolymer facilities are significant point sources of GenX contamination in surface waters.

Application of AFFF for firefighting has also been linked to PFAS contamination of water sources, especially groundwater. AFFF is a type of synthetic Class B firefighting foam used for extinguishing liquid hydrocarbon fires, which contains high levels of mixed PFAS, (Mueller and Yingling 2017, 2018). Due to AFFF application, the groundwater around 420 US Department of Defense facilities including many Air Force Bases are contaminated with PFAS at concentrations ranging from 2.8 ng/L to 7090 ug/L (Backe et al. 2013; Houtz et al. 2013; Moody et al. 2003; Moody and Field 1999, 2000). There have been cases where drinking water wells were shut down

due to AFFF contamination from firefighting training areas (Dauchy et al. 2017a; Department of Defense 2017).

1.3 Treatment of PFAS

Due to the adverse health effects, persistence, and widespread detection of PFAS in groundwater and surface water, it is essential to ensure their removal from drinking water (Giesy and Kannan 2002). PFAS are highly recalcitrant to conventional and many advanced treatments practiced in drinking water treatment plants (Liang et al. 2018). Current treatment practices for managing PFAS in shown in Fig. 1.3. In the US, the most popular practices for removing PFAS from drinking water are by adsorption using activated carbon, ion exchange, reverse osmosis, and nanofiltration. The disadvantage of these treatment strategies is that capturing PFAS by adsorption or filtration only transfers PFAS from one matrix to another. Once saturated with PFAS, the carbon needs to be sent to landfills. In landfills, the adsorbed PFAS can leach out from the carbon and end up in the leachate. PFAS then travel along with the leachate to wastewater treatment plants. Similarly, the brine containing concentrated PFAS from resin regeneration in ion exchange systems and reject from nanofiltration are sent to wastewater treatment plants, eventually discharged back to surface water since wastewater treatment plants are not designed to remove PFAS. Hence, it is essential to use a destructive treatment strategy to manage PFAS.

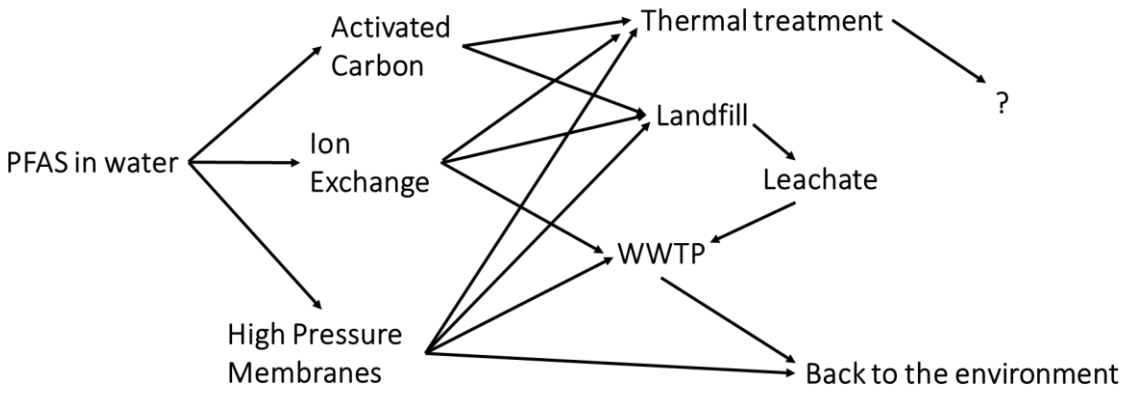

Fig. 1.3 Current treatment practices for managing PFAS in surface water and groundwater

One of the most popular type of process utilized for destructive treatment is advanced oxidation. Advanced oxidation processes (AOP) is an umbrella term for various destructive treatments that generate highly reactive oxidative radicals such as hydroxyl radicals and sulfate radicals at sufficient concentration to degrade recalcitrant organic compounds (Trojanowicz et al. 2018). AOP include various chemical and photochemical processes such as UV/O_3, UV/H_2O_2, Fenton reaction, sonolysis, electrochemical oxidation, among others.

Among various AOP, different innovative techniques to destruct PFAS have been investigated (Li et al. 2010; Schaefer et al. 2015a), such as sonolysis, photochemical oxidation, and plasma-based treatments. Sonolysis uses sound energy to induce water pyrolysis, releasing hydroxyl radicals to break down PFAS molecules in a solution (Rodriguez-Freire et al. 2015). Photochemical oxidation, also known as photocatalytic decomposition, uses UV light and chemical catalysts like TiO_2 to oxidize PFAS (Chen et al. 2015). Plasma-based treatments use electric power to create a plasma that generates oxidative radicals to degrade PFAS (Stratton et al. 2017). Nevertheless, these methods are energy-intensive, uneconomical in PFAS degradation, or not scalable, making them difficult to adopt for drinking water treatment. Furthermore, most of these methods show a steep

decline in degradation efficiency, even when PFAS concentrations are reduced from 100 mg/L to 10 mg/L.

Among the explored PFAS removal methods, electrochemical mineralization is a promising option, utilizing the electric power to transform PFAS into bicarbonate, fluoride, and possibly other inorganic species (Li et al. 2015; Lin et al. 2012, 2018; Yang et al. 2017; Zhuo et al. 2014). During electrolysis, PFAS were degraded via a stepwise CF2 elimination to form various radicals as intermediates (Kutsuna and Hisao 2007). This process takes place on a time scale of minutes to days. A study on the electrochemical oxidation of PFOA showed complete removal of PFOA at 50 mA/cm^2 at a detention time of 8 hours (Schaefer et al. 2017). A study published on the electrochemical oxidation of GenX confirmed direct electron transfer as the underlying mechanism behind GenX degradation (Pica et al. 2019a).

1.4 Data gaps and objectives

Although a large collection of literature is available on various PFAS destruction techniques, there are still data gaps on PFAS electrochemical mineralization. Therefore, the objectives of this study are to assess electrochemical mineralization of PFOA as an example of legacy PFAS, GenX as an alternative PFAS, and a mixture of known and unknown PFAS in AFFF waste streams from firefighting practice. In particular, this study aims to address the following data gaps:

1.4.1 Electrochemical mineralization of PFOA

- Low percentage mineralization: Most studies show high percentages of PFOA removal but fail to demonstrate complete mineralization (Lin et al. 2012; Yang et al. 2017). Complete mineralization was not achieved because PFOA is degraded to both known and unknown short-

chain intermediate PFAS during electrolysis, but complete degradation to inorganic fluoride is challenging.

- Incomplete mass balance: While some studies quantified reaction products and some intermediates, the complete fluorine mass balance before and after electrolysis was established by most previous studies. Incomplete mass balance might be due to the gas phase loss of HF and short-chain PFAS, as well as the possible formation of unknown reaction products (Lin et al. 2012; Trautmann et al. 2015). Without a convincing mass balance, some reaction products and intermediates remain unknown, so it is impossible to declare a reduction in environmental risk after treatment.
- Problematic supporting electrolyte: Supporting electrolyte is needed in electrochemical reactions to facilitate electric current flow. Most earlier PFOA studies used sodium perchlorate ($NaClO_4$) or sodium chloride (NaCl) as supporting electrolytes (Ma et al. 2015; Trautmann et al. 2015; Zhuo et al. 2014). However, perchlorate is not suitable for water treatment due to its toxicity, whereas chloride can be oxidized to toxic substances like perchlorate, chlorate, and chlorine gas during electrolysis. Thus, environmentally benign electrolytes are needed for PFOA electrochemical degradation.

1.4.2 Electrochemical mineralization of GenX

- Electrochemical mineralization of GenX needs further optimization since limited studies are available on this topic. During the formulation of the hypothesis and performance of tasks for the current study, only one study was available (Pica et al. 2019a). However, recently four more studies on electrochemical degradation of GenX were published and are included in identification of knowledge gap.

- Including the recently published studies on electrochemical degradation of GenX, no studies have compared the effectiveness of various absorption solutions for capturing fluoride and PFAS gases generated during electrochemical process.
- A comparison of various reactor models for improving GenX degradation has not been explored even after considering the recent publications.
- Out of the five studies available of electrochemical degradation of GenX, only one incorporated combustion ion chromatography analysis for fluorine mass balance.

1.4.3 Electrochemical mineralization AFFF waste streams from firefighting practice

Previous literature focused on electrochemical degradation of PFAS in AFFF impacted groundwater (Schaefer et al. 2015a, 2017, 2018; Trautmann et al. 2015). However, direct capture and electrochemical treatment of AFFF waste streams are expected to be advantageous due to higher PFAS concentrations and lower volume that requires treatment. Since there are no previous studies on electrochemical degradation treatment of AFFF waste streams, it is essential to explore the efficiency and suitability of such a treatment option.

1.5 Dissertation overview

This dissertation is presented in five chapters. Chapter 1 provides an introduction to the work, brief background information, and research objectives. Chapters 2 through 4 presented research on electrochemical mineralization of PFOA, GenX, and simulated AFFF waste streams, respectively, and each chapter is prepared for publication as a peer-reviewed journal paper. Chapter 5 contains conclusions, novel contributions, environmental implications of this research, and suggestions for future work.

2. Electrochemical mineralization of PFOA

2.1 Literature review

During electrochemical degradation, oxidation of organic compounds happens by direct electron transfer at the surface of the anode (Shi et al. 2019). Hydroxyl radicals are also produced by anodic oxidation of water, but some studies suggest that hydroxyl radicals do not play a significant role in PFAS degradation (Schaefer et al. 2017). Previous studies have used various commercially available as well as lab synthesized anodes for PFAS degradation (Lin et al. 2012; Schaefer et al. 2017). For this study, three commercially available anodes, Ebonex Plus, Ti/RuO_2, and boron-doped diamond (BDD), were compared for their efficiency at PFOA degradation (Figure 2.1).

Ebonex Plus electrode is a commercially available Magneli phase titanium suboxide-ceramic anode used as discrete cathodic protection for reinforced concrete structures and steel-framed buildings (Lin et al. 2018; Vector Corrosion Technologies 2012). Studies have shown its effectiveness in degrading various organic compounds, including PFAS (Geng et al. 2015; Lin et al. 2018). A study using Magneli phase titanium oxide electrodes achieved 96% PFOA removal within 3 hours of electrochemical oxidation (Liang et al. 2018).

Ti/RuO_2 is a dimensionally stable electrode (Zhuo et al. 2011). One study had achieved more than 90% PFOA and PFOS degradation using Ti/RuO_2 in spiked groundwater samples (Schaefer et al. 2015b).

BDD electrodes are highly stable chemically, mechanically, and thermally. They have a high overvoltage for oxygen evolution and produce oxidants like hydroxyl radicals (Trautmann et al. 2015). Various studies have found BDD to be effective in degrading PFAS (Gomez-Ruiz et al. 2017, 2019; Gorri and Urtiaga 2017; Schaefer et al. 2017; Trautmann et al. 2015).

Fig. 2.1 (From Left) Ebonex Plus, Ti/RuO_2, Boron Doped Diamond electrodes used in this study

2.1.1 PFOA degradation mechanism

The electrochemical degradation of PFOA occurs in a stepwise elimination of one carbon atom and two fluorine atoms forming shorter perfluorinated carboxylic acids (PFCA). Initially, the C-C bond between the carboxylate group and the carbon chain breaks, followed by cleavage of the C-F bonds (Schaefer et al. 2017).

Based on experimental results from previous literature, a possible pathway electrochemical oxidation of PFOA is given below (Ma et al. 2015). When electrolysis starts, electrons are stripped from the carboxylic group of PFOA and transferred to the anode. The electron transfer leads to the formation of PFOA radicals (Kormann et al. 1991).

$$C_7F_{15}COO^- \rightarrow C_7F_{15}COO^{\cdot} + e^- \qquad (1)$$

Since the PFOA radical formed is highly unstable, it undergoes Kolbe decarboxylation reaction to form C_7F_{15} radicals. This step flakes out a carbon atom.

$$C_7F_{15}COO^{\cdot} \rightarrow C_7F_{15}^{\cdot} + CO_2$$

(2)

C_7F_{15} radical reacts with hydroxyl radicals formed due to electrolysis of water to form an alcohol $C_7F_{15}OH$, which is thermally unstable.

$$C_7F_{15}^{\cdot} + HO^{\cdot} \rightarrow C_7F_{15}OH \quad (3)$$

$C_7F_{15}OH$ then undergoes fluorine elimination. This flakes off the first fluorine atom.

$$C_7F_{15}OH \rightarrow C_6F_{13}COF + HF \quad (4)$$

In the next step, $C_6F_{13}COF$ undergoes hydrolysis reaction eliminating another fluorine atom in the process. This step produces perfluoroheptanoic acid.

$$C_6F_{13}COF + H_2O \rightarrow C_6F_{13}COO^- + HF + H^+ \quad (5)$$

The above reactions complete the first CF_2 flake off, and the next shorter chain PFAS of the parent compound is formed. This process is repeated until only inorganic end products such as bicarbonate and fluoride remain.

Another pathway for PFOA, degradation is also suggested (Kutsuna and Hisao 2007). The pathway is similar until the formation of perfluoroheptyl radical ($C_7F_{15}^{\cdot}$) in reaction (2). This radical reacts with oxygen produced during water electrolysis to form a perfluoroheptylperoxy radical.

$$C_7F_{15}^{\cdot} + O_2 \rightarrow C_7F_{15}OO^{\cdot} \quad (6)$$

The perfluoroheptylperoxy radical formed then reacts with another perfluoroheptylperoxy radical to form a perfluoroalkoxy radical ($C_7F_{15}O.$).

$$C_7F_{15}OO^{\cdot} + C_7F_{15}OO^{\cdot} \rightarrow C_7F_{15}O^{\cdot} + C_7F_{15}O^{\cdot} + O_2 \quad (7)$$

Further reaction of perfluoroalkoxy radical follows two paths.

First path: perfluoroalkoxy radical reacts with hydroperoxyl radical to form an alcohol.

$$C_7F_{15}O^{\cdot} + HO_2^{\cdot} \rightarrow C_7F_{15}OH + O_2 \quad (8)$$

Second path: perfluoroalkoxy radical undergoes a decomposition reaction to form a perfluorohexyl radical and a carbonyl fluoride (COF_2).

$$C_7F_{15}O^{\cdot} \rightarrow C_6F_{13}^{\cdot} + COF_2 \quad (9)$$

Carbonyl fluoride then undergoes hydrolysis to form carbon dioxide and hydrogen fluoride. This carbon dioxide is the source of bicarbonate at the end.

$$COF_2 + H_2O \rightarrow CO_2 + 2HF \quad (10)$$

The above reactions are repeated until all PFAS species are converted to inorganic end products.

2.1.2 Proposed Treatment Train

As discussed before, the concentrations of PFAS in natural water sources range from ng/L to low ug/L levels. Since the efficiency of electrochemical oxidation reduces significantly when the concentration of the target compound decreases, it is economically desirable to concentrate PFAS into a small volume before electrochemical treatment. Hence a sequential treatment is proposed to remove PFAS from drinking water derived from contaminated surface water or groundwater in treatment plants or groundwater for site remediation purposes (Fig. 2.2).

The system includes

a) An ion-exchange treatment to exchange ionic PFAS by a non-toxic anion, making the treated water suitable for consumption or discharge

b) Regeneration of the exhausted resin to release the adsorbed PFAS using a concentrated brine containing the exchange anion

c) Electrochemical treatment of the spent brine to mineralize the released PFAS.

Advantages of such sequential treatment over a direct electrochemical treatment are:

i. The volume of water to be electrochemically treated can be reduced by over 100 times.

ii. PFAS are concentrated in the spent brine, making the electrochemical treatment more energy efficient.

iii. The brine naturally becomes the supporting electrolyte for the electrochemical reactions, so no extra salts are needed.

iv. Such treatment is also better than a single-stage ion exchange treatment because ion exchange alone does not destruct PFAS, leaving the management of PFAS contaminated resin another environmental concern.

This dissertation focussed only on the electrochemical mineralization part of the treatment train. Lab-prepared solutions that reflect the PFAS and salt concentration present in the spent brine from resin regeneration were used as electrochemical study samples. PFOA, being a well-studied compound, was selected as an example PFAS to study electrochemical degradation.

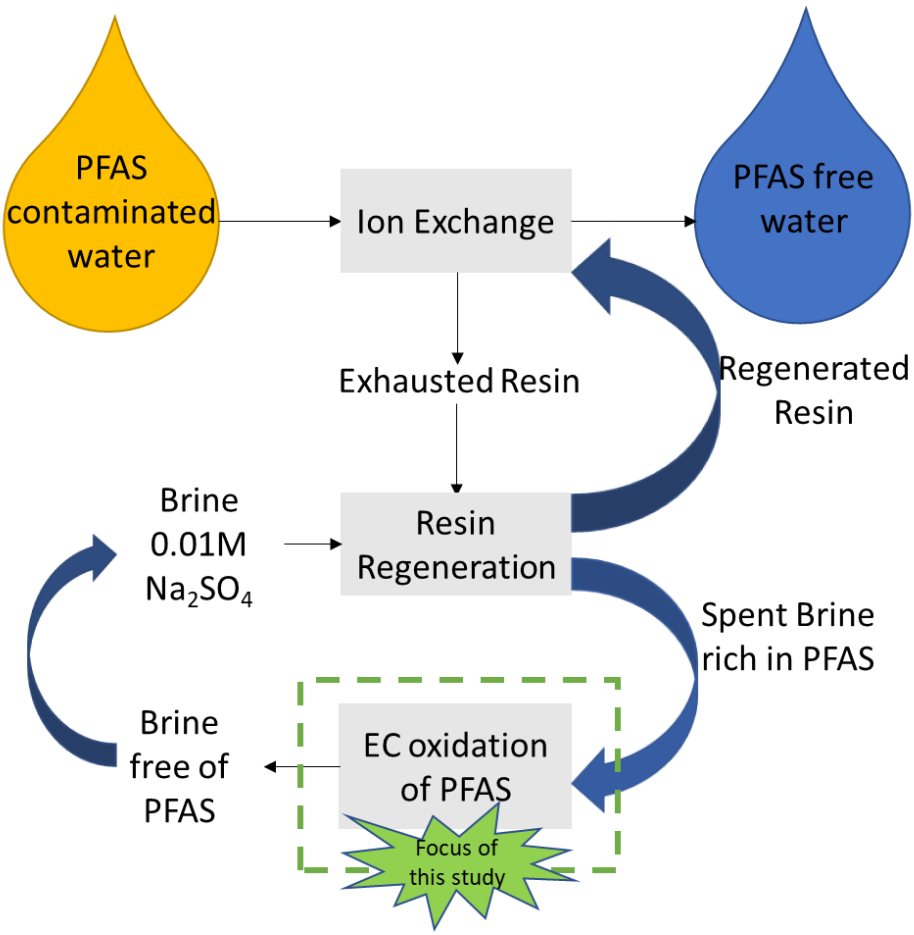

Fig. 2.2 Proposed flow diagram of PFAS removal from contaminated water

2.2 Study overview

2.2.1 Task 1- Identify suitable anode materials for electrochemical degradation of PFOA

A comparison of Ebonex Plus, Ti/RuO_2, and BDD anodes for their PFOA degradation performance was made. The anode with the highest PFOA degradation efficiency was selected as the best anode.

Hypothesis: Various anodes would have different oxidation potentials and characteristics that can influence PFOA degradation. By studying the PFOA degradation using these anodes at different current densities, the best-suited anode for PFOA degradation can be found.

2.2.2 Task 2- Assess PFOA mineralization and mass balance

The fluorine mass balance of PFOA electrochemical oxidation using each anode material needs to be established to ascertain the safety of the electrochemical treatment. One of the tools used for establishing fluorine mass balance was adsorbable organic fluorine (AOF) analysis. AOF is a measurement of the total concentration of fluorinated organic compounds, including both identified and unidentified species (Wagner et al. 2013).

Hypothesis: With AOF analysis, individual PFAS analysis by liquid chromatography-tandem spectrometry (LC-MS/MS), and fluoride analysis, the mass balance of PFOA electrochemical degradation would be available, and a more thorough assessment of if such treatment can achieve mineralization and risk reduction will be possible.

2.2.3 Task 3- Evaluate the efficiency of a plug flow reactor (PFR) with recirculation for PFOA mineralization

PFOA degradation using a PFR was tested at different current densities. PFR possess improved treatment efficiency compared to completely mixed reactors. In addition, the anode area to sample volume ratio inside the reactor is greatly improved to 5 cm^2/mL in the plug flow reactor we built.

Hypothesis: The new reactor design with an increased anode area to volume ratio will improve the contact between electrodes and the target compound, resulting in higher PFOA degradation.

2.3 Materials and methods

Chemical Reagents: PFOA potassium salt was purchased from Matrix Scientific. Sodium sulfate (Na_2SO_4) was purchased from Acros Organics. LC-MS grade methanol was purchased from Fisher Scientific. PFAS standards with a mixture of 21 PFAS compounds (PFAC-MXC) and mass-

labeled PFAS as internal standards (MPFAC-C-ES) were purchased from Wellington Laboratories. Anhydrous sodium fluoride was obtained from VWR. Potassium nitrate for AOF analysis was purchased from Acros Organics.

Electrodes: Three types of commercially available electrodes were tested for electrochemical mineralization of PFOA: Ebonex Plus, Ti/RuO_2, and boron-doped diamond (BDD). Ebonex Plus electrodes were purchased from Vector Corrosion Technologies, Ti/RuO_2 plates from American Elements, and boron-doped diamond from Fraunhofer USA.

Water matrix: To better understand the underlying mechanisms, PFOA electrochemical mineralization was studied in laboratory-prepared synthetic water samples. Such samples mimicked the composition of spent brine after ion exchange resin regeneration as shown in Fig. 2.2 and have concentrated PFOA and sodium sulfate. Typical concentrations of PFOA in contaminated groundwater are at low µg/L levels (Schaefer et al. 2015a). Assuming the ion exchange and resin regeneration process can concentrate PFOA for 100 folds, PFOA concentration in the spent brine will be at a few mg/L. Thus, an initial concentration of 1.5 mg/L of PFOA was used in this study. Sulfate is proposed to be used as the ion exchange resin regenerant instead of commonly used chloride, since chloride will be oxidized to undesirable chlorine gas, chlorate, or perchlorate in electrochemical reactions. Sodium sulfate concentration in the synthetic samples was at 1.42g/L (0.01 M) to mimic the regenerant used in the resin regeneration practice. At the end of each experiment, the electrodes, reactor vessel, and tubings were rinsed with methanol to extract any adsorbed PFAS. The rinse solution collected was then blow dried to 1 mL using nitrogen gas in a 40˚C water bath.

Reactors: PFOA electrochemical mineralization was studied in bench-scale electrolyzers. The information on various reactor types used in this study and their comparison to previous literature

is given in Table 2.1. PS-305DM direct current (DC) power supplies were used to power the reactors.

Different types of reactors were built for this study depending on the type of electrodes, gas capture mechanism, and whether the experiment is batch type or plug flow. Detailed information of each type of reactor used for Ebonex Plus, Ti/RuO_2, and BDD is given below under the respective anode.

a. Ebonex Plus

Studies on electrochemical mineralization of PFOA by the Ebonex Plus anodes used batch reactors that worked under a continuous vacuum pull. This vacuum allowed the movement of evolved gases towards the absorption solution and their eventual capture in the absorption solution. The air intake was on top of the reactor vessel, while the absorption solution was housed in a glass flask connected to a vacuum pump. A schematic diagram of the reactor that works under continuous vacuum pull is given in Fig. 2.3.

The Ebonex Plus electrodes are cylinders with a diameter of 18 mm and a length of 15 cm. The tests were carried out at a current density of 0.14 mA/cm^2. This current density was chosen based on the current rating provided by the manufacturer and the length of the electrode immersed in the PFOA solution (12 cm). In this test, Ebonex Plus electrodes were used as both the cathode and anode. Each reactor contained 900 mL solution with 1.5 mg/L PFOA and 0.01 M Na_2SO_4 as the supporting electrolyte (Trautmann et al. 2015). Aqueous samples of 10 mL were taken every hour to monitor the depletion of PFOA and the production of PFAS intermediates and fluoride. The absorption solution was a mixture of methanol and water (1:1 v/v) with a total volume of 10 mL. A polyether ether ketone (PEEK) tubing was employed to connect the reactor to the vacuum flask to prevent PFAS adsorption or leaching. The electrolysis conditions were: a distance of 5 mm

between the electrodes, a stirring speed of 500 rpm, and a total electrolysis time of 8 hours (Lin et al. 2012; Ma et al. 2015; Niu et al. 2013; Schaefer et al. 2017; Yang et al. 2017; Zhuo et al. 2014). Comparison of this reactor to other reactors used in this study and previous literature is given in Table 2.1.

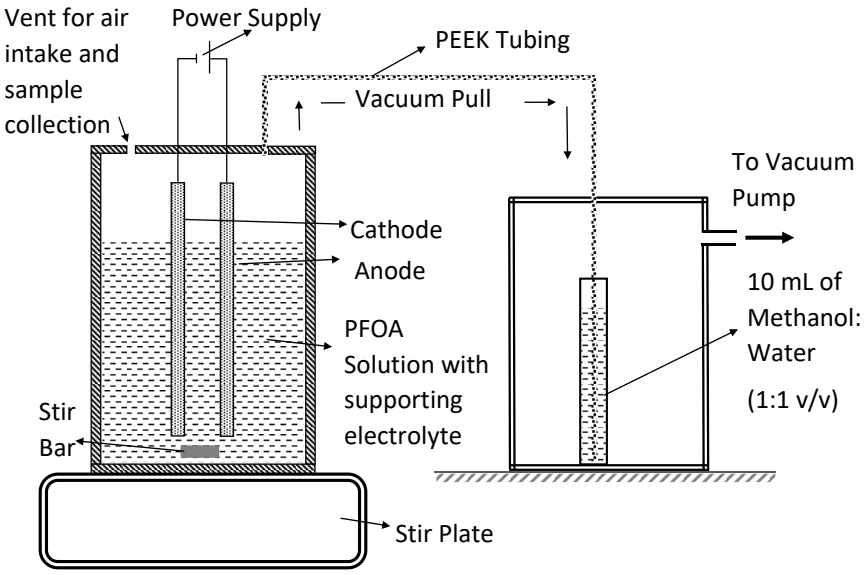

Fig. 2.3 Schematic diagram of the reactor that works under continuous vacuum pull. This type of reactor was used for electrochemical mineralization of PFOA by anodes such as Ebonex Plus and Ti/RuO_2.

b. <u>Ti/RuO_2</u>

Electrochemical mineralization of PFOA by the Ti/RuO_2 anode was carried out in batch reactors that work under continuous vacuum pull similar to the reactors used in Ebonex Plus study. Tests using Ti/RuO_2 anodes and titanium cathodes were conducted at 5, 20, 30, and 40 mA/cm^2. The Ti/RuO_2 anode had an effective submerged surface area of 97 cm^2. All other experimental conditions were the same as in the Ebonex Plus anode study. The schematic diagram of the reactor used for Ti/RuO_2 study is given in Fig 2.3, and the actual reactor setup is given in Fig. 2.4.

Comparison of this reactor to other reactors used in this study and previous literature is given in Table 2.1.

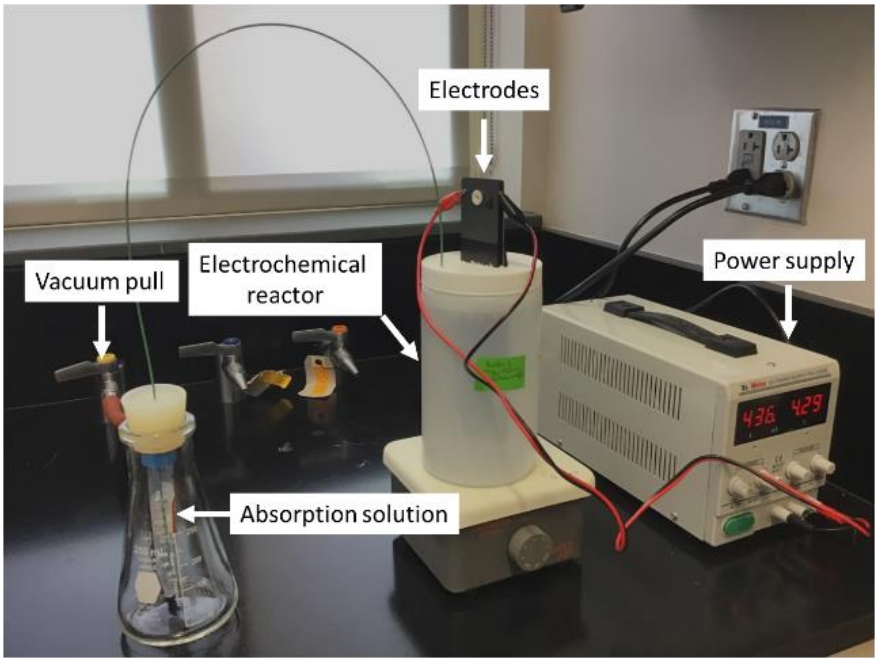

Fig. 2.4 Reactor setup used for Ti/RuO_2 study

c. Boron-Doped Diamond (BDD)

Electrochemical mineralization of PFOA by the BDD anode was carried out in two types of reactors: airtight batch reactors and plug flow reactors (PFR) with recirculation. The BDD plates were manufactured by depositing a boron-doped diamond on a niobium backbone. Each plate had a dimension of 12.5 mm x 100 mm x 2 mm. The BDD film coating was on just one side and had a thickness of 5 µm.

Airtight batch reactors

Airtight batch reactors differ from the reactors shown in Fig. 2.3 as the main reactor was airtight without a vent, and the whole system worked under positive pressure due to the buildup of gases evolved during electrochemical mineralization. From the results of the Ti/RuO_2 anode study,

which used reactors that work under continuous vacuum pull, it was evident that high concentrations of PFOA and other PFASs were present in the absorption solution. PFOA and other PFASs that end up in the absorption solution became unavailable for electrochemical degradation, thus reduced the overall system performance. Airtight reactors could mitigate this issue since they do not promote pulling the gas or aerosol phase PFASs towards the absorption solution; instead, the evolved gases are captured by the absorption solution only when there is a pressure build-up in the reactor.

Different types of airtight batch reactors were designed for electrochemical mineralization of PFOA. The models were named BDD-I, BDD-II, and BDD-III based on the electrode placement, reactor size, and other factors. All three reactor types used BDD as the anode and titanium as the cathode.

BDD-I used 130 mL reactor volume whereas BDD-II used 200 mL. The same PFOA/Na_2SO_4 solutions used for Ebonex Plus and Ti/RuO_2 anode studies were used in BDD anode tests, and the applied currents density was 5 and 10 mA/cm^2. BDD-II replaced BDD-I to further minimize aerosol-based PFOA losses. In BDD-I reactors, a portion of both electrodes projected out of the reactors, and sealant had to be used in the gaps between the electrodes and the reactor cap to make the reactor airtight.

The BDD-II model used a larger reactor so that the entire length of the anode and cathode fit inside the reactor. Only tiny holes for electric connections were needed, which significantly improved the tightness and eliminated the use of sealants. The other differences of BDD-II from BDD-I are: the 1/16” PEEK tubing in BDD-I connecting the reactor to the absorption solution was replaced with 1/8” silicone tubing in BDD-II to reduce resistance during gas transfer; a horizontal shaker

was used for mixing in BDD-II instead of magnetic stir plates in BDD-I; a water bath was used in BDD-I but not for BDD-II as it turned out unnecessary.

The schematic diagram and photos of BDD-I reactor setup is shown in Fig. 2.5 and Fig. 2.6 respectively. The schematic diagram and photos of BDD-II reactor setup is given in Fig. 2.7 and Fig. 2.6 respectively. The gaps between anode and cathode were kept at 2 mm, and each experiment was carried out for 6 h. Comparison of BDD-I and BDD-II reactor to other reactors used in this study and previous literature is given in Table 2.1.

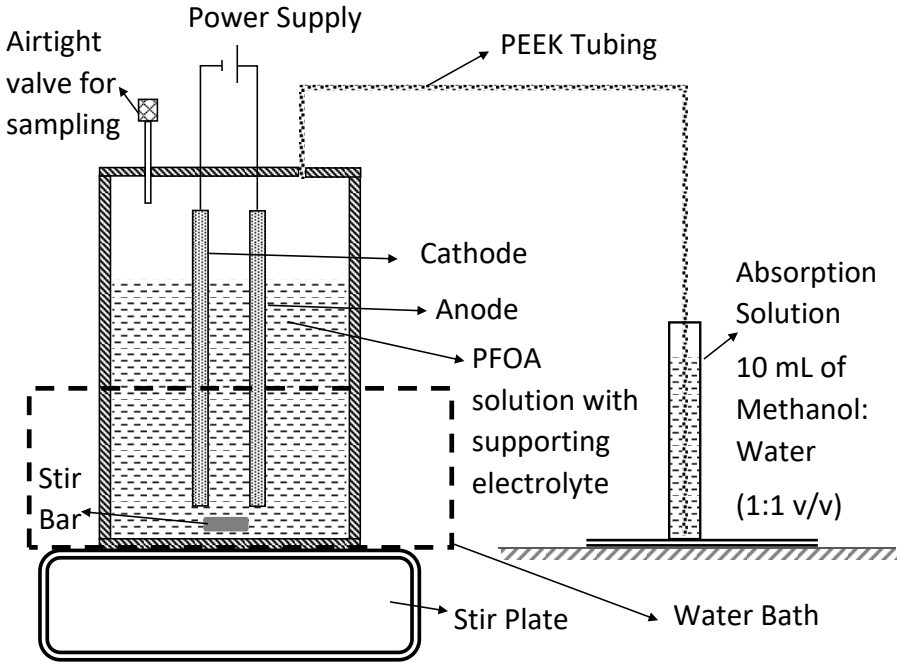

Fig. 2.5 Schematic diagram of the BDD-I type airtight batch reactor used for electrochemical mineralization of PFOA by BDD anodes. BDD served as the anode whereas Ti served as the cathode

Fig. 2.6 (From Left) BDD-I type reactor, and BDD-II type reactor

The BDD-III reactor further improved based on BDD-II by using a reduced reactor volume of 35 mL and a higher anode area to reactor volume ratio of 0.56 as given in Table 2.1. A schematic diagram of BDD-III type reactor is given in Fig 2.7. The actual reactor setup is given in Fig. 2.8.

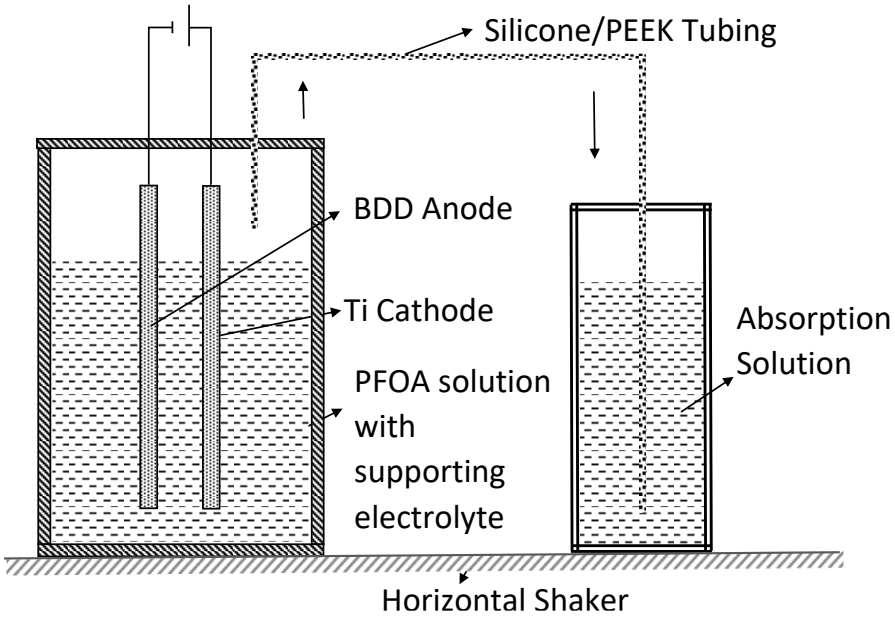

Fig. 2.7 Schematic diagram of BDD-II and BDD-III type airtight reactor. This reactor was used for electrochemical mineralization of PFOA. The reactor used boron-doped diamond (BDD) as the anode and titanium as the cathode.

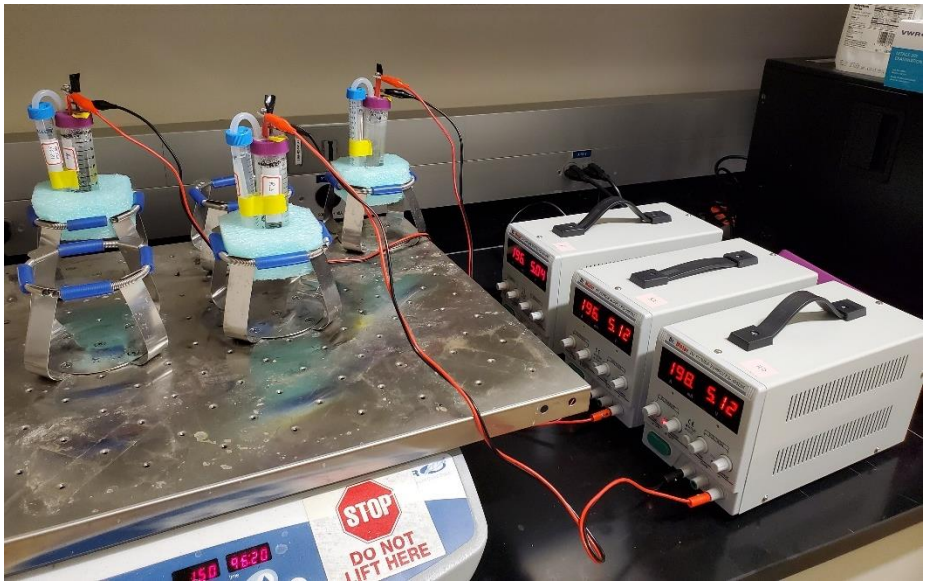

Fig. 2.8 BDD-III type airtight reactor used electrochemical mineralization of PFOA. The reactor used boron-doped diamond (BDD) as the anode and titanium as the cathode.

Plug flow reactor with recirculation

The plug flow reactors with BDD electrodes (BDD-PFR) were designed using AutoCAD 3D and computer numerical control (CNC) machined from polypropylene. The BDD-PFR with recirculation setup consisted of a plug-flow electrolytic reactor, a reservoir, and an absorption solution. The PFOA/Na_2SO_4 solution was circulated between the reservoir and electrolytic reactor at a constant flow rate of 1 mL/min. The solution and the gases evolved during electrochemical mineralization came out of the electrolytic reactor from the same outlet. A schematic diagram of the PFR is given in Fig 2.9. The inlet of the electrolytic reactor was placed at the bottom and the outlet at the top. Electric connections were given from the sides of the reactor. The electrolytic reactor had a high anode area to sample volume ratio of 5 cm^2/mL. The actual reactor setup is given in Fig. 2.10. Comparison of this reactor to other reactors used in this study and previous literature is given in Table 2.1.

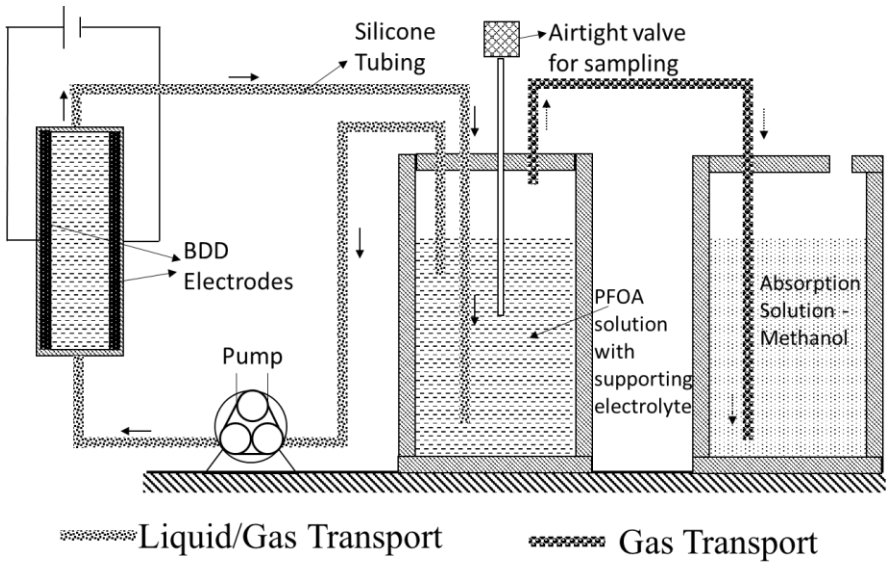

Fig. 2.9 Schematic diagram of the plug flow reactor used for electrochemical mineralization of PFOA by boron-doped diamond (BDD) anode and cathode

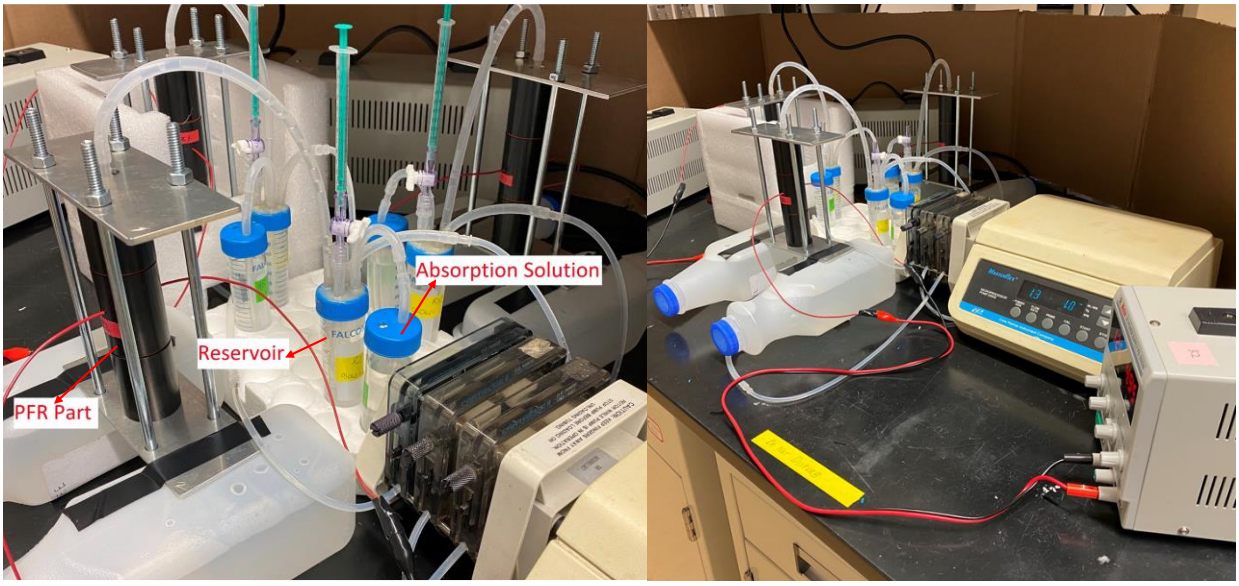

Fig. 2.10 The plug flow reactor with recirculation used for electrochemical mineralization of PFOA by boron-doped diamond (BDD) anode and cathode. The left panel shows a labeled close-up view of the PFR reactor. The right panel shows the complete reactor setup with the peristaltic pump and DC power supply

Additionally, two other reactor models, BDD-continuous reactor with recirculation and BDD-IV airtight batch reactor were used in electrochemical mineralization of GenX and AFFF waste streams. Detailed information on these reactors is given in the "Materials and method" section of electrochemical mineralization of GenX. The comparison of BDD-continuous reactor with recirculation and BDD-IV airtight batch reactor with other reactor types is given in Table 2.1.

Sulfuric Acid Treatment of BDD electrodes

Surface fluorination of BDD electrodes can lead to lower PFAS mineralization efficiency during electrochemical mineralization of PFAS. Sulfuric acid treatment can prevent surface fluorination, and was carried out after each electrochemical mineralization experiment. Two BDD electrodes 2 mm apart were immersed in a 5% sulfuric acid solution in a 50 mL centrifuge tube. A low anode potential of around 3V was applied for 15 min by setting the power supply to a constant current input of 50 mA, with one of the BDD electrodes serving as the anode and the other cathode. After 15 min, the polarities were reversed, and the same voltage was applied for another 15 min.

Table 2.1 Comparison of the different types of electrochemical reactors used in this study to those in previous literature

Reactor	Reactor Vol. (mL)	Anode	Cathode	Anode Area/ volume (cm^2/mL)	Reference
Ebonex Plus	900	Ebonex Plus	Ebonex Plus	0.08	This study
Ti/RuO_2	900	Ti/RuO_2	Titanium	0.10	This study
BDD-I	130	BDD	Titanium	0.12	This study
BDD-II	200	BDD	Titanium	0.10	This study
BDD-III	35	BDD	Titanium	0.56	This study
BDD-PFR with recirculation	60	BDD	BDD	0.21	This study
BDD- Continuous with recirculation	55	BDD	BDD	0.36	This study
BDD-IV	30	BDD	BDD	0.59	This study
Microflow Cell	250	BDD	Tungsten	0.15	(Schaefer et al. 2017)
Multipurpose Flow Cell	2000	Ti/RuO_2	Stainless Steel (SS)	0.05	(Schaefer et al. 2015b)
Glass Beaker	200	Ti_4O_7	SS	0.5	(Lin et al. 2018)
Open Electrolytic Cell	100	Ti_4O_8	SS	1	(Liang et al. 2018)
Open Electrolytic Cell	100	Ti/PbO_2	Titanium	0.12	(Zhuo et al. 2016)
Open Electrolytic Cell	200	Ti/PbO_2	Titanium	0.18	(Zhuo et al. 2017)
Open Electrolytic Cell	200	Ti/SnO_2–Sb/Yb–PbO_2	Titanium	0.05	(Ma et al. 2015)

Chemical Analysis: Fluoride was measured using a Dionex ICS-3000 ion chromatography (IC) from Thermo Fisher Scientific with a Dionex IonPac AS22 analytical column. AOF concentrations were analyzed using a Mitsubishi combustion unit coupled with the IC. An AR15 pH meter from Accumet Research was used to measure the pH of all the samples. Detailed information on LC-MS/MS analysis of PFOA and short-chain PFAA is given below.

Liquid chromatography-tandem mass spectrometry

PFAS, including PFOA and seven short-chain perfluoroalkyl acids (PFAA), were analyzed by a direct injection method using LC-MS/MS system (Agilent 1100 LC liquid chromatography coupled with a 6410 triple quadrupole MS). Individual analytes were separated by a Poroshell 120 EC-C18 column (4.6 mm x 50 mm x 4 μm). The temperature of the column was maintained at 50˚C. An injection volume of 500 μL was used. For both PFOA and short-chain PFAA, mobile phases A and B were 2 mM ammonium acetate in water and 2 mM ammonium acetate in 98% methanol, respectively. Electrospray ionization (ESI) in negative mode was used to ionize PFAS. The multiple reaction monitoring (MRM) method was used to quantify targeted PFAS compounds.

Since LC-MS/MS analysis of PFOA and short-chain PFAA required different dilution factors, two separate methods were used with details given below.

PFOA analysis:

The mobile phase proportion and gradient used for PFOA analysis are given in Table 2.2. The initial condition was 60% B and a flow rate of 0.5 mL/min. Other parameters of mass spectrometry are given in Table 2.3 and Table 2.5.

Table 2.2 Proportion and gradient of mobile phase during LC-MS/MS analysis of PFOA

Time (min)	Mobile Phase A (%)	Mobile Phase B (%)
0.00	40	60
4.20	40	60
4.30	5	95
6.00	5	95
6.10	40	60
8.00	40	60

Table 2.3 Acquisition parameters of mass spectrometry

Parameter	Value
Gas Temperature	300˚C
Gas Flow	13 L/min
Nebulizer	50 psi
Capillary	3000 V

Short-chain PFAA analysis:

The mobile phase proportion and gradient during LC-MS/MS analysis of short-chain PFAA are given in Table 2.4. Details of the compounds analyzed, their internal standards and other mass spectrometry parameters are given in Table 2.3 and Table 2.5.

Table 2.4 Proportion and gradient of mobile phase during LC-MS/MS analysis of short chain PFAA

Time (min)	Mobile Phase A (%)	Mobile Phase B (%)
0.00	90	10
4.20	90	10
14.00	5	95
19.00	5	95
19.10	90	90
22.00	90	90

Table 2.5 Detailed instrument parameters of PFAS tested and their internal standards during mass spectrometry

Compound	Precursor ion (m/z)	Product ion 1 (m/z)	Product ion 2 (m/z)	Dwell	Fragmentor volt (V)	Collision Energy-1 (V)	Collison Energy-2 (V)
PFOA	412.96	369	169	28	88	8	20
PFBA	212.98	169	n.a	28	83	4	n.a
PFPeA	263.97	219	n.a	28	83	4	n.a
PFBS	298.94	99	80	28	73	36	40
PFHxA	312.97	269	118.9	28	83	4	20
PFPeS	348.94	98.9	80	28	84	40	48
PFHpA	362.97	319	169	28	88	4	20
PFHxS	398.93	99	80	28	84	40	52
M8PFOA (IS[a])	420.99	376	172	28	83	8	20
MPFBA (IS[a])	216.99	172	n.a	28	64	4	n.a
M5PFPeA (IS[a])	267.99	223	n.a	28	78	4	n.a

Compound	Precursor ion (m/z)	Product ion 1 (m/z)	Product ion 2 (m/z)	Dwell	Fragmentor volt (V)	Collision Energy-1 (V)	Collison Energy-2 (V)
M5PFHxA (IS[a])	317.99	273	n.a	28	78	4	n.a
M4PFHpA (IS[a])	366.99	322	169	28	88	8	16
M3PFHxS (IS[a])	401.99	99	80	28	190	40	56

n.a- Not applicable

[a] Internal standard

PFOA depletion

PFOA depletion in the reservoir of the PFR with recirculation setup, or in the main electrolytic reactor in all other reactor setups in this study, is calculated using the following equation:

$$PFOA\ depletion\ (\%) = \left(\frac{cPFOA_0 - cPFOA_t}{cPFOA_0}\right) \times 100 \qquad (Eq.\ 2.1)$$

where,

$cPFOA_0$= Initial PFOA concentration (µg/L)

$cPFOA_t$= Concentration of PFOA at time 't' (µg/L)

PFOA degradation

PFOA degradation represents the decrease in PFOA mass in the entire reactor system at the end of the electrochemical mineralization experiment. PFOA masses in the reactor, reservoir, absorption solution and rinse solution are considered. PFOA degradation is calculated using the following equation:

$$PFOA\ degradation\ (\%) = \left(\frac{mPFOA_0 - mPFOA_f}{mPFOA_0}\right) \times 100 \qquad (Eq.\ 2.2)$$

where,

$mPFOA_0$= Initial PFOA mass in the entire reactor system (µg)

$mPFOA_f$= Final PFOA mass remaining in the entire reactor system at the end of the electrochemical experiment (µg/L)

Defluorination Ratio

Defluorination ratio is the percentage of organic fluorine in the degraded PFOA that was converted to fluoride. The defluorination ratio is calculated using the following equation:

$$R = \frac{n_{F-}}{(nPFOA_0 - nPFOA_f) \times n} \times 100\%$$

where,

R- Defluorination ratio (%)

n_{F-} - moles of fluoride in the entire reactor system at the end of the electrochemical experiment (mmol)

$nPFOA_0$ – Initial moles of PFOA in the entire reactor system (mmol)

$nPFOA_f$ – moles of PFOA remaining in the entire reactor system at the end of electrochemical experiment (mmol)

n - Number of fluorine atoms in each PFOA molecule (15 for PFOA)

2.4 Results and Discussion

2.4.1 Ebonex Plus anode

LC-MS/MS analysis of the samples showed no decrease in PFOA concentrations in the reactors. If the 1.5 mg/L PFOA were completely mineralized, 1 mg/L fluoride would have been produced. However, IC analysis of samples taken each hour showed that fluoride concentrations in all samples were below the limit of quantification (LOQ) of 1 µg/L. Given that the IC samples were diluted 20 times before analysis, the non-detect results suggest PFOA defluorination was no more than 2%. Such results further indicate that the applied current density was too low for PFOA mineralization. Given that the electrode material cannot withstand a higher current density based on the manufacturer's instruction, this material was concluded not capable of supporting PFOA degradation.

2.4.2 Ti/RuO_2 anode

The study was conducted to determine the effect of applied current density on PFOA degradation efficiency using a Ti/RuO_2 anode and a Ti cathode. The study included a control (no current) and tested current densities of 5, 20, 30, and 40 mA/cm^2.

The variation of pH observed during the 8-hour reaction time is given in Table 2.6. The pH dropped slightly during the reaction indicating release of H^+ ions. Based on PFOA degradation mechanism

given in Section 2.1.1, the drop in pH an be attributed to the release of hydrofluoric acid and H+ ions during the stepwise degradation of PFOA.

Table 2.6 Variation of pH during Ti/RuO_2 anode study

Test	Initial		Final	
	pH	Std. Dev.	pH	Std. Dev.
Control	5.54	0.03	5.38	0.04
5 mA/cm^2	5.63	0.10	4.11	0.07
20 mA/cm^2	5.56	0.05	5.16	0.09
30 mA/cm^2	5.49	0.02	5.28	0.25
40 mA/cm^2	5.44	0.02	4.81	0.10

The DC power supply maintained a constant current by regulating voltage. Figure 2.11 shows the variation of applied voltage over the reaction period of 8 hours. As the electrochemical reaction progressed, there was a drop in voltage, more evident in the initial hours. The voltage drop indicates a decrease in resistance of the solution in the reactor as time progressed, which might be due to the increase in ionic concentrations after bond cleavage.

The results of PFOA depletion from the reactor solution and distribution of PFOA mass between the reactor and absorption solution at various current densities are shown in Fig. 2.12 and Fig. 2.13, respectively. The control experiment showed no significant change in PFOA concentration, indicating minimal adsorption or any other losses (Fig. 2.13). Under no current condition, PFOA was observed in the absorption solution even though it was just 0.001% of the initial PFOA mass in the reactors (too small to be visual in Fig. 2.13), suggesting the possibility that a small amount of PFOA might have migrated to the absorption solution in the aerosol form (Fig. 2.13).

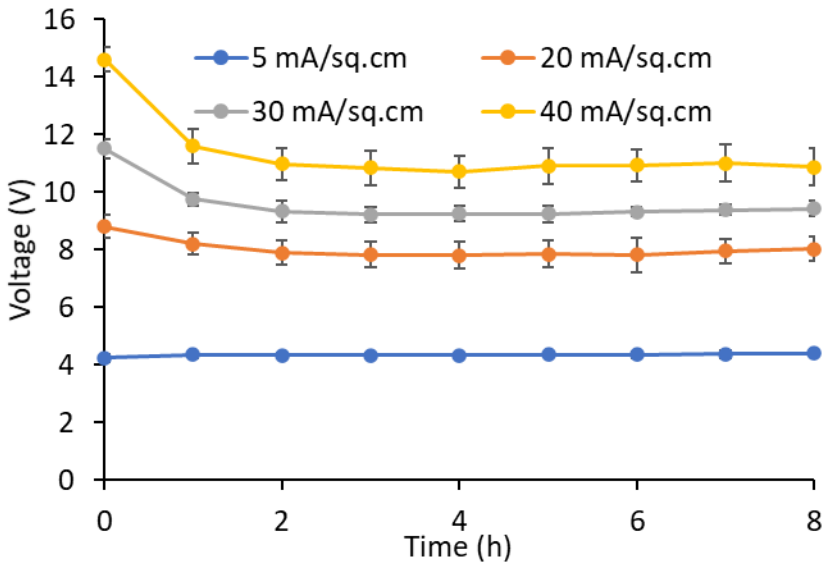

Fig. 2.11 Variation of voltage over time during electrochemical mineralization of PFOA using Ti/RuO_2 anode and Ti cathode. Experiments were done in triplicates.

The PFOA depletion results for 5, 20, and 30 mA/cm^2 experiments showed a trend of increasing PFOA depletion with increasing current density. At 30 mA/cm^2, a decrease of more than 50% in PFOA concentration in the reactor solution was observed in 2 hours (Fig. 2.12). However, no short-chain PFAS compounds as intermediates were detected. The result is in line with previous studies since most studies showed a decrease in PFOA concentration over time but no short-chain intermediates (Schaefer et al. 2015b). The non-detect of short-chain intermediates is because most PFAS degradation occurs on the electrode surface, thus short chain intermediates will be concentrated on the electrode surface, while the electrodes were not rinsed to recover any PFAS adsorbed on the surface in this experiment. Fluoride concentrations of 30 µg/L and 46 µg/L were detected in the reactor samples taken at the hour-8 of 20 mA/cm^2 and 30 mA/cm^2 experiments, respectively, indicating the Ti/RuO_2 anode is capable of mineralizing PFOA.

Meanwhile, significant amounts of PFOA were found in the absorption solution at 5 and 20 mA/cm^2, accounting for ~20% of the initial PFOA mass in the reactor. Almost no PFOA was

detected in the absorption solution at 30 mA/cm^2, due to a possible failure in the vacuum system or the reactor sealing during the experiment.

PFOA being a soluble compound with a pKa of 2.8 will be completely dissociated at a pH of 5.5 (initial pH in the reactors) and is not expected to go to the gas phase (USEPA 2016c). Hence the plausible explanation for the presence of PFOA in the absorption solutions is that, during the electrochemical reactions, aerosol was generated due to water electrolysis/gas production and associated heat generation. PFOA has a high tendency to partition into the air-water interface (Costanza et al. 2019), and hence it is concentrated on the aerosol surface. Some aerosol transported to and was captured by the absorption solutions, some got condensed on the reactor lids, and some might escape to the atmosphere either due to the inefficiency of the absorption solution for full PFOA capture or through the small gaps between the electrodes and the lids. The part that escaped to the atmosphere may explain the incomplete mass balance in Fig. 2.13.

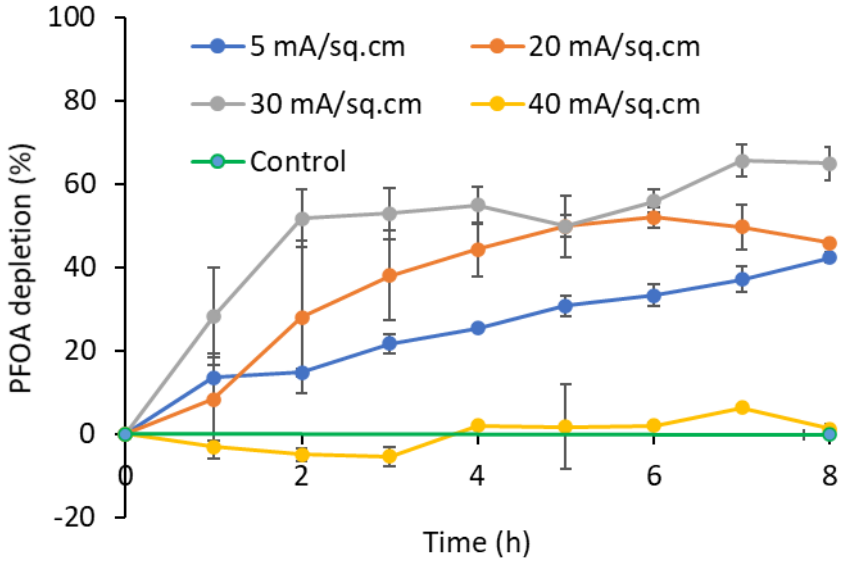

Fig. 2.12 PFOA depletion over time during electrochemical mineralization using Ti/RuO_2 anode and Ti cathode. Experiments were done in triplicates.

However, the results of 40 mA/cm^2 showed no decrease in PFOA concentration as given in Fig.

2.12. Further, no fluoride was detected in the reactor samples. The normalized fluorine mass balance in Fig. 2.13 showed no change in PFOA mass in the system, indicating that no PFOA degradation took place. From these results, it can be inferred that Ti/RuO_2 anodes have a short lifespan and lost their PFOA degradation capacity after few experiments.

One previous study reported that Ti/RuO_2 electrode is effective for PFOA degradation, and their tests did not show a decline in the PFOA degradation efficiency with use (Schaefer et al. 2015b). However, the maximum current density studied by Schaefer et al. was 20 mA/cm^2, much lower than the 40 mA/cm^2 current density where the sharp decline in PFOA degradation efficiency was observed in this study. Hence, the high current density used in this study might have accelerated the decline in electrochemical mineralization efficiency of the Ti/RuO_2 electrode.

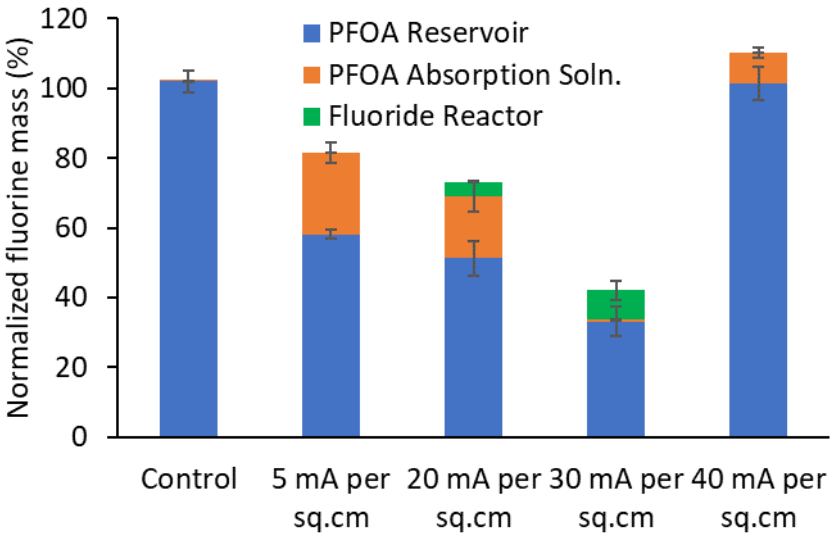

Fig. 2.13 Normalized fluorine mass balance based on PFAS and fluoride for electrochemical mineralization of PFOA using Ti/RuO_2 anode and Ti cathode. No short-chain PFAS were detected. Experiments were done in triplicates.

The high concentrations of PFOA detected in the absorption solution at 5 and 20 mA/cm^2 indicate that aerosol-based transport of PFOA is significant. If this aerosol-based PFOA loss is not

accounted for in the fluorine mass balance, PFOA degradation will be overestimated. Interestingly, many previous papers have reported high PFOA removal while failing to report a fluorine mass balance or achieve complete fluorine mass balance. A study on the electrochemical oxidation of PFOA using PbO_2 electrodes showed more than 90% PFOA removal but a lower defluorination ratio (Zhuo et al. 2017), and no data on fluorine mass balance was provided. Similarly, a study using novel PbO_2 electrodes showed around 75% PFOS degradation but a defluorination ratio of just 12%, and no mass balance was reported (Zhuo et al. 2016). Another study showed high defluorination, but could not close the fluorine mass balance and fell short by 15% even though they looked for short-chain PFAS intermediates (Yang et al. 2017). Similar results were observed by various other studies (Lin et al. 2012; Xiao et al. 2011; Yu et al. 2015; Zhao et al. 2013; Zhuo et al. 2011, 2014). Particularly, a study that used the same Ti/RuO_2 anode as used in this study reported 90% PFOA removal and 58% defluorination without short-chain PFASs detected (Schaefer et al. 2015a). Since none of these studies tried to capture PFASs in the gas/aerosol phase, it is thus reasonable to speculate in these studies, a notable portion of the PFAS that disappeared from the electrolytic reactors was due to aerosol loss into the environment rather than electrochemical mineralization, and the actual PFAS removal in these studies was lower than the reported values.

It should be noted that a few studies have displayed high PFOA degradation as well as a high recovery of the fluorine mass balance. For instance, a study on PFOA degradation using a stable Zirconium doped PbO_2 electrode showed 90% PFOA degradation, 50% defluorination, and more than 90% fluorine recovery (Xu et al. 2016). Similar results were observed by another study that employed Yb doped Ti/SnO_2-Sb/PbO_2 anodes to degrade PFOA (Ma et al. 2015). However, the small missing 10% in these studies could also be aerosol phase PFOA loss.

Nevertheless, the results from this study point out that aerosol-based PFOA loss during electrochemical studies can be significant. Capturing such losses will be an essential part of achieving complete fluorine mass balance. To better control such losses, the batch reactors under continuous vacuum-pull were replaced with airtight batch reactors in the electrochemical mineralization study of PFOA using BDD anodes.

Effect of pH Adjustment on Electrochemical degradation of PFOA

In other experiments under this project, the test solution had a natural initial pH of ~5.5 after PFOA addition, and these solutions were tested as is for PFOA electrochemical removal. In this experiment, the pH of the initial solution was adjusted to 7 to assess the effect of initial pH on PFOA electrochemical removal at an applied current density of 20 mA/cm^2. The change in PFOA concentrations in the reaction vessel was similar with and without initial pH adjustment (Fig. 2.14).

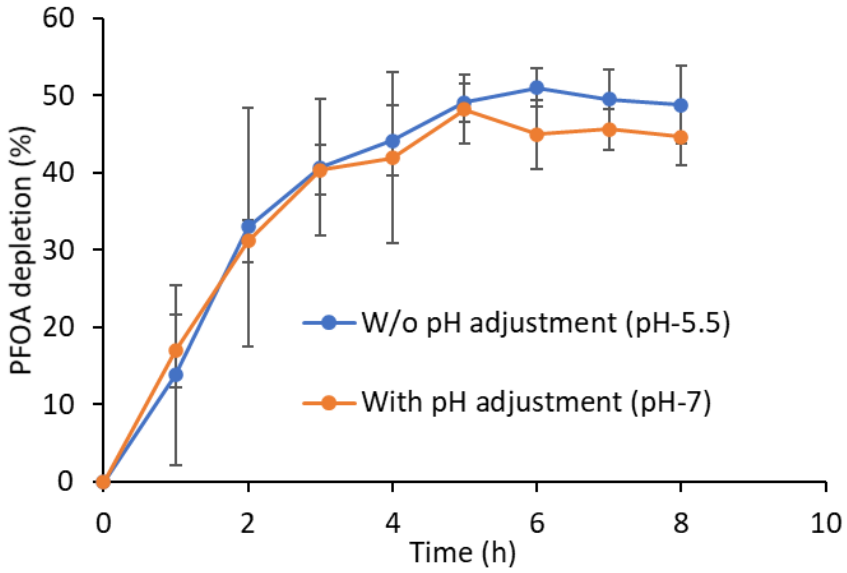

Fig. 2.14 Effect of adjusting initial pH of the PFOA solution in the electrolytic reactor to 7 on PFOA depletion. Experiments were done in triplicates.

The reduced PFOA mass captured in the absorption solutions when the initial pH was adjusted to 7 (Fig. 2.15) is more likely to result from inconsistent vacuum pull across experiments rather than

the pH effect. No short-chain PFAS intermediates were detected with or without pH adjustment. Hence, it can be concluded that a pH adjustment to 7 did not significantly affect PFOA degradation.

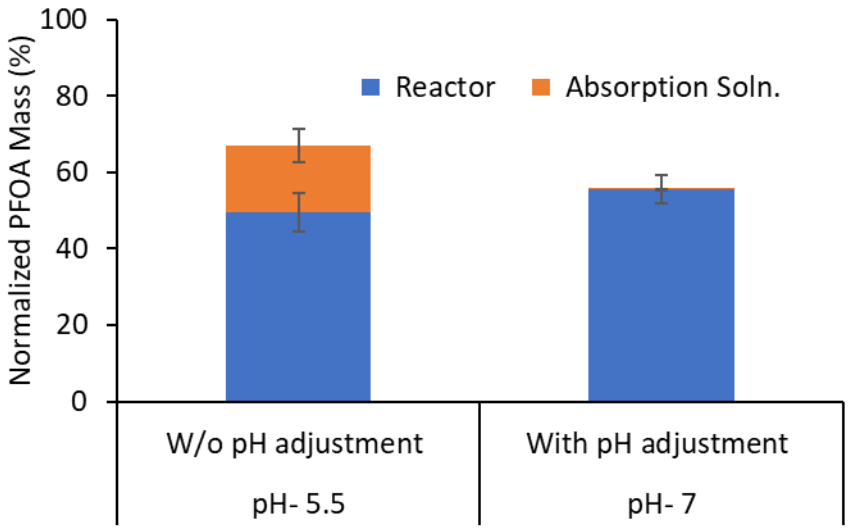

Fig. 2.15 Effect of initial pH adjustment of the PFOA sample to 7 on the final mass distribution of PFOA between reactor and absorption solution during electrochemical mineralization of PFOA. Experiments were done in triplicates.

2.4.3 Boron doped diamond (BDD)

For the study on PFOA degradation using BDD anode and Titanium cathode, three types of airtight batch reactor and one type of PFR were tested. The airtight reactor models were BDD-I, BDD-II, BDD-III and one plug flow reactor model, BDD-PFR with recirculation. The details of each reactor type are given in Section 2.5 and Table 2.1.

2.4.3.1 Airtight Batch Reactors

Control Experiments

The control experiments without current were carried out in triplicates for 6 h. In BDD-I reactors, PFOA concentrations dropped by 10 to 15% (Fig. 2.16), possibly due to small leaks in the reactors

or absorption of PFOA to the sealant used to make the reactors airtight. Meanwhile, PFOA loss was negligible in BDD-II and BDD-III reactors. pH values at the beginning and end of each control test are given in Table 2.9. No significant change in pH occurred in any of the three reactor models during the control experiments.

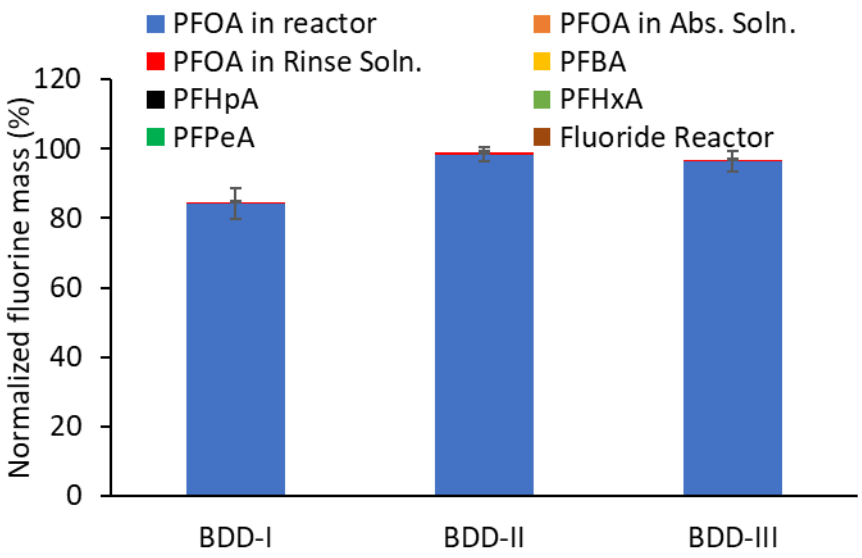

Fig. 2.16 Normalized fluorine mass balance based on PFAS and fluoride during control experiments in the three airtight batch reactor models using BDD anodes. PFAS other than PFOA are reported based on total mass present in the entire reactor system. Experiments were done in triplicates.

Electrochemical mineralization experiments

Experiments conducted using different types of airtight batch reactors are listed in Table 2.7. Except for one experiment, all tests had an initial PFOA concentration of 1.5 mg/L. Two current densities, 5 and 10 mA/cm^2, were studied using airtight batch reactors.

Table. 2.7 Tests conducted using airtight batch reactors equipped with BDD anode and Ti Cathode

Test	PFOA Conc. (mg/L)	Current Density (mA/cm^2)	Reactor Model
1	1.5	5	BDD-I
2	15	10	BDD-I
3	1.5	10	BDD-I
4	1.5	5	BDD-II
5	1.5	10	BDD-III

i. pH results

Table 2.8 below shows the variation in pH during the five electrochemical mineralization experiments carried out using BDD anode and Ti cathode. For experiments with an initial PFOA concentration of 1.5 mg/L, the pH reduced from around 5.5 to 3.5 for BDD-I and BDD-II reactor models. The drop in pH observed can be attributed to the release of hydrofluoric acid during electrochemical oxidation of PFOA (Kormann et al. 1991) or other side reactions such as oxygen evolution. However, at the same initial concentration, BDD-III reactor showed an increase in pH from around 5.5 to 8.8 in six hours. The increase in pH indicates that the cathodic reduction of water to hydroxide during electrolysis dominated hydrofluoric acid generation from PFOA. The plausible reason might be better kinetics due to increased anode area to volume ration resulting in faster arrival at stable PFAS intermediates. Thereafter, cathodic reduction of water to hydroxide might have dominated. formation of stable PFAS intermediates.

As expected, when the initial PFOA concentration was raised to 15 ppm, the starting pH was lower than 1.5 ppm PFOA at 4.84, reflecting the acidic nature of PFOA. For the 15 ppm PFOA study at 20 mA/cm^2, the pH dropped from 4.84 to 2.85.

Table 2.8 Variation of pH in BDD anode study

Test	Hour-0		Hour-6		Hour-8	
	pH	Std. Dev.	pH	Std. Dev.	pH	Std. Dev.
Control Test- BDD-I	5.56	0.06	5.83	0.09	-----	-----
Control Test- BDD-II	5.5	0.00	5.79	0.11	-----	-----
Control Test- BDD-III	5.5	0.00	5.71	0.07	-----	-----
1.5 ppm- 5 mA/ cm^2 – BDD-I	5.52	0.03	-----	-----	3.40	0.10
15 ppm- 10 mA/ cm^2 – BDD-I	4.84	0.14	2.85	0.05	-----	-----
1.5 ppm- 10 mA/ cm^2 – BDD-I	5.58	0.06	3.54	0.03	-----	-----
1.5 ppm- 5 mA/cm^2- BDD-II	5.45	0.00	3.42	0.06	-----	-----
1.5 ppm- 10 mA/cm^2- BDD-III	5.46	0.00	8.78	0.32	-----	-----

ii. Variation of voltage

The variation in voltage over the electrolytic reactors with time is given in (Fig. 2.17). To apply a higher current density, a higher voltage is required. The voltage required for the 15 ppm- 10 mA/cm^2 test was lower than 1.5 ppm 10 mA/cm^2 test using the same BDD-I reactors, because the 15 ppm solution has higher ionic strength, hence higher conductivity and lower the voltage requirement. There was no significant difference between voltage reading between BDD-I and BDD-II reactors during the 5 mA/cm^2 tests, indicating that the resistance of the reactors remained the same between BDD-I and BDD-II models.

iii. PFOA depletion in the reactor

The depletion of PFOA in the reactors over time is given in Fig 2.18. The initial test with 1.5 ppm PFOA at 5 mA/cm^2 showed more than 93% PFOA depletion in the reactors. The second test was conducted in 15 ppm PFOA at 10 mA/cm^2 to better establish fluorine mass balance, but the PFOA

depletion was just 27%. The decreased PFOA depletion might be because the PFAS degradation reaction had become kinetically limited.

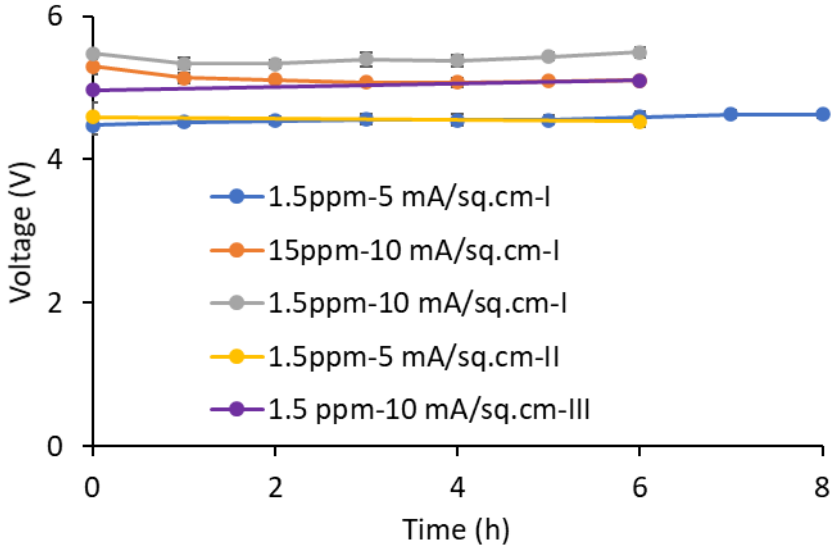

Fig. 2.17 Variation in voltage observed during BDD anode study. Experiments were done in triplicates.

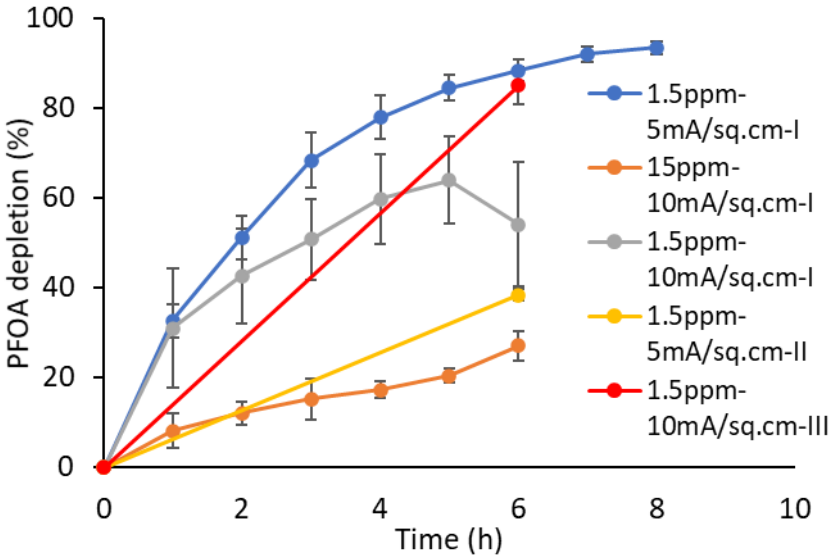

Fig. 2.18 PFOA depletion observed during electrochemical mineralization of PFOA in airtight batch reactors using BDD anode and Ti cathode. Experiments were conducted in triplicates

The third experiment with 1.5 ppm PFOA at 10 mA/cm^2 had PFOA depletion around 54%, lower than that in the 5 mA/cm^2 test. Such unexpected low depletion might indicate the surface fluorination of the BDD anodes, which can cause the loss of electrochemical efficiency. Previous studies have shown that electrochemical oxidation of PFOA causes surface fluorination of the BDD anodes (Gayen and Chaplin 2017; Jawando et al. 2015). Surface fluorination results in the formation of ≡C-F and ≡C-C_nF_{2n+1} ($1 \leq n \leq 7$) functional groups on the BDD surface. These functional groups inhibit PFOA degradation via steric hindrance, opposing dipole-dipole interactions, and lowered van der Waals attraction. Deprotonated PFOA molecules need to reach the electrode surface to undergo electrochemical degradation by direct electron transfer. However, if the BDD anode has surface fluorination, the highly electronegative fluorine atoms in the functional groups on BDD surface will repel incoming deprotonated PFOA molecules and prevent PFOA degradation.

In the fourth test, the reactor was modified to the BDD-II type. The experiment was done in 1.5 ppm PFOA at 5 mA/cm^2. The PFOA removal achieved in the reactor was just 38%, much less than the 93% achieved in the first test under the same conditions. Such results further support the speculation that surface fluorination has occurred.

After the BDD anodes underwent hydrogen plasma treatment by the manufacturer to remove surface fluorination, electrochemical mineralization of PFOA using the restored anodes was conducted in a new reactor model, BDD-III. The test was conducted at 10 mA/cm^2, with around 85% PFOA depletion achieved in 6 hours (Fig. 2.18). Such results confirmed that the decreased PFOA degradation in earlier experiments was due to surface fluorination.

For all future experiments, sulfuric acid treatment was performed as given in Section 2.5 after each electrochemical mineralization experiment to prevent surface fluorination.

iv. Electrochemical degradation of PFOA at 5 mA/cm^2 using BDD-II reactor

The electrochemical degradation of PFOA at 5 mA/cm^2 using BDD-II reactor achieved less than 40% PFOA degradation and less than 10% defluorination (Fig 2.19). The fluorine mass balance based on PFAS species and fluoride of the 5 mA/cm^2 BDD-II experiment is given in Fig. 2.20. PFOA and short-chain intermediates like perfluorobutanoic acid (PFBA), perfluoroheptanoic acid (PFHpA), perfluorohexanoic acid (PFHxA), and perfluoropentanoic acid (PFPeA), as well as fluoride were quantified and used to calculate the fluorine mass balance. No perfluoroalkyl sulfonates (PFSA) were detected. Around 72% fluorine mass balance was achieved.

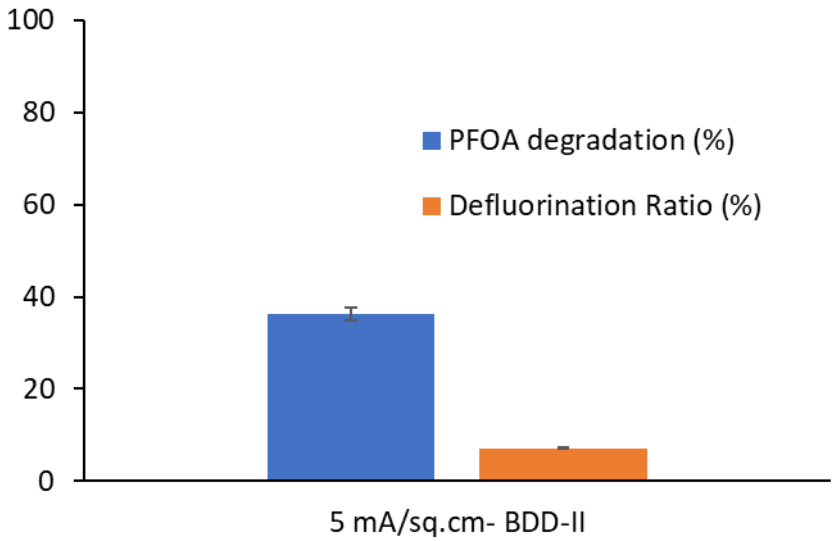

Fig. 2.19 PFOA degradation and defluorination observed in 5 mA/cm^2 BDD-II study. Experiments were conducted in triplicates

However, the fluoride generation was less than 3% of the initial fluorine mass. The low fluoride generation indicates low PFOA mineralization and could be attributed to the surface fluorination of the BDD anodes lowering the available anode area. More than 60% PFOA remained in the reactor, indicating the low PFOA degradation due to surface fluorination (Fig. 2.20). Short-chain PFAS intermediates were found in the reactors but not in the absorption solutions. Short-chain

PFAS accounted for 5% of the total fluorine mass (Fig. 2.20). PFHpA had the highest concentrations among the short-chain PFAS intermediate, accounting for 3% of the initial PFOA mass.

PFOA was detected in the reactor and rinse solution. However, PFOA detected in the absorption solution was negligible (Fig. 2.20), confirming that the airtight batch reactors were able to minimize aerosol-based transport of PFOA from the reactors to the absorption solutions. In contrast, batch reactors under continuous vacuum pull showed around 20% PFOA in the absorption solutions (Fig. 2.13). Hence it could be concluded that the airtight batch reactors are superior to batch reactors under continuous vacuum pull for electrochemical mineralization of PFOA.

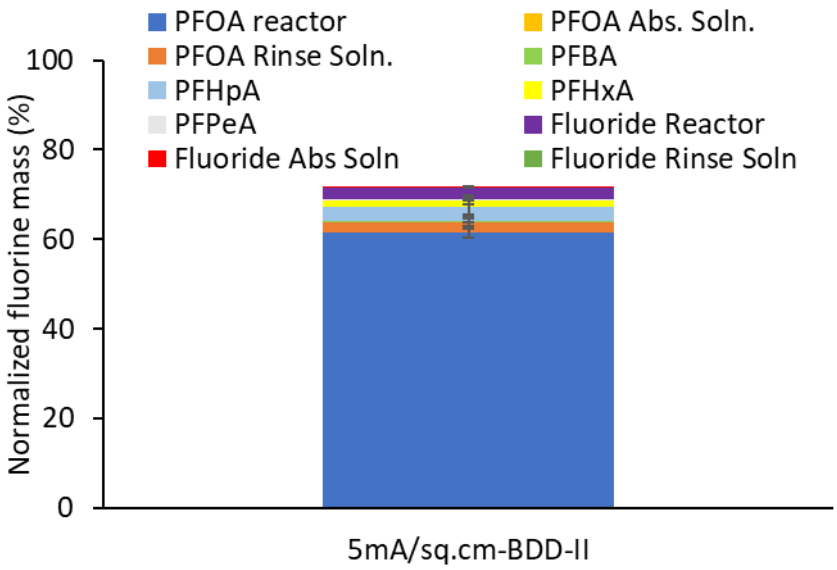

Fig. 2.20 Normalized fluorine mass balance based on PFAS and fluoride achieved in 5 mA/cm^2 BDD-II study. PFAS other than PFOA are reported based on total mass present in the entire reactor system. Experiments were conducted in triplicates

The fluorine mass balance based on AOF and fluoride is given in Fig. 2.21. AOF results include fluorine present in unknown PFAS in addition to the limited number of PFAS species analyzed by

LC-MS/MS, thus capturing a wider range of reaction intermediates yet to be identified. As expected, complete fluorine mass balance was achieved, clearly showing the benefit of using AOF over individual PFAS concentrations to account for fluorine mass balance.

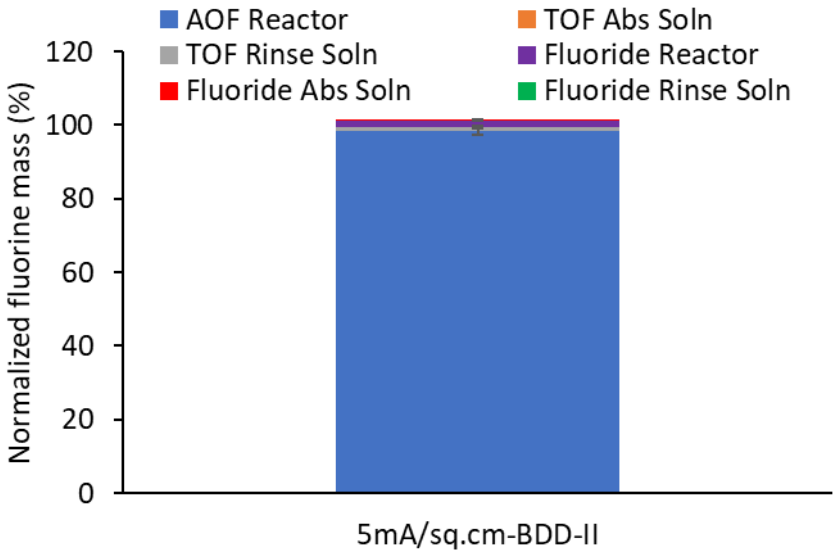

Fig. 2.21 Normalized fluorine mass balance based on AOF and fluoride achieved in 5 mA/cm^2 BDD-II study. Experiments were conducted in triplicates

v. Electrochemical degradation of PFOA at 10 mA/cm^2 using BDD-III reactor

The electrochemical experiment at 10 mA/cm^2 using BDD-III achieved around 80% PFOA degradation and 42% defluorination (Fig. 2.22). This indicates the hydrogen plasma treatment performed on the BDD electrodes was able to remove surface fluorination and restore the electrochemical efficiency of the electrodes. The high PFOA degradation obtained indicate that BDD anode is effective at PFOA degradation even at a low current density like 10 mA/cm^2. The PFOA degradation and defluorination ratio are significantly higher than the 5 mA/cm^2- BDD-II test (Fig. 2.19) because of a better anode area to volume ratio, higher current density and use of BDD anodes restored by hydrogen plasma treatment.

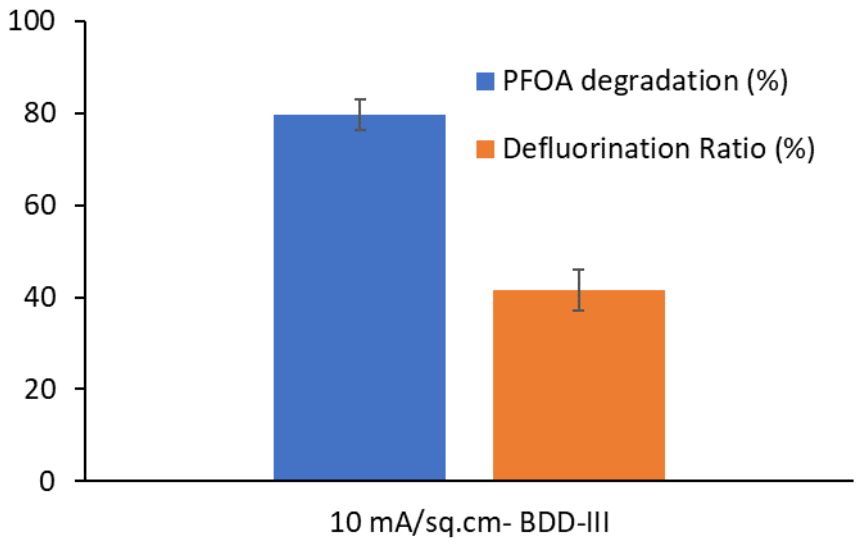

Fig. 2.22 PFOA degradation and defluorination ratio achieved in 10 mA/cm^2 BDD-III study. Experiments were conducted in triplicates

Fluorine mass balance based on PFAS and fluoride achieved around 62% (Fig. 2.23). The treatment achieved more than 30% fluoride generation. PFOA remaining in the reactor was just 15% of the initial PFOA mass. Similar to the 5 mA/cm^2 BDD-II test, no PFOA was detected in the absorption solution further confirming the superiority of airtight batch reactors over batch reactors under continuous vacuum pull. Short-chain PFAS intermediates accounted 8% of initial fluorine mass with PFHA dominating at 3% of initial fluorine mass.

Fluorine mass balance based on AOF and fluoride is shown in Fig. 2.24. Almost complete fluorine mass balance was achieved compared to just 62% when fluorine from PFAS and fluoride were used. The comparison further confirms the superiority of fluorine mass balance based on AOF and fluoride over the one using PFAS and fluoride.

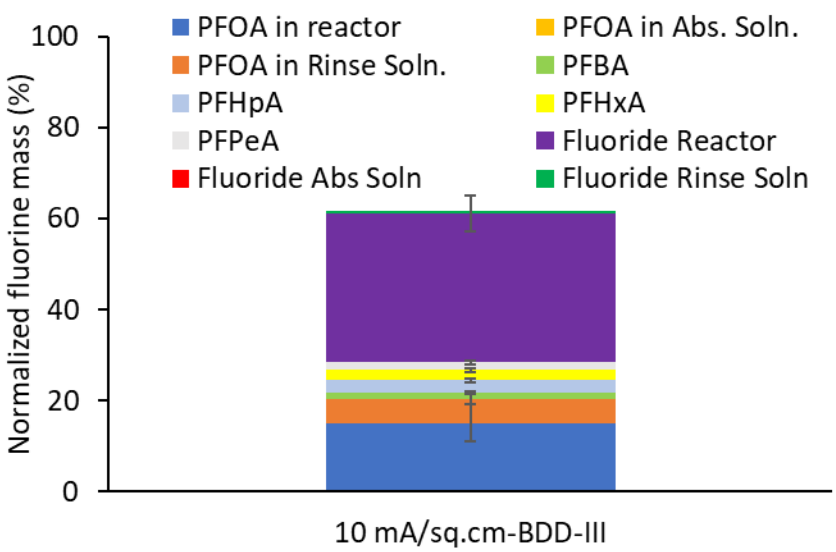

Fig. 2.23 Fluorine mass balance based on PFAS and fluoride in 10 mA/cm^2 BDD-III study. PFAS other than PFOA are reported based on total mass present in the entire reactor system. Experiments were conducted in triplicates

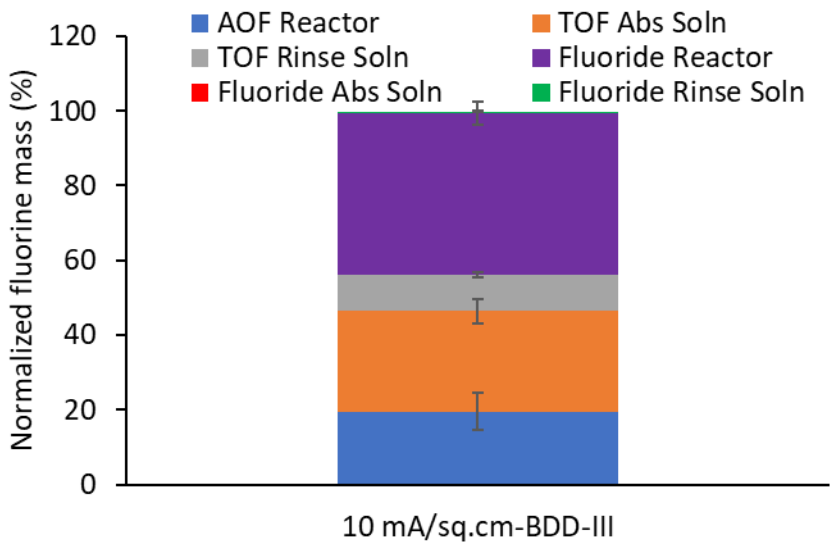

Fig. 2.24 Fluorine mass balance based on AOF and fluoride in 10 mA/cm^2 BDD-III study. Experiments were conducted in triplicates

Around 27% organic fluorine was detected in the absorption solution as shown by Fig 2.24. However, no PFOA was detected in the absorption solution as given by Fig. 2.23. Except for a

negligible amount of PFPeA, no other short-chain intermediates were detected in the absorption solution. This confirms the presence of unknown PFAS in the absorption solution. Organic fluorine in the rinse solution accounted for 10% of the total fluorine mass. This organic fluorine is from PFAS that were adsorbed on the electrodes, reactor walls and tubing.

The organic fluorine that ends up in the absorption solution is not available for electrochemical mineralization. The key to high PFAS mineralization will be the prevention of the transport of organic fluorine to absorption solution or the reintroduction of this organic fluorine back to the reactor solution.

2.4.3.2 Plug flow reactor with recirculation

The electrolytic system was further modified to a plug flow reactor with recirculation to minimize the amount of organic fluorine transported to the absorption solution and improve the anode area to reactor volume ratio. A control test and two electrochemical tests (10 mA/cm^2 and 20 mA/cm^2) were performed using this reactor.

The variation of pH observed during all the tests are given in Table 2.9. During both electrochemical tests, pH slightly increased after 8 hours. The variations of voltage observed during both tests were minimal (Fig.2.25).

The depletion of PFOA in the reservoir solution during the tests is given in Fig 2.26. Tests at 10 mA/cm^2 and 20 mA/cm^2 achieved around 30% PFOA depletion. The low depletion is possibly due to hydrogen and oxygen gases building up between the electrodes, causing large gas pockets. The gas pockets significantly reduced the anode area available for reactions, resulting in poor PFOA depletion. This problem was caused by insufficient mechanical mixing and the lack of a dedicated

gas outlet separate from the outlet for the PFOA solution in the PFR. Hence, the current PFR model is not suitable for PFOA degradation and needs to be redesigned.

Table 2.9 Variation of pH during electrochemical mineralization of PFOA using BDD electrodes in the plug flow reactor with recirculation

Test	Hour-0		Hour-8	
	pH	Std. Dev.	pH	Std. Dev.
Control Test	5.47	0.00	5.57	0.12
10 mA/cm^2	5.50	0.00	6.22	0.45
20 mA/cm^2	5.56	0.00	6.56	0.33

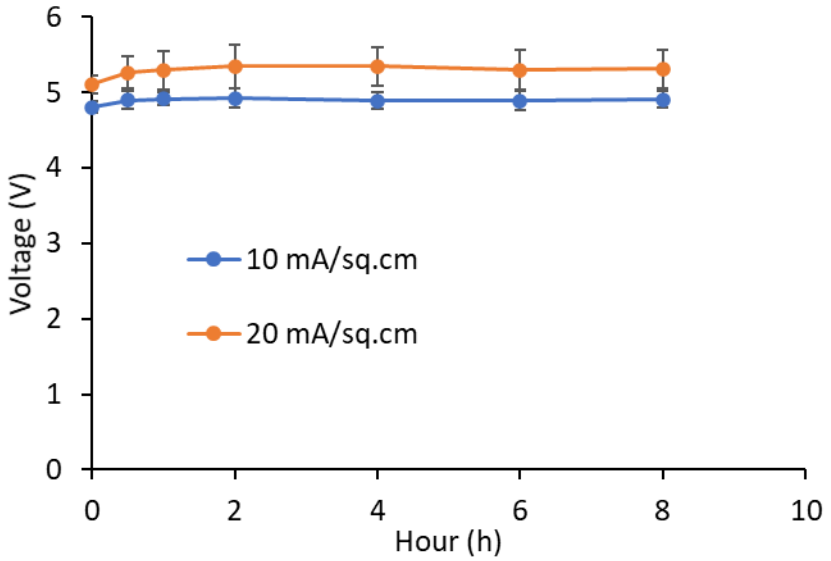

Fig. 2.25 Variation of voltage observed during electrochemical mineralization of PFOA using plug flow reactor with recirculation at 10 and 20 mA/cm^2

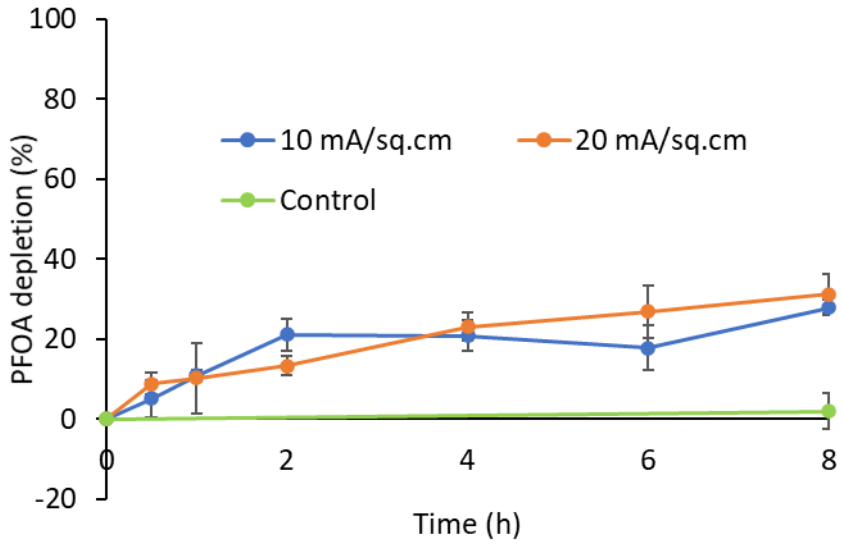

Fig. 2.26 PFOA depletion observed during electrochemical mineralization of PFOA at 10 and 20 mA/cm^2

2.5 Conclusions

- Ebonex Plus electrodes are not suitable for electrochemical degradation of PFOA due to its low current rating
- Ti/RuO_2 anode has short lifespan and is concluded not suitable for electrochemical degradation of PFOA
- BDD anode was selected as the best electrode for PFOA degradation due to its high PFOA degradation efficiency and long lifespan
- BDD-III model airtight batch reactor equipped with BDD anode and Ti cathode achieved 80% PFOA degradation and 42% defluorination ratio

- Complete fluorine mass balance was achieved using AOF and fluoride compared to just 62% mass balance achieved using PFAS and fluoride. Hence mass balance based on AOF and fluoride is superior to the one based on PFAS and fluoride
- Airtight batch reactor was able to prevent aerosol-based transport of PFOA to the absorption solution
- Around 27% organic fluorine was detected in the BDD-III airtight batch reactor indicating that aerosol-based transport is significant
- Reintroducing the organic fluorine that ends up in the absorption solution back to the reactor solution will be key to achieve higher PFOA mineralization
- PFR with recirculation showed poor PFOA degradation due to development of air pockets between the electrodes resulting in poor contact between PFAS and anode

3. Electrochemical mineralization of GenX

3.1 Literature Review

Studies on electrochemical mineralization of GenX are limited. So far there are just five studies on electrochemical degradation of GenX including the four recently published ones. Pica et. al. explored electrochemical oxidation of GenX in nanofiltration reject by BDD anodes (Pica et al. 2019a). The nanofiltration reject had a GenX concentration of 4.98 mg/L. The electrochemical cell utilized a boron-doped ultra-nanocrystalline diamond anode on niobium substrate and stainless steel as the cathode. The sample was recirculated at 3 L/min, and a current density of 50 mA/cm^2 was applied (Pica et al. 2019a). Results revealed that direct electron transfer was the primary reaction mechanism. The electrochemical degradation of GenX followed a first-order kinetic model with a rate constant of 0.0041 min^{-1} in the nanofiltration reject, almost double that in raw water. In 240 min, around 40% of GenX was degraded in both the nanofiltration reject and in raw water. In the nanofiltration reject, 60% GenX degradation and 80% of fluorine mass balance was achieved. The missing fluorine could be unknown intermediates from GenX degradation or loss of aerosol-based GenX. The electric energy consumption per order of GenX removal in the nanofiltration reject was 237 kWh/m^3, less than 1/6 of the energy required in treating raw water. The nanofiltration treatment before electrochemical oxidation reduced the energy requirement by 97% and the anode material needed by 93% (Pica et al. 2019a). Scavenger and replacement tests showed that when sulfate was not present or sulfate radicals were scavenged, the GenX degradation rate constant went down. Hence it was concluded that sulfate was imperative for faster degradation kinetics.

Yang et. al., 2022 compared electrochemical degradation of PFOA and GenX and found that PFOA was more susceptible to electrochemical oxidation than GenX with 2.4 folds more degradation than GenX (Yang et al. 2022). Babu et. al. studied electrochemical oxidation of GenX using BDD anodes at a high concentration of 15 mg/L and mainly compared the effect of different electrolytes and electrolyte concentrations for degrading GenX. At lower electrolyte concentration, more voltage was needed to achieve the same current density. They observed that at the same current density, higher applied voltage achieved more GenX degradation possibly due to the higher energy input needed for higher voltages. However, the increase in GenX degradation when using 0.1M and 0.05M sodium sulfate was not significant. While comparing different current densities, they observed increased GenX degradation and defluorination with increasing current density with 97% degradation and 95% defluorination achieving at 30 mA/cm^2(Suresh Babu et al. 2022). Olvera-Vargas et. al., paired electro-Fenton process using a graphene-Ni foam cathode with anodic oxidation by BDD. Using total organic carbon (TOC) analysis a GenX mineralization of 92% was ascertained in the treatment carried at 16 mA/cm^2 for 6 hours while 73% GenX mineralization was observed when only BDD was used (Olvera-Vargas et al. 2022). Baldaguez Medina et. al., combined electrosorption and electrochemical oxidation. Electrosorption was achieved using a redox co-polymer acting as anode during sorption to attract deprotonated GenX. This was followed by reversing the polarity to attract GenX towards the new anode of BDD which degraded GenX. At a current density of 10 mA/cm^2 around 70% defluorination was achieved in 10 hours and complete mineralization was achieved in 24 hours (Baldaguez Medina et al. 2021).

GenX degradation mechanism

Pica et al. proposed a degradation mechanism for electrochemical mineralization of GenX by the BDD anode using density functional theory (Pica et al. 2019a). The proposed degradation mechanism is given in Fig. 3.1. Compounds enclosed in boxes represent non-radical stable intermediates, and blue arrows represent direct electron transfer. Initially, GenX undergoes a direct electron transfer and decarboxylation at anode potentials above 3.4V to form a radical of alkyl ether. This radical undergoes an immediate reaction with a hydroxyl radical to form a potentially stable intermediate ether alcohol. Degradation could occur through two different paths. In the first path, a reaction with a hydroxyl radical followed by the loss of $\cdot CF_3$ results in a second stable intermediate, an acyl fluoride labeled as (5). The second path, which is more favored above an anode potential of 5.1V, occurs via direct electron transfer followed by loss of $\cdot CF_3$ and H^+ to form the stable intermediate similar to the other path. The acyl fluoride can then undergo direct electron transfer or react with hydroxyl radicals; however, direct electron transfer is preferred over 4.5V. A carbocation is formed, which reacts with water immediately, then deprotonates to form radical (7). The reaction of the acyl fluoride with a hydroxyl radical under 4.5V also results in radical (7). This radical then gives out fluoroformic acid (FCOOH) and radical (8). FCOOH degrades to hydrogen fluoride and carbon dioxide. Radical (8) loses carbonyl fluoride to form radical (9). The carbonyl fluoride and radical (9) then degrades to carbon dioxide and hydrogen fluoride. Theoretical calculations also revealed that sulfate radicals could help GenX degradation by producing hydroxyl radicals, resulting in indirect oxidation of radicals (3) and (5) mediated by hydroxyl radicals.

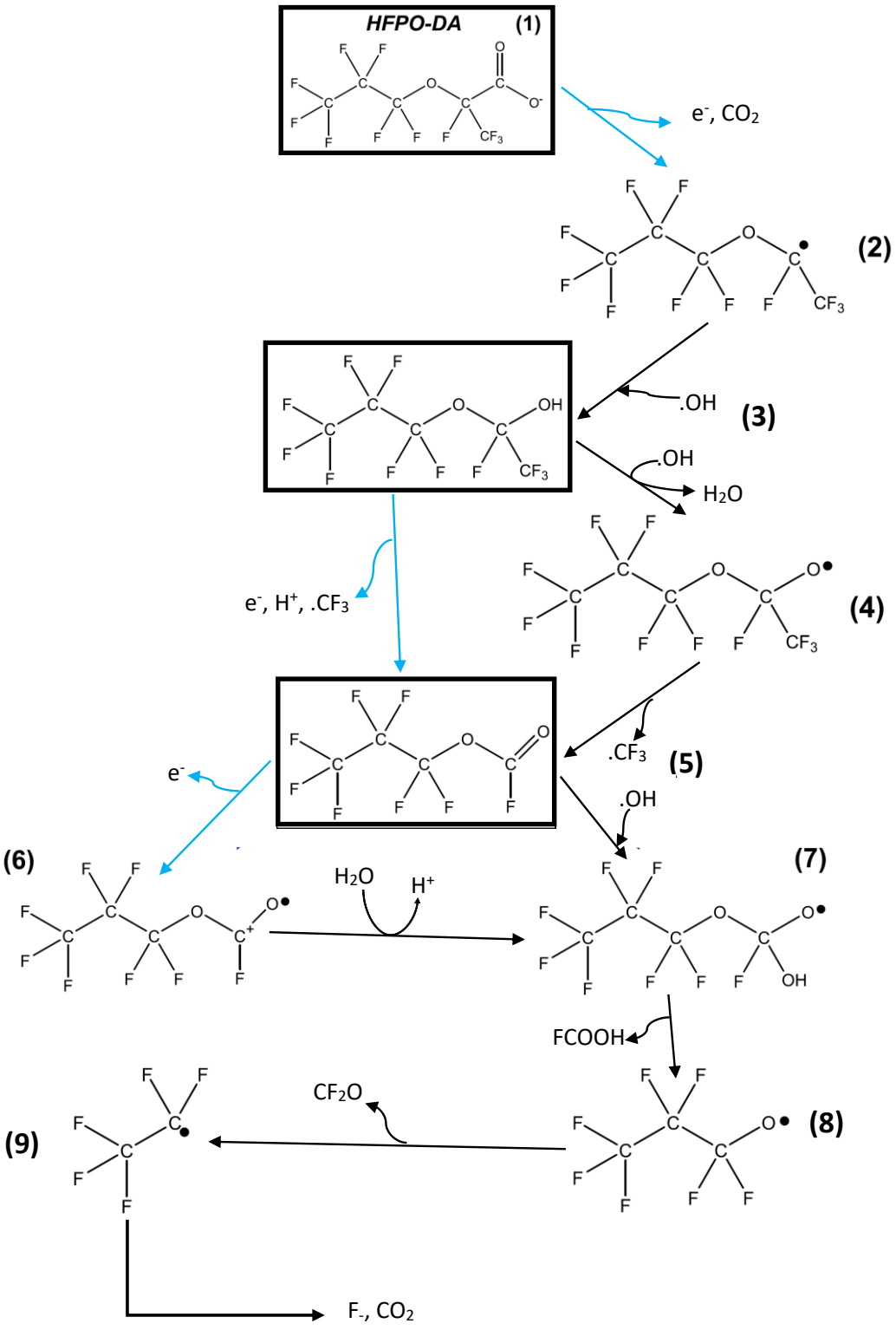

Fig. 3.1 Pathway of electrochemical mineralization of GenX proposed by Pica et. al., 2019. Compounds inside solid boxes represent stable intermediates. Blue arrows represent direct electron transfer

Knowledge gap

The available literature on advanced oxidation is limited with just one study reporting electrochemical mineralization of GenX (Pica et al. 2019a). Even though Pica et. al. conducted the test at a high current density of 50 mA/cm^2, the GenX degradation was just 40% and a fluorine mass balance of 80%. The missing fluorine could be unknown PFAS or loss of aerosol-based GenX since the study use 0.5M NaOH as absorption solution.

Hence, it is necessary to optimize electrochemical mineralization of GenX to improve GenX degradation, fluorine mass balance and determine the most suitable absorption solution.

Proposed treatment train

The same treatment train proposed for PFOA electrochemical mineralization as shown in Fig 2.2 which involves a two-stage treatment process is considered for electrochemical mineralization of GenX. Detailed description of the treatment train can be found in Section 2.1.

3.2 Study overview

3.2.1 Task 1: Identify optimum current density for electrochemical mineralization of GenX by BDD electrodes in a continuous reactor with recirculation

Current density drives both GenX mineralization and undesired side reactions and affects the operational cost of the treatment. The first task was to identify the optimum current density for electrochemical mineralization of GenX among 10, 20, 25, and 30 mA/cm^2. The current density with GenX degradation and defluorination ratio significantly higher than its nearest lower current density tested was considered optimal.

Hypothesis: We hypothesize that GenX degradation rate will increase with increasing current density but become relatively constant beyond a certain threshold due to the competition from side reactions and ohmic heating

3.2.2 Task 2: Assess the effect of sodium hydroxide as absorption solution during electrochemical mineralization of GenX

Sodium hydroxide solution is expected to have higher efficiency for capturing the acidic hydrogen fluoride gas due to its basic nature. Three different concentrations (0.01M, 0.5M and 1M) of NaOH solutions were studied to find the optimum concentration for capturing fluoride generated during electrochemical mineralization of GenX in batch reactors. The NaOH solution concentration with significantly higher fluoride capture than its immediately lower concentration tested was considered optimal.

Hypothesis: Fluoride capturing efficiency will increase with the concentration of NaOH solution.

3.2.3 Task 3: Assess the effect of methanol as absorption solution during electrochemical mineralization of GenX

Methanol and the optimum NaOH solution selected from Task 2 were compared for their suitability as absorption solutions for electrochemical mineralization of GenX in batch reactors. The selection of the optimum absorption solution was based on both organic fluorine and fluoride capture. However, since completely mineralizing GenX to fluoride is the treatment goal, fluoride capture was given more weightage.

Hypothesis: Both methanol and sodium hydroxide solution may be able to capture some fluoride and aerosol-based PFAS. However, methanol as an organic solvent has higher efficiency

at capturing aerosol-based PFAS gases generated during electrochemical mineralization, where sodium hydroxide as a base has higher efficiency for capturing the acidic hydrogen fluoride gas.

3.2.4 Task 4: Study the effect of shaker speed on electrochemical mineralization of GenX

Two shaker speeds (150 and 200 rpm) were compared to determine if GenX electrochemical degradation in batch reactors is limited by available GenX molecules at the anode surface. The conclusion was made by comparing the GenX electrochemical degradation and defluorination between the two shaker speeds.

Hypothesis: A higher shaker speed may enhance GenX electrochemical degradation by preventing PFASs from concentrating at the air-water interface, which are unavailable for electrochemical reaction, and reducing the mass transfer resistance for GenX molecules to transport from the bulk solution to the anode surface.

3.2.5 Task 5: Comparison of batch reactor and continuous reactor with recirculation for electrochemical mineralization of GenX

In the study on electrochemical mineralization of PFOA in batch reactors, around 28% organic fluorine was found in the absorption solution, and this portion of organic fluorine was not available for further electrochemical degradation. To achieve a more complete electrochemical degradation, it is essential to reintroduce the organic fluorine in the absorption solution back to the reactors, which can be achieved by using a continuous reactor with recirculation. Batch reactors and continuous reactors with recirculation were compared for their effectiveness at GenX mineralization at the optimum current density selected from Task 1. The better reactor configuration was determined by higher GenX degradation and defluorination ratio.

Hypothesis: The continuous reactor with recirculation will be able to capture aerosol-based organic fluorine generated during electrochemical reactions and reintroduce it back to the reactor solution. Thus, this new reactor configuration will have higher GenX degradation and defluorination ratio than the batch reactor configuration.

3.3 Materials and Methods

Chemical Reagents: GenX as hexafluoropropylene oxide dimer acid (HFPO-DA) was purchased from Acros Organics. Mass-labeled HFPO-DA (M3HFPO-DA) as the internal standard was purchased from Wellington Laboratories. All other chemicals were from the same sources listed in Section 2.3.

Electrodes: For electrochemical mineralization of GenX, BDD was used as both the anode and cathode in both batch reactors and continuous reactors with recirculation.

Water Matrix: Electrochemical mineralization experiments were carried out in lab-prepared solution in deionized water with 1.5 mg/L GenX and 0.01M sodium sulfate. As discussed in Chapter 2, the GenX and sodium sulfate concentrations reflected the composition of spent brine after ion exchange resin regeneration. Sodium sulfate acted as the supporting electrolyte during electrochemical mineralization.

Reactors: Two types of reactors were used for electrochemical mineralization of GenX: continuous reactors with recirculation (BDD-continuous with recirculation) and airtight batch reactors (BDD-IV).

a. Continuous reactor with recirculation

The schematic diagram of the continuous reactor with recirculation used for electrochemical mineralization of GenX is given in Fig 3.2. The actual reactor setup is shown in Fig 3.3. The setup consisted of the main electrolytic reactor, a reservoir, and an absorption solution. The GenX solution is circulated between the main reactor and reservoir at 0.6 mL/min by a peristaltic pump. The BDD electrodes were used as both anode and cathode in this setup.

The main reactor contained 30 mL solution while the reservoir had 25 mL. The anode area to sample volume ratio was 0.36 (Table 2.1). The absorption solution for this reactor setup contains 40 mL mathanol. This reactor had separate outlets for gas and liquid transport.

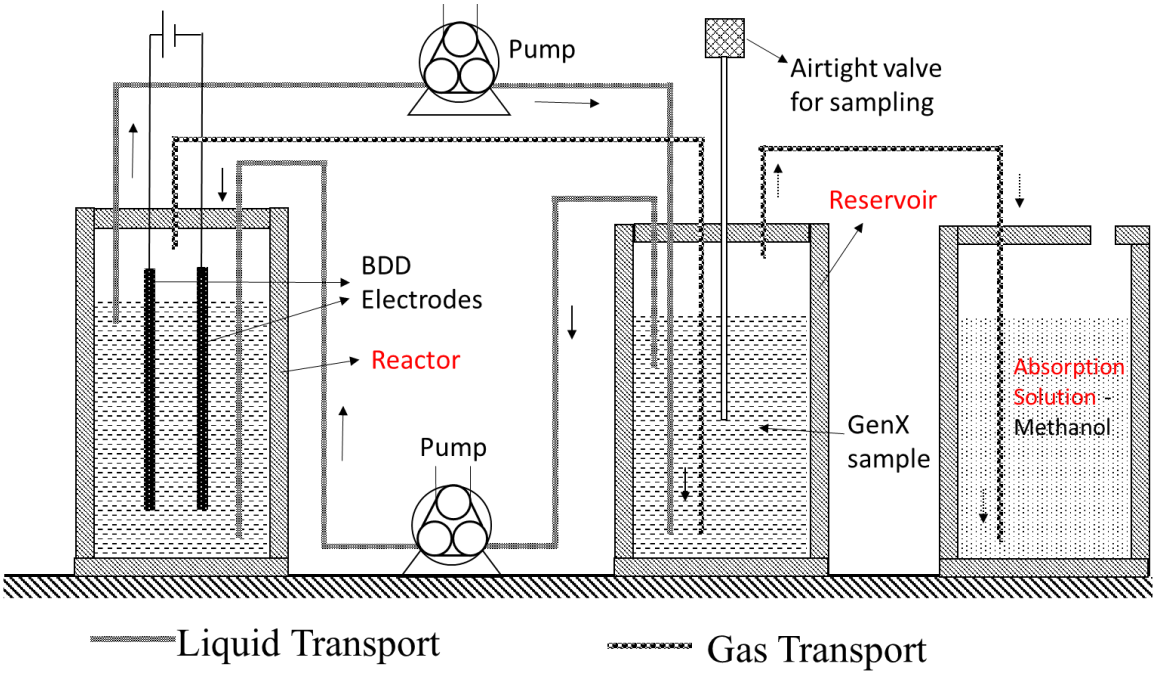

Fig. 3.2 Schematic diagram of the continuous reactor with recirculation used for electrochemical mineralization of GenX

Fig. 3.3 Continuous reactor with recirculation setup used for electrochemical mineralization of GenX

b. Batch reactor

The BDD-IV type airtight batch reactor is similar to BDD-III type with two differences: (1) the BDD-IV reactor used BDD as both the anode and cathode, while BDD-III used Ti as the cathode; (2) BDD-IV used a smaller reactor volume of 30 mL while BDD-III used 35 mL. The anode area to volume ratio of the BDD-IV reactor was 0.59 cm^2/mL (Table 2.1). The schematic diagram of the BDD-IV airtight batch reactor is given in Fig. 3.4. The actual reactor setup is shown in Fig. 3.5.

Sulfuric Acid Treatment of BDD electrodes

Sulfuric acid treatment of the BDD electrodes was carried out after each electrochemical mineralization experiment to prevent surface fluorination. The procedure for sulfuric acid treatment is discussed under reactors in Section 2.3.

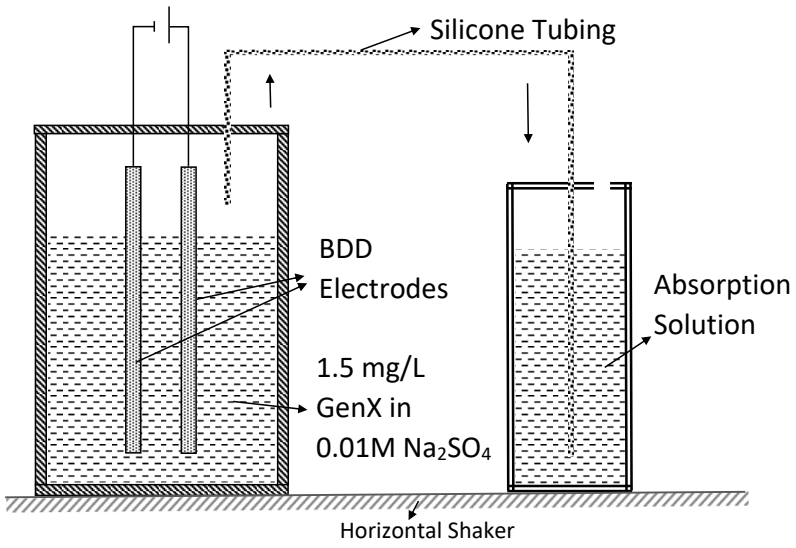

Fig. 3.4 Schematic diagram of the BDD-IV model of airtight batch reactor used for electrochemical mineralization of GenX

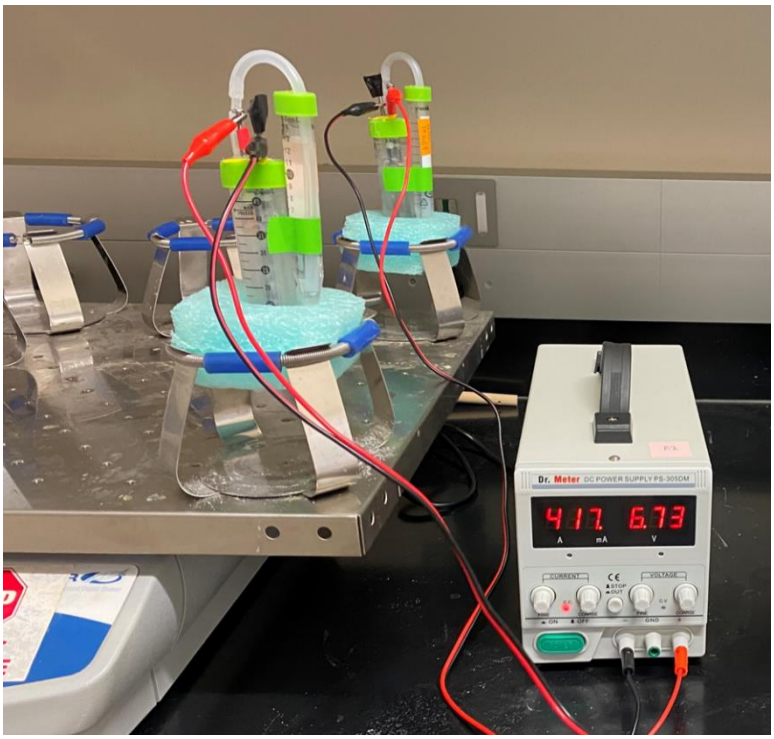

Fig. 3.5 Setup of BDD-IV model of airtight batch reactor used for electrochemical mineralization of GenX

Chemical Analysis: Analysis of PFAAs, fluoride, AOF, and pH were the same as described in Section 2.3. Quantification for GenX, which is described below:

The mobile phase proportion and gradient used for GenX analysis are given in Table 3.1. The initial condition was 60% B and a flow rate of 0.5 mL/min. Other parameters of mass spectrometry are given in Table 3.2 and Table 3.3. LC-MS/MS analysis required a lower gas temperature of 230˚C.

Table 3.1 Proportion and gradient of mobile phase during LC-MS/MS analysis of GenX

Time (min)	Mobile Phase A (%)	Mobile Phase B (%)
0.00	90	10
4.20	90	10
5.00	5	95
12.00	5	95
12.10	90	10
14.00	90	10

Table 3.2 Acquisition parameters of mass spectrometry

Parameter	Value
Gas Temperature	230˚C
Gas Flow	13 L/min
Nebulizer	40 psi
Capillary	3000 V

Table 3.3 Detailed instrument parameters of GenX and its internal standard during mass spectrometry

Compound	Precursor ion (m/z)	Product ion 1 (m/z)	Product ion 2 (m/z)	Dwell	Fragmentor volt (V)	Collision Energy-1 (V)	Collison Energy-2 (V)
GenX	328.97	285	169	150	59	0	4
GenX	285	169	----	150	59	0	----
M3HFPO-DA (IS[a])	331.99	185.1	----	150	88	12	----
M3HFPO-DA (IS[a])	287	169	----	150	59	0	-----

[a] Internal standard

GenX depletion, degradation, and the defluorination ratio were defined similarly to those defined for PFOA mineralization in Chapter 2**.**

3.4 Results & Discussion

3.4.1 Continuous reactor with recirculation

Continuous reactors with recirculation were introduced to minimize the amount of organic fluorine reaching the absorption solution. This is achieved by having a reservoir solution that absorbs part of the aerosol-based PFASs and recirculates it back to the reactor.

Control tests and electrochemical mineralization tests at four different current densities (10, 20, 25, and 30 mA/cm^2) were conducted using the continuous reactor with recirculation. The variation of pH during these tests is given in Table 3.4. pH during all tests increased, with higher current density leading to higher pH increase, and the highest pH of 10.22 was observed at the highest current density. The voltage variation during the electrochemical mineralization was negligible. As expected, the highest voltage application was required for the highest current density. The applied voltage and its variation during the electrochemical process are given in Fig. 3.6.

Table 3.4 pH variation during electrochemical mineralization of GenX in continuous reactors with recirculation

Test	Hour-0		Hour-8	
	pH	Std. Dev.	pH	Std. Dev.
Control Test	5.50	0.00	6.17	0.19
10 mA/cm^2	5.45	0.00	9.32	0.52
20 mA/cm^2	5.77	0.00	9.05	0.14
25 mA/cm^2	5.48	0.00	9.99	0.30
30 mA/cm^2	5.64	0.00	10.22	0.04

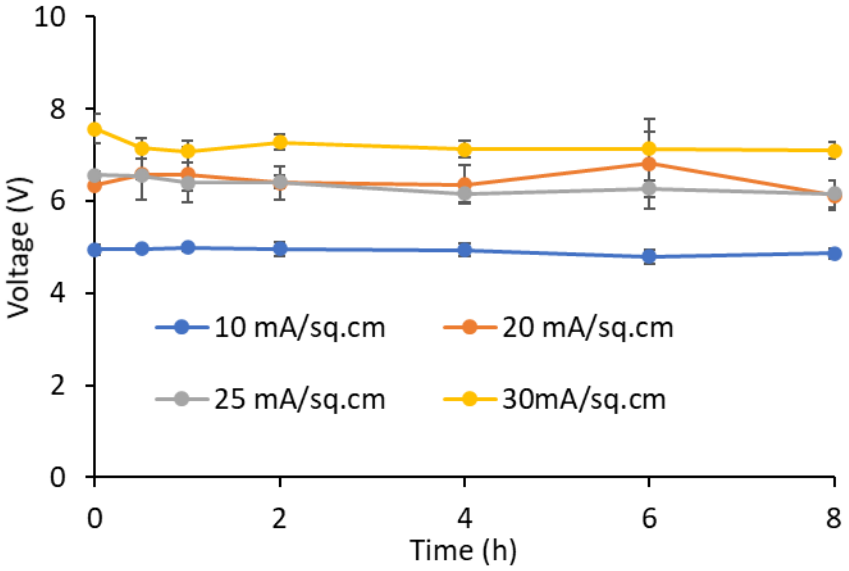

Fig. 3.6 Variation of voltage observed during electrochemical mineralization of GenX using continuous reactor with recirculation at different current densities. Experiments were conducted in duplicates

GenX depletion over time during electrochemical mineralization using the continuous reactors with recirculation is given in Fig. 3.7. There was a significant jump in GenX depletion from 10 mA/cm^2 to 20 mA/cm^2. While GenX depletion at 10 mA/cm^2 reached around 34% after 8 hours, GenX depletion at mA/cm^2 reached around 68%. However, no significant increase in GenX depletion was observed for current densities higher than 20 mA/cm^2, possibly due to increased competition from side reactions and energy loss due to Ohmic heating.

Fig. 3.8 shows the GenX degradation and defluorination ratio achieved at each current density tested. Similar GenX degradation and defluorination ratio was obtained at current densities 20 mA/cm^2 and above. As discussed before, no further increase in GenX degradation was obtained above 20 mA/cm^{2,} possibly due to competition from side reactions and Ohmic heating. From these results, it can be concluded that 20 mA/cm^2 is the optimum current density for GenX degradation among the four current densities tested.

By comparison, at 10 mA/cm^2, 80% PFOA degradation was achieved whereas just 65% GenX degradation was obtained at 20 mA/cm^2, a current density twice the one applied for PFOA. This shows that GenX is more recalcitrant to electrochemical oxidation compared to PFOA. Similar results were obtained during previous studies which investigated different advanced oxidation treatments for GenX. A recent study on electrochemical degradation of GenX found that PFOA was 2.4 times more easy to oxidize than GenX (Yang et al. 2022). Bao et. al., 2018 studied UV/persulfate oxidation for GenX and PFOA degradation. The results revealed that while UV/persulfate oxidation caused 26% PFOA degradation in 3 hours, however the GenX degradation achieved in the same time was less than 5% (Bao et al. 2018). A study conducted on electrochemical oxidation of GenX achieved just 60% degradation at a high current density of 50 mA/cm^2 (Pica et al. 2019b). Whereas many studies conducted on PFOA degradation reported near complete PFOA degradation in less time duration and lower applied current densities (Ma et al. 2015; Yang et al. 2015; Zhuo et al. 2017). From these comparisons it could be concluded that GenX is more recalcitrant to electrochemical oxidation than PFOA. For the current study, it could be argued that reduction by the cathode also plays a role since the electrochemical reactors housed both anode and cathode in the same solution without any separation of catholyte and anolyte. However, electrochemical oxidation by anode could be considered dominant over reduction by cathode since GenX with its low pKa is mostly in its anionic form and gets attracted and adsorbed on the positively charged anode.

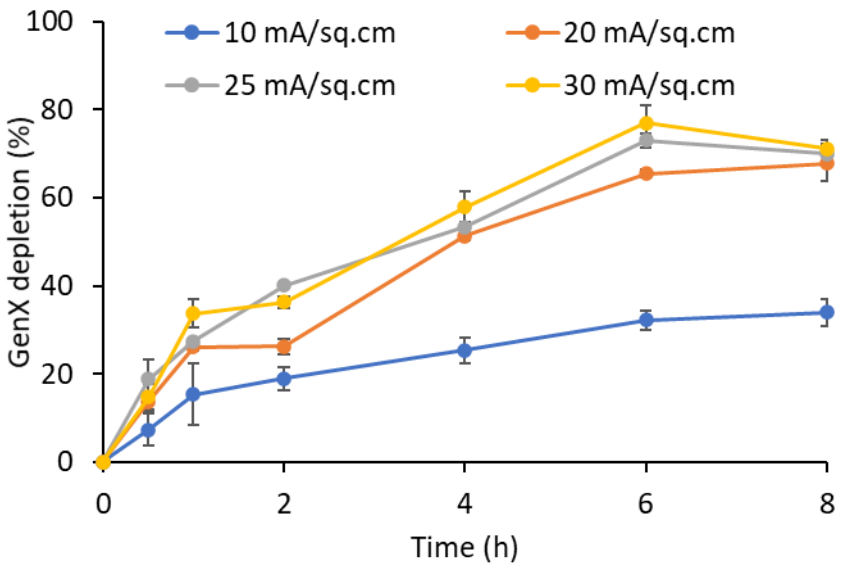

Fig. 3.7 GenX depletion over time during electrochemical mineralization of GenX using continuous reactor with recirculation at different current densities. Experiments were conducted in duplicates

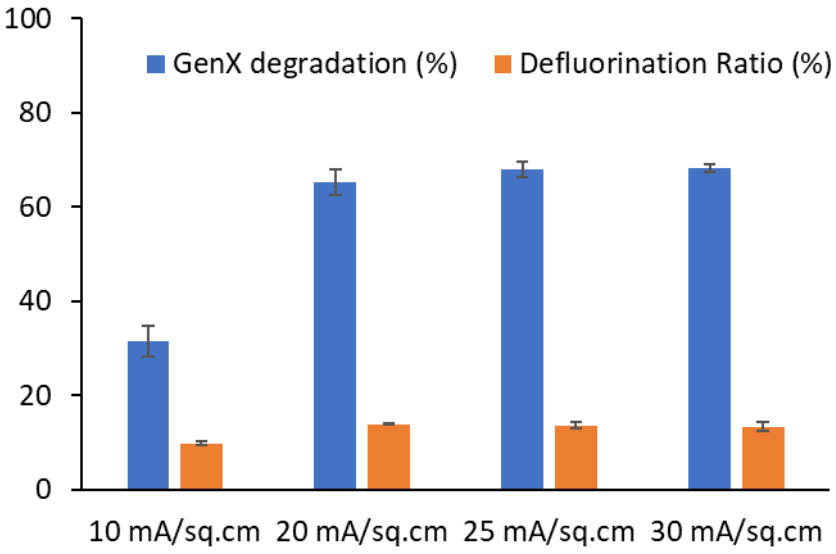

Fig. 3.8 GenX degradation and defluorination ratio achieved at each current density during electrochemical mineralization of GenX in continuous reactor with recirculation. Experiments were conducted in duplicates

The fluorine mass balance based on PFAS and fluoride is given in Fig. 3.9. LC-MS/MS analysis of the samples did not detect any PFAS other than GenX in either the reactor or the absorption solution, indicating that the degradation intermediates were not on the LC-MS/MS analyte list. The best fluorine mass balance was obtained at the lowest current density tested, suggesting that at higher current densities, more GenX gets degraded to unknown short-chain PFAS. At 10 mA/cm^2, a fluorine mass balance of 72% was achieved; however, at 20 mA/cm^2, it lowered to 44%. At higher current densities, the fluorine mass balance decreased even further.

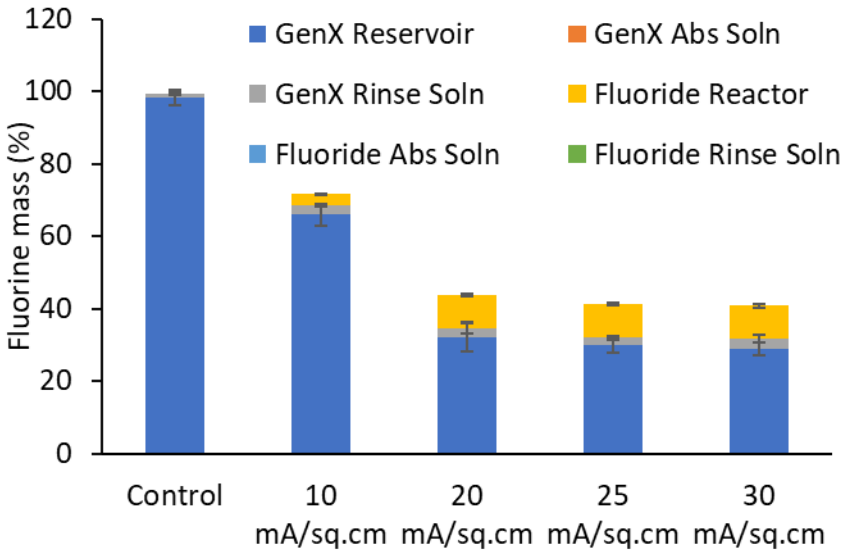

Fig. 3.9 Fluorine mass balance based on PFAS and fluoride for electrochemical mineralization studies of GenX using continuous reactor with recirculation at different current densities. Experiments were conducted in duplicates

The fluorine mass balance during electrochemical mineralization of GenX based on AOF and fluoride achieved at different current densities is given in Fig. 3.10. At the optimum current density of 20 mA/cm^2, 70% fluorine mass balance was achieved. For comparison, at the same current density, the mass balance based on PFAS and fluoride was only 44%. The difference reflects the

benefit of using AOF to calculate the fluorine mass balance over individual PFAS, since the AOF analysis accounts for fluorine contents in unknown PFAS intermediates.

A decreasing trend in fluorine mass balance with increasing current density was observed (Fig. 3.10). The fluorine mass balance based on AOF and fluoride depends on a various factors such as affinity of the PFAS compounds towards the carbon used, efficiency of PFAS mass transfer between the gas bubbles and the absorption solution, and the loss of fluorine due to surface fluorination. With increasing current density, more electrochemical energy is available for PFAS degradation resulting in more short-chain PFAS intermediates at higher current densities. Since short-chain PFAS are less hydrophobic than longer-chain ones, short-chain PFAS will have poor recovery during AOF analysis (Han et al. 2021) . This poor recovery of short-chain intermediates results in lower fluorine mass balance at higher current densities. The second reason for decreasing fluorine mass balance with increasing current density is due to the lowered PFAS mass transfer between the gas bubbles and absorption solution at higher current densities. At higher current densities, more H_2 and O_2 gases are generated resulting in increased number and size of gas bubbles entering the absorption solution. Hence the area and time available for mass transfer is reduced leading to poor efficiency in PFAS capture by the absorption solution. This poor recovery in turn results in a lower fluorine mass balance at higher current densities. Surface fluorination is not expected to significantly impact fluorine mass balance since complete fluorine mass balance was achievable for PFOA electrochemical degradation.

Another important observation from Fig 3.10 is that around 13% organic fluorine was detected in the absorption solution in the 20 mA/cm^2 test, while no GenX or short-chain PFAA were detected in the absorption solution (Fig 3.9). This observation confirms the presence of potential unidentified PFAS as degradation byproducts during electrochemical mineralization of GenX.

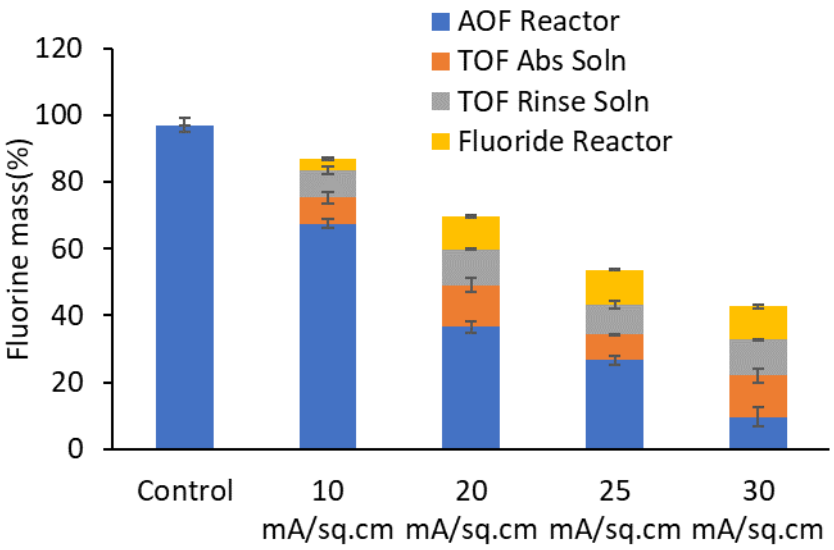

Fig. 3.10 Fluorine mass balance based on AOF and fluoride at each current density tested during electrochemical mineralization of GenX in a continuous reactor with recirculation. Experiments were conducted in duplicates

3.4.2 Batch Reactor Studies

Various tests were carried out in BDD-IV airtight batch reactors to ascertain the effect of sodium hydroxide and methanol as absorption solution and the effect of shaker speed on electrochemical mineralization of GenX. All batch reactor studies were conducted at a current density of 20 mA/cm^2.

3.4.2.1 Effect of NaOH as absorption solution

Three different NaOH solution concentrations (0.01M, 0.5M, and 1M) were tested for their suitability as an absorption solution for electrochemical mineralization of GenX. The variation of pH during the electrochemical process with different NaOH concentrations is given in Table 3.5. Since only the absorption solution was different in the three electrochemical tests, while chemicals in the absorption solution did not return to the electrolytic reactors, all electrochemical tests had a similar pH of around 10.5 at the end of the reaction.

Table 3.5 Variation of pH during electrochemical mineralization of GenX in BDD-IV type airtight batch reactor

Test	Hour-0		Hour-8	
	pH	Std. Dev.	pH	Std. Dev.
Control Test	5.48	0.00	5.91	0.24
0.01M NaOH as absorption solution	5.51	0.00	10.49	0.31
0.5M NaOH as absorption solution	5.63	0.00	10.33	0.13
1M NaOH as absorption solution	5.48	0.00	10.57	0.15

Fig. 3.11 shows GenX degradation and defluorination ratio achieved during electrochemical mineralization of GenX at 20 mA/cm^2 by each absorption solution. While all absorption solutions showed the same GenX degradation, the highest defluorination ratio of around 37% was achieved by the 1M NaOH absorption solution. The 1M NaOH solution achieved the highest defluorination ratio due to its highest fluoride capture, further suggesting that the 1M NaOH is the best for fluoride capture among the three concentrations tested.

The fluorine mass balance based on PFAS and fluoride using the three concentrations of NaOH as the absorption solution is given in Fig. 3.12. Other than GenX, no other PFAS tested were detected in any of the samples. The mass of GenX in the whole system, and fluoride in the reactors and rinse solutions were relatively constant at different NaOH concentrations since the electrochemical reactions were not affected by the absorption step. The test with 1M NaOH as the absorption solution achieved the highest fluorine mass balance of 61% among the three different concentrations tested as expected, because a more concentrated base can capture more hydrogen fluoride generated during electrochemical mineralization of GenX. While the 1M NaOH absorption solution captured around 13% fluorine mass as fluoride, just 7% was captured by the 0.5M NaOH solution, and no fluoride was observed in the 0.01M NaOH solution. Hence, the 1M

NaOH solution is concluded the best absorption solution among the three NaOH solutions tested for fluoride capture.

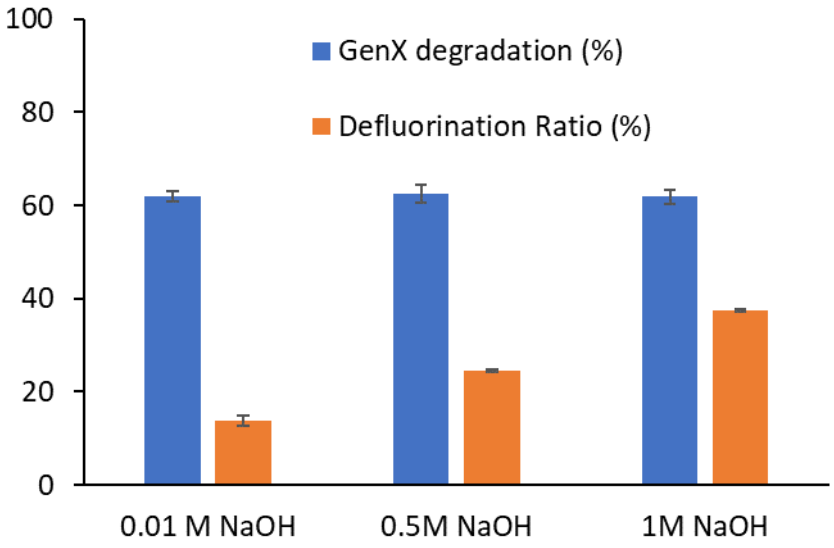

Fig. 3.11GenX degradation and defluorination observed for batch studies carried out in BDD-iv type airtight batch reactor comparing 0.01M, 0.5M and 1M NaOH solutions as absorption solutions. Experiments were conducted in duplicates.

All absorption solutions showed similar GenX capture as shown in the mass balance shown in Fig. 3.12. This is also the reason for observing similar GenX degradation (Fig. 3.11). GenX degradation is calculated based on the amount of GenX remaining in the reactor, absorption solution, and rinse solution. Since the tests were carried out at the same current density, the only factor that can vary is the GenX capture by absorption solution. From this, it can be concluded that the concentration of NaOH absorption solution did not affect GenX capture.

The mass balance based on AOF and fluoride is shown in Fig 3.13. As expected, the batch reactor with 1M NaOH as the absorption solution showed the highest fluorine mass balance of 68% due to its highest fluoride capture.

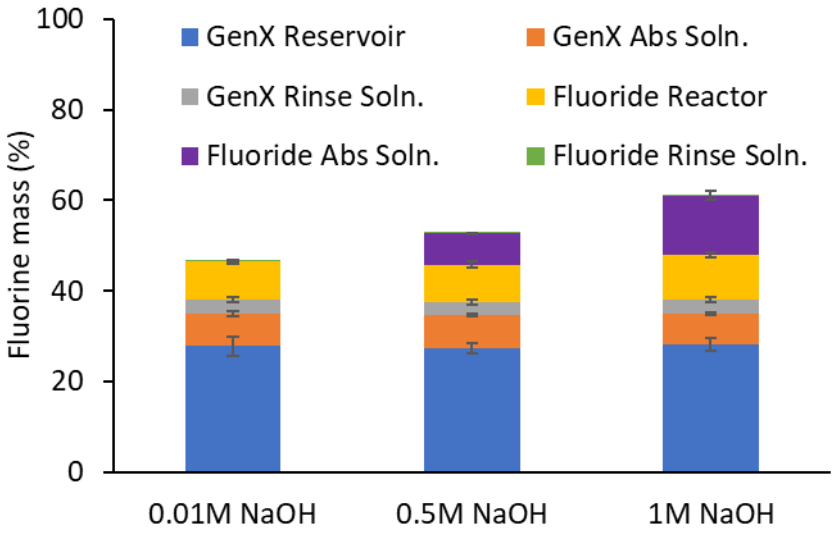

Fig. 3.12 Fluorine mass balance based on PFAS and fluoride for the batch studies carried out in BDD-iv type airtight batch reactor comparing 0.01M, 0.5M and 1M NaOH solutions as absorption solutions. Experiments were conducted in duplicates

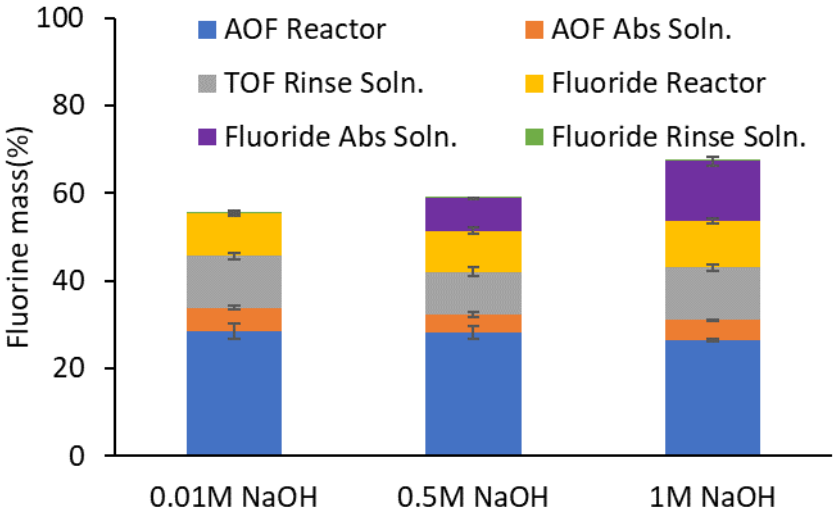

Fig. 3.13 Fluorine mass balance based on AOF and fluoride achieved for batch studies carried out in BDD-iv type airtight batch reactor comparing 0.01M, 0.5M and 1M NaOH solutions as absorption solutions. Experiments were conducted in duplicates.

3.4.2.2 Comparison of methanol and 1M NaOH as absorption solution

Methanol was tested as the absorption solution, and its performance was compared to the 1M NaOH solution selected as the best from the previous study. The variation in pH of the reactor solution at the end of the reaction is given in Table 3.6. Since both tests were carried out at the same current density, the final pH was similar. Fig. 3.14 shows GenX degradation and defluorination when methanol and 1M NaOH were used as the observation solution. Both GenX degradation and defluorination were higher when 1M NaOH was used as the absorption solution.

Table 3.6 Variation of pH during batch reactor studies comparing methanol and 1M NaOH as absorption solutions

Test	Hour-0		Hour-8	
	pH	Std. Dev.	pH	Std. Dev.
Methanol as absorption solution	5.47	0.00	10.20	0.26
1M NaOH as absorption solution	5.48	0.00	10.57	0.15

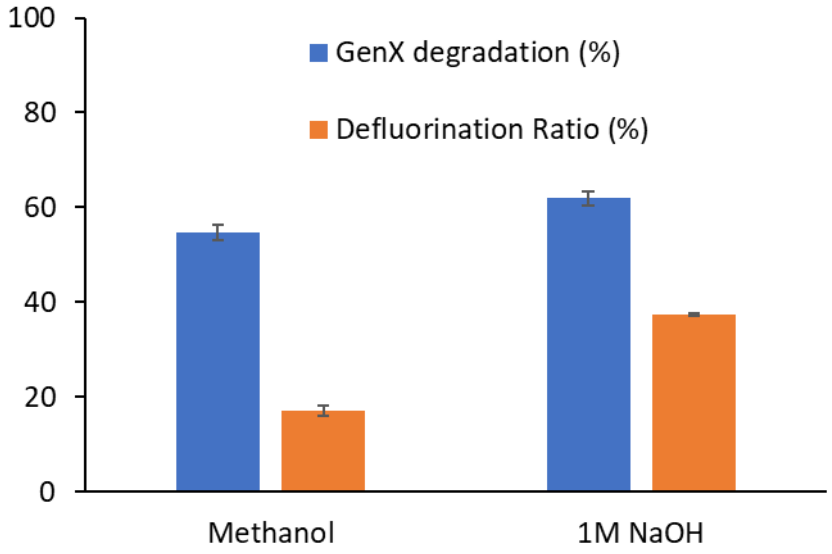

Fig. 3.14 GenX degradation and defluorination for batch studies carried out in BDD-iv type airtight batch reactor comparing methanol and 1M NaOH solutions as absorption solutions. Experiments were conducted in duplicates.

The mass balance based on PFAS and fluoride for the two test conditions is shown in Fig. 3.15. While around 14% of fluorine was captured as fluoride by the 1M NaOH absorption solution, no fluoride capture was observed in the methanol solution, indicating that 1M NaOH is better than methanol for capturing fluoride gases evolved during electrochemical mineralization of GenX. Meanwhile, around 14% fluorine as GenX was captured by the methanol absorption solution, while 7% was captured by the 1M NaOH absorption solution, suggesting that methanol is better than 1M NaOH for GenX capture. Overall, 1M NaOH as the absorption solution achieved a higher fluorine mass balance than methanol (61% vs. 54%). The lower GenX degradation observed when methanol was used as the absorption solution is because methanol is better at capturing GenX than the 1M NaOH as shown by Fig. 3.15. Meanwhile, the higher fluoride capture and lower GenX capture by the 1M NaOH solution than methanol resulted in a higher defluorination ratio when 1M NaOH was used as the absorption solution.

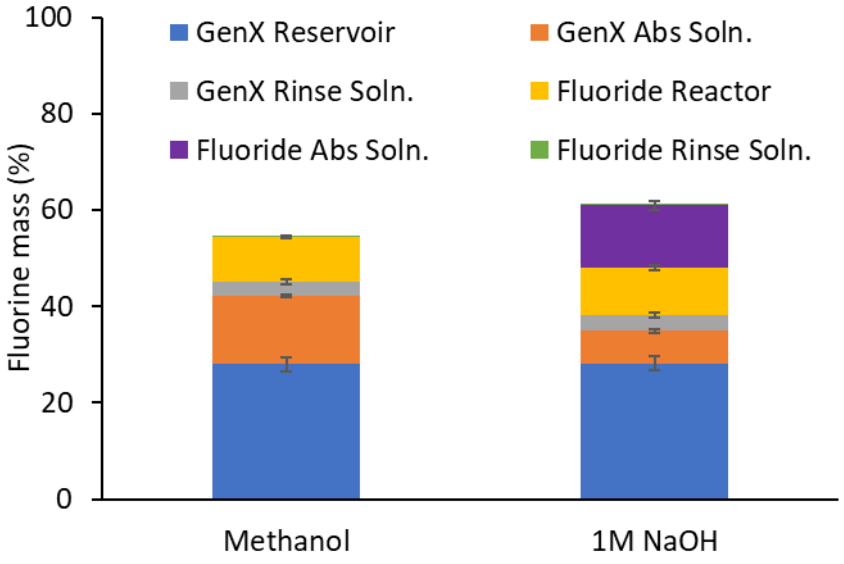

Fig. 3.15 Fluorine mass balance based on PFAS and fluoride achieved for batch studies carried out in BDD-iv type airtight batch reactor comparing methanol and 1M NaOH solutions as absorption solutions. Experiments were conducted in duplicates.

Fluorine mass balance based on AOF and fluoride is shown in Fig. 3.16. In contrast to mass balance based on PFAS and fluoride, the higher fluorine mass balance based on AOF and fluoride was achieved when methanol was used as the absorption solution (73%) than when the 1M NaOH was used (68%). Such results are because a large portion of fluorine was present in unidentified PFAS intermediates and was better captured by methanol (25%) than 1M NaOH (5%). The amount of these organic PFAS intermediates was so large that even though methanol did not capture any fluoride while the 1M NaOH captured around 14% fluoride, the methanol solution still achieved a higher overall fluorine mass balance.

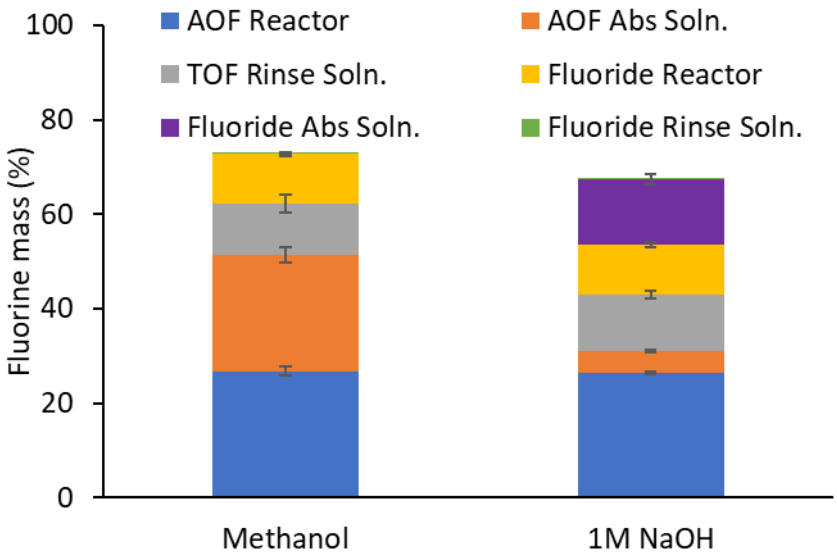

Fig. 3.16 Fluorine mass balance based on AOF and fluoride achieved for batch studies carried out in BDD-iv type airtight batch reactor comparing methanol and 1M NaOH solutions as absorption solutions. Experiments were conducted in duplicates.

Overall, methanol is better at capturing organic fluorine transported from the reactor as aerosol-based PFAS, while the 1M NaOH is better at capturing fluoride gases generated during electrochemical mineralization. Hence to achieve simultaneous high fluoride and organic fluorine capture, the 1M NaOH and methanol should be used in series as absorption solutions. The 1M

NaOH solution will be able to capture fluoride and some organic fluorine, and the organic fluorine not captured by the 1M NaOH will be captured by methanol. Theoretically, if 1M NaOH and methanol was used in series as the absorption solution for the batch study discussed above, a fluorine mass balance of 87% could have been achieved.

3.4.2.3 Effect of shaker speed on electrochemical mineralization of GenX

The effect of shaker speed at 150 rpm and 200 rpm were compared at 20 mA/cm^2, using 1M NaOH as the absorption solution. The variation of pH during the two tests is given in Table 3.7. No significant difference in pH variation was observed between the two tests, with the final pH for both tests around 10.5.

Fig. 3.17 shows GenX degradation and defluorination ratio for the electrochemical tests carried out at the two shaker speeds. Slightly less GenX degradation was observed at 200 rpm; however, the difference is not significant. Similar observations can be made in Fig. 3.18 which shows the mass balance based on PFAS and fluoride Even though there is a slightly better fluorine mass balance at 200 rpm, the difference is not significant.

Table 3. 7 pH variation observed during electrochemical mineralization of GenX in BDD-IV type airtight batch reactor operated at different shaker speeds

Test	Hour-0		Hour-8	
	pH	Std. Dev.	pH	Std. Dev.
150 rpm	5.48	0.00	10.57	0.15
200 rpm	5.59	0.00	10.65	0.23

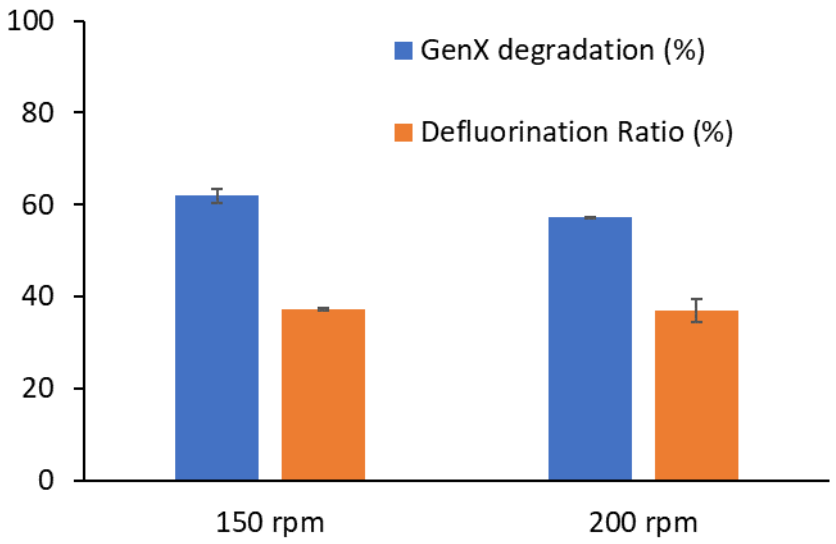

Fig. 3.17 GenX degradation and defluorination for batch studies carried out in BDD-iv type airtight batch reactor comparing 150 rpm and 200 rpm shaker speeds. Experiments were conducted in duplicates.

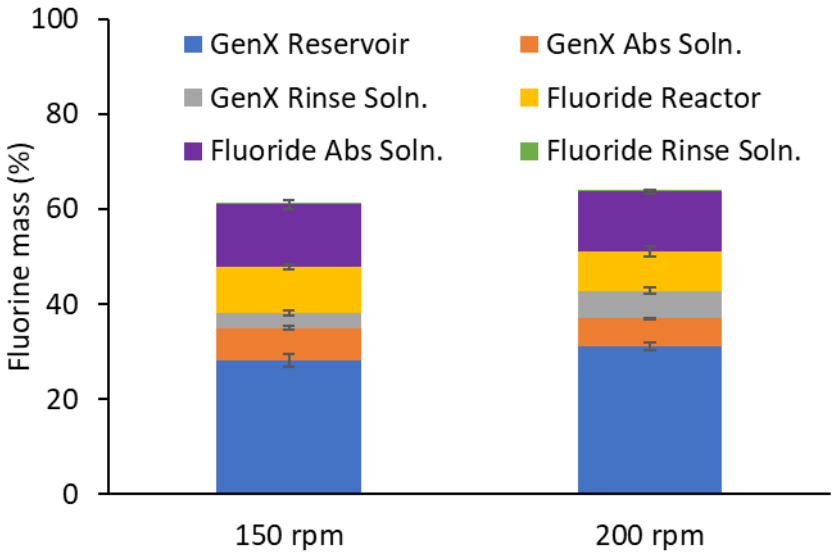

Fig. 3.18 Fluorine mass balance based on PFAS and fluoride achieved for batch studies carried out in BDD-iv type airtight batch reactor comparing 150 rpm and 200 rpm shaker speeds. Experiments were conducted in duplicates.

The fluorine mass balance based on AOF and fluoride is shown in Fig. 3.19. No significant difference was observed between the fluorine mass balance achieved at the two shaker speeds. At

both shaker speeds, around 68% fluorine mass balance was achieved. The results indicate that changing shaker speeds did not significantly affect the electrochemical mineralization of GenX.

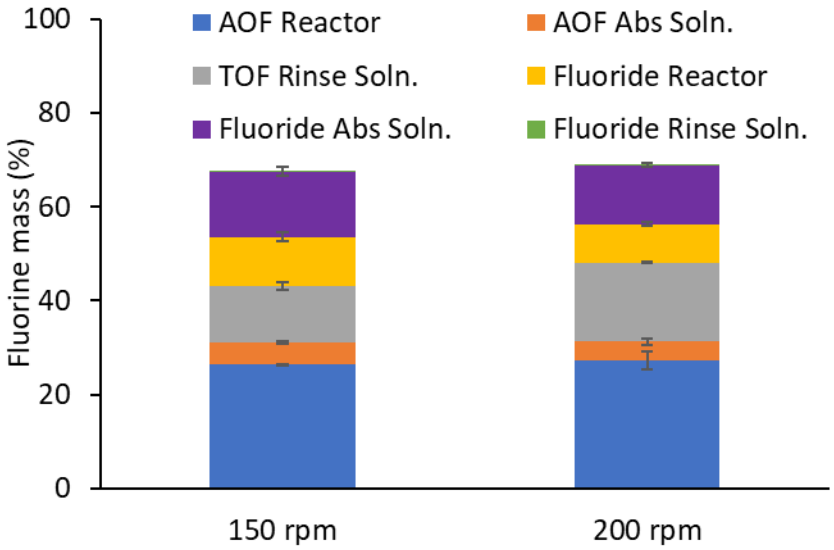

Fig. 3.19 Fluorine mass balance based on AOF and fluoride for batch studies carried out in BDD-iv type airtight batch reactor comparing 150 rpm and 200 rpm shaker speeds. Experiments were conducted in duplicates.

3.4.3 Comparison of batch reactor and continuous reactor with recirculation

This section compares the effectiveness of batch reactors and continuous reactors with recirculation for electrochemical mineralization of GenX. Continuous reactor with recirculation was designed to minimize organic fluorine carried over by gases evolved in electrochemical side reactions to the absorption solution. The reservoir added to this reactor design reintroduces this portion of organic fluorine to the liquid phase and circulates it back to the reactor. The test conditions used for each reactor are given in Table 3.8. The continuous reactor had a higher volume thus a lower anode area to volume ratio. Both tests were carried out at 20 mA/cm^2 and used methanol as the absorption solution.

Table 3. 8 Test conditions used for electrochemical mineralization of GenX using batch reactor and continuous reactor with recirculation

Test	Reactor model	Sample volume (mL)	Anode area/sample volume ratio (cm^2/mL)	Current density (mA/cm^2)	Absorption Solution
Batch reactor	BDD-IV	30	0.59	20	Methanol
Continuous reactor with recirculation	BDD-Continuous with recirculation	55	0.36	20	Methanol

GenX degradation and defluorination ratio achieved during electrochemical mineralization of GenX in both reactor types are given in Fig. 3.20. Both reactor types achieved a similar defluorination ratio. However, the continuous reactors with recirculation achieved a higher GenX degradation of 65% compared to the batch reactors (55%), because aerosol-based GenX loss was captured by the reservoir and reintroduced to the reactor solution for electrochemical degradation.

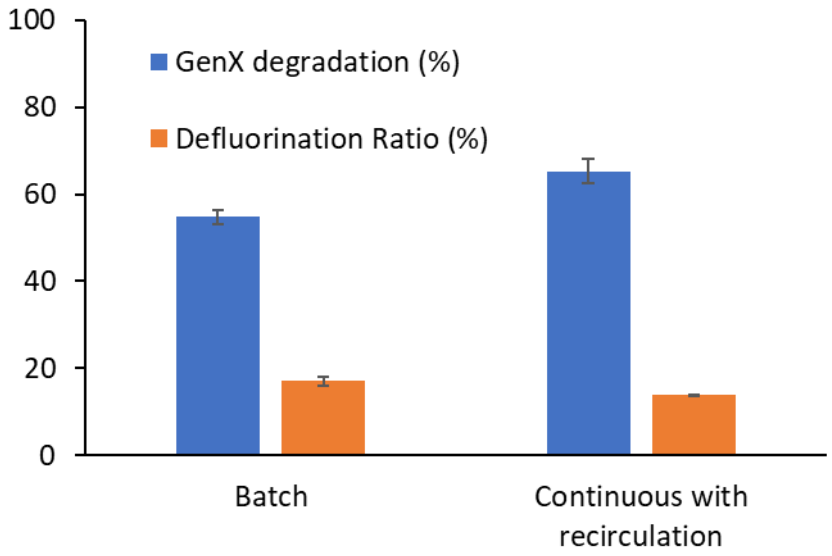

Fig. 3.20 GenX degradation and defluorination ratio achieved by batch reactor and continuous reactor with recirculation during electrochemical mineralization of GenX at 20 $mA/cm^{2.}$ Experiments were conducted in duplicates.

In contrast, GenX in the aerosol form generated in the batch reactor was transported directly to the absorption solution and became unavailable for further degradation. It should also be noted that the continuous reactors achieved a higher GenX degradation even though they had to treat a higher sample volume compared to the batch reactors at the same current density. Hence, the continuous reactors with recirculation are considered superior to the batch reactors for electrochemical mineralization of GenX.

Fig. 3.21 shows the fluorine mass balance based on PFAS and fluoride. The test in batch reactors achieved around 55% fluorine mass balance, whereas the continuous reactors with recirculation achieved 44%. Since PFAS other than GenX were not detected, it is not possible to confirm the best reactor configuration based on just this result. Around 14% GenX was detected in the absorption solution of the batch reactors.

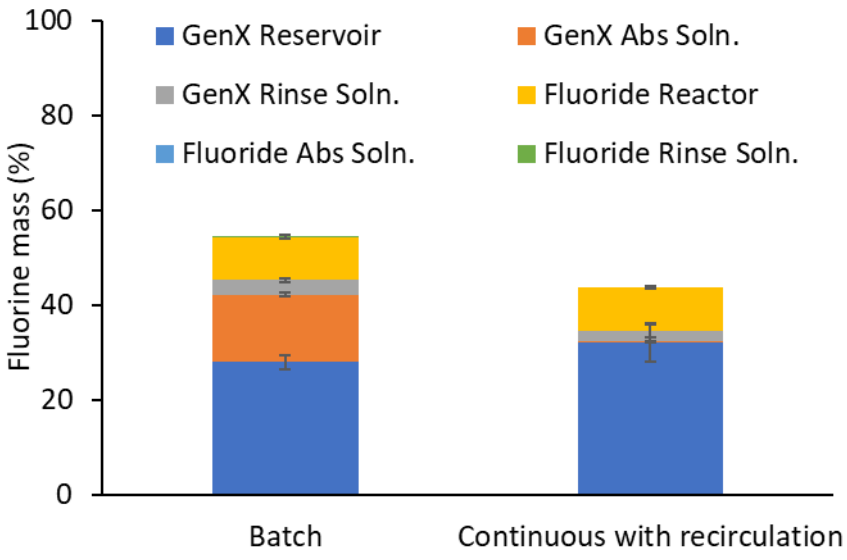

Fig. 3.21 Fluorine mass balance based on PFAS and fluoride achieved by batch reactor and continuous reactor with recirculation for electrochemical mineralization of GenX at 20 mA/cm$^{2.}$ Experiments were conducted in duplicates.

In contrast, no GenX was observed in the absorption solution of the continuous reactors with recirculation, indicating that the reservoir solution itself was sufficient to capture all the aerosol-based GenX transported from the reactor to the absorption solution. In that aspect, the continuous reactors with recirculation are advantageous over the batch reactors.

Fig. 3.22 shows mass balance based on AOF and fluoride achieved by the batch reactors and continuous reactors with recirculation. Organic fluorine in the absorption solution of the continuous reactors with recirculation (13%) was much less than that of the batch reactors (25%), further indicating the ability of the continuous reactors to capture aerosol-based organic fluorine in the reservoir solution and circulate it back to the reactor solution for further electrochemical degradation. Accordingly, more organic fluorine remained in the reactor solution of the continuous reactors with recirculation than the batch reactors. These results again suggest that the continuous reactors with recirculation are more effective than the batch reactors for electrochemical mineralization of GenX.

Batch reactor had a slightly better fluorine mass balance with 73% but continuous reactor was closely behind with 70%. The lower mass balance could be explained by the lower affinity of shorter chain PFAS intermediates towards the carbon used for AOF analysis compared to GenX. The sum organic fluorine in the whole reactor systems was also similar with batch reactor showing 62% while continuous reactor with recirculation showing 60%. Comparing these results with those shown in Fig. 3.20, one speculation is that some GenX was converted into certain unknown PFAS intermediates, which were recalcitrant to further mineralization even when they were reintroduced to the electrolytic reactors in the recirculation design.

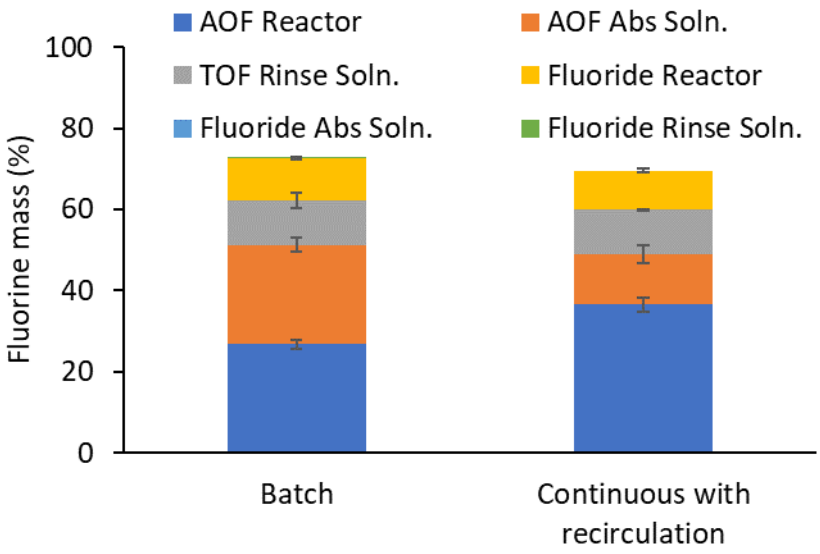

Fig. 3.22 Fluorine mass balance based on AOF and fluoride achieved by batch reactor and continuous reactor with recirculation for electrochemical mineralization of GenX at 20 mA/^{cm2}. Experiments were conducted in duplicates.

3.5 Conclusions

- Optimum current density for electrochemical mineralization of GenX was found to be 20 mA/cm^2
- Compared to the airtight batch reactor, the use of continuous reactor with recirculation reduced the aerosol-based transport of organic fluorine to the absorption solution from 25% to 13%
- Absence of GenX and presence of organic fluorine in the absorption solution confirmed the presence of potential unidentified PFAS as degradation byproducts
- Continuous reactor with recirculation was able to achieve higher GenX degradation (65%) compared to airtight batch reactor (55%) even when treating a larger volume using lower anode area.

- GenX degradation (65%) achieved during electrochemical oxidation at at 20 mA/cm^2 is lower compared to PFOA degradation (80%) at 10 mA/cm^2, indicating that GenX is more recalcitrant to electrochemical oxidation than PFOA
- Around 70% fluorine mass balance was achieved in both continuous reactor with recirculation and BDD-III airtight batch reactor
- Recirculating aerosol-based GenX back to the reactor solution helped achieve higher GenX degradation
- Methanol is best for capturing organic fluorine, while 1M NaOH is best for capturing HF gases
- Increasing shaker speed from 150 rpm to 200 rpm did not have a significant effect on GenX degradation or mass balance

4. Electrochemical mineralization of PFAS in AFFF Waste Streams from Firefighting Practice

4.1 Literature review

One of the major applications of PFAS is in aqueous film-forming foams (AFFF) for firefighting. AFFF is a complex mixture of known and unidentified PFAS together with other ingredients (Mueller and Yingling 2017, 2018; USEPA 2017a). AFFF are of three types: legacy PFOS, legacy fluorotelomer, and modern fluorotelomer AFFF. Legacy PFOS AFFF consists of PFOS and precursors that breakdown into PFOS, legacy fluorotelomer AFFF consists of precursors that breakdown into PFOA and other perfluorinated carboxylic acids, and modern fluorotelomer AFFF consists of precursors that breakdown into short-chain PFAS and do not contain perfluorohexanoic acid (PFHxA), PFOS, PFOA or any other long-chain PFAS (Mueller and Yingling 2018). In 2004, the total inventory of AFFF in the US was around 9.9 million gallons, out of which 4.6 million gallons were PFOS-based (Darwin 2004), and 2 million gallons of PFOS-based AFFF remains in the US (Darwin 2011)

AFFF application in firefighting areas like Air Force bases is a significant point source of PFAS contamination in soil and groundwater. There are around 420 facilities under the US Department of Defense with known or suspected release of PFOS or PFOA due to AFFF application. The runoff from such firefighting training areas contaminates nearby soil and groundwater (Houtz et al. 2013; Moody and Field 1999). Previous studies on AFFF contaminated groundwater at Air Force bases across the US found various PFAS at concentrations ranging from 2.8 ng/L to 7090 ug/L (Backe et al. 2013; Houtz et al. 2013; Moody et al. 2003; Moody and Field 2000). There have been cases where drinking water wells were shut down due to AFFF contamination from firefighting training areas (Dauchy et al. 2017b; Department of Defense 2017).

While there are studies on electrochemical degradation of PFAS in AFFF impacted groundwater with PFAS concentrations in the range of 0.7-300 µg/L (Schaefer et al. 2015a, 2018; Trautmann et al. 2015), no studies are available on treating the more concentrated AFFF waste streams from the firefighting training areas. Collecting and treating AFFF waste streams at their sources has three benefits:

(i) It prevents soil and groundwater contamination

(ii) It reduces the quantity of water to be treated

(iii) Electrochemical degradation is more efficient at higher PFAS concentration in waste streams than in groundwater.

Hence, the objective of this study is to explore the effectiveness of electrochemical treatment in mineralizing simulated AFFF waste streams from firefighting practice.

4.2 Study overview

4.2.1 Task: Evaluate electrochemical mineralization of two AFFF solutions at 20 mA/cm^2

Electrochemical mineralization of two AFFF solutions was carried out at 20 mA/cm^2. This current density was selected based on the results of the GenX electrochemical mineralization study. However, since the AFFF formulas are typically proprietary, and the electrochemical degradation pathways for different PFAS have not been completely revealed, a large portion of PFAS involved in the electrochemical treatment may be unidentified species not captured in the traditional targeted analysis by LC-MS/MS. Thus, additional analytical tools are needed to determine the extent of AFFF degradation.

The total oxidable precursor (TOP) assay measures the amount of PFAA precursors in a sample. TOP assay uses heat activated persulfate at elevated pH to generate hydroxyl radicals that transforms PFAA precursors to PFCA which can be quantified by targeted analysis. Comparing concentration of PFCA before and after the persulfate treatment, PFAA precursors can be quantified (Houtz and Sedlak 2012). The AFFF solutions before and after electrochemical treatment were analyzed using both targeted and TOP assay analysis to reflect the degradation of both PFAA and their precursors.

Fluorine mass balance of the AFFF solution before and after treatment will be examined by AOF analysis, TOP assay, intermediates (short-chain PFAS with available standards), and mineralization products (fluoride). Two types of mass balances were made, one using TOP assay and fluoride, and the other using AOF and fluoride.

Hypothesis: The electrochemical treatment will transform the unknown precursors to PFAA, and some PFAA to fluoride with unknown intermediates. AOF analysis and the TOP assay will give a more comprehensive fluorine mass balance assessment by incorporating unknown PFAA precursors and degradation intermediates. A more thorough assessment of whether electrochemical treatment can achieve mineralization and risk reduction will be possible with the mass balance available.

4.3 Materials and Methods

AFFF samples: Two AFFF concentrates, FireAde and Williams T-STORM 703LV (T-Storm), were obtained from Denver Fire Department, North Carolina. The organic fluorine concentration of FireAde and T-Storm concentrates was determined by TOF analysis in our lab and reported in a previous publication (Han et al. 2021).

Water Matrix: All electrochemical experiments were conducted in AFFF solutions diluted around 1000 times with ultrapure water to achieve an organic fluorine content of 1 mg/L to represent concentrations in AFFF waste streams. As a supporting electrolyte, sodium sulfate was added to the diluted AFFF solutions to achieve a concentration of 0.01M.

Reactors: Electrochemical mineralization of AFFF was studied in the BDD-IV reactors equipped with BDD anode and cathode, the same setup used for the batch study on electrochemical mineralization of GenX. The schematic diagram and the actual reactor setup are given in Fig. 3.4 and Fig. 3.5, respectively. Each reactor contained 30 mL AFFF solutions, and the absorption solution was 10 mL 1M NaOH solution.

Analytical methods: Analysis of PFAA, fluoride, AOF, and pH were the same as described in Section 2.5. TOP assay to quantify PFAA precursors was carried out following the procedure in a previous study (Houtz and Sedlak 2012). Additional PFAS were included in the LC-MS/MS analysis and are detailed below.

Information on mobile phase gradient and other detailed LC-MS/MS parameters are given in Table 2.3 and Table 2.4 of Chapter 2 and Table 4.1. The initial condition was 10% B and a constant flow rate of 0.5 mL/min was used. Table 2.3 and Table 2.4 in Chapter 2.

Table 4.1 Detailed instrument parameters of PFAS and their internal standards during mass spectrometry

Compound	Precursor ion (m/z)	Product ion 1 (m/z)	Product ion 2 (m/z)	Dwell	Fragmentor volt (V)	Collision Energy-1 (V)	Collison Energy-2 (V)
PFBA	212.98	169	n.a	5	83	4	n.a
PFPeA	263.97	219	n.a	5	83	4	n.a
PFBS	298.94	99	80	5	73	36	40
PFHxA	312.97	269	118.9	5	83	4	20
4:2 FTS	326.97	306.9	80.8	5	73	20	32
PFPeS	348.94	98.9	80	5	84	40	48
PFHpA	362.97	319	169	5	88	4	20
PFHxS	398.93	99	80	5	84	40	52
PFOA	412.96	369	169	5	88	8	20
PFHpS	448.93	98.9	79.9	5	84	48	52
PFOS	498.93	99.1	79.9	5	50	48	68
PFNA	462.96	419	219	5	88	8	16
PFDA	512.96	469	269	5	98	8	16
MPFBA (IS[a])	216.99	172	n.a	5	64	4	n.a

Compound	Precursor ion (m/z)	Product ion 1 (m/z)	Product ion 2 (m/z)	Dwell	Fragmentor volt (V)	Collision Energy-1 (V)	Collison Energy-2 (V)
M3PFBS (IS[a])	301.99	98.9	80	5	73	32	36
M5PFHxA (IS[a])	317.99	273	n.a	5	78	4	n.a
M2 4:3FTS (IS[a])	328.99	308.9	80.9	5	107	24	32
M4PFHpA (IS[a])	366.99	322	169	5	88	8	16
M3PFHxS (IS[a])	401.99	99	80	5	190	40	56
MPFOA (IS[a])	420.99	376	172	5	83	8	20
MPFOS (IS[a])	506.99	99	80	5	84	52	56
MPFNA (IS[a])	471.99	427	223	5	93	8	16
MPFDA (IS[a])	518.99	474	270	5	103	8	20

Sulfuric Acid Treatment of BDD electrodes

After each electrochemical mineralization experiment, BDD electrodes underwent sulfuric acid treatment to prevent surface fluorination. The procedure for sulfuric acid treatment is discussed under reactors in Section 2.3.

4.4 Results & Discussion

4.4.1 pH Results

The change in pH after 8 hours of electrochemical mineralization is given in Table 4.2. Both FireAde and T-Storm had a similar starting pH around 5.5. After 8 hours of treatment, the pH rose to around 11 for the two AFFF formulations. Like what was observed during electrochemical mineralization of PFOA and GenX using BDD anode, the increase in pH observed might be due to the reduction reaction of water molecules to hydrogen gas and hydroxide ions dominating.

Table 4.2 pH variation observed during electrochemical mineralization of AFFF solutions FireAde and T-Storm in BDD-IV type airtight batch reactors at 20 mA/cm^2

Test	Hour-0		Hour-8	
	pH	Std. Dev.	pH	Std. Dev.
FireAde	5.57	0.00	11.13	0.34
T-Storm	5.48	0.00	11.19	0.24

4.4.2 Variation of voltage

The variation in voltage observed during the electrochemical treatment of AFFF formulations FireAde and T-Storm is given in Fig. 4.1. The two AFFF formulations showed a similar trend in voltage variation. At the applied current density of 20 mA/cm^2, voltage for both tests started around

7 V. A slight decrease in voltage was observed during the initial hours, indicating an increase in ionic strength which reduced the resistance of the treated solution.

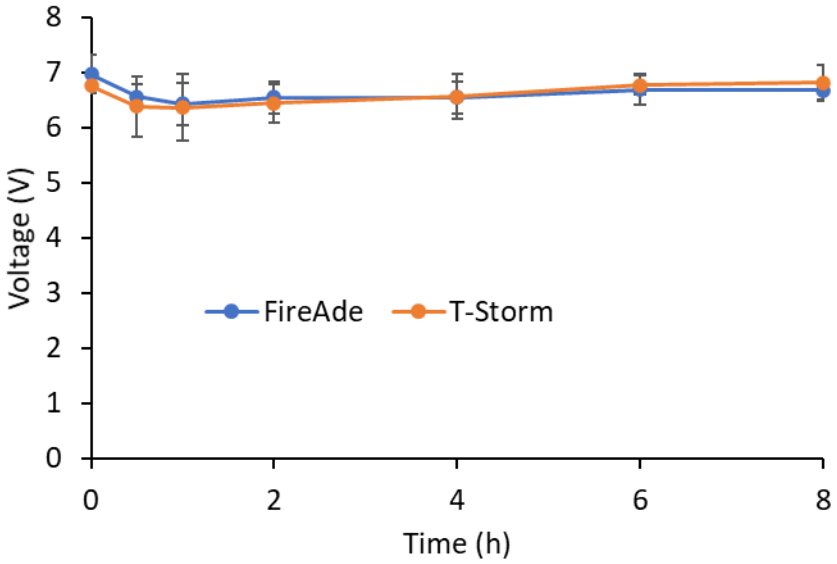

Fig. 4.1 Variation in voltage observed during electrochemical mineralization of AFFF solutions, FireAde and T-Storm in BDD-IV airtight batch reactors at 20 mA/cm^2

4.4.3 Variation of PFAS compositions and concentrations over time

PFBA, PFPeA, PFHxA and PFHpA were detected in the samples collected at different time points during the electrochemical mineralization of the FireAde solution (Fig. 4.2). Before the electrochemical treatment (t=0), none of the PFAS listed in Table 4.1 were detected. After 0.5 hour, PFBA and PFHxA were detected followed by detection of PFPeA and PFHpA. PFHxA had the highest concentration of any detected PFAS at 30 µg/L in sample taken at four hours. The production of these perfluoroalkyl carboxylic acids (PFCA) indicates that PFAS precursors present in the FireAde solution got degraded during electrochemical mineralization. The highest concentration of PFBA was detected after 1 hour and completely disappeared after 4 hours. Similar, PFPeA was produced then degraded in the 8-hour test. This suggests that sources of PFBA

and PFPeA declined resulting in the degradation rate of PFBA and PFPeA dominating their production. Meanwhile, the longer chain PFHxA and PFHpA persisted in the system, suggesting their production from their precursors is faster than their degradation. The comparatively stable PFHxA concentration implies either the production and degradation rate were similar or that further degradation or production of PFHxA did not occur.

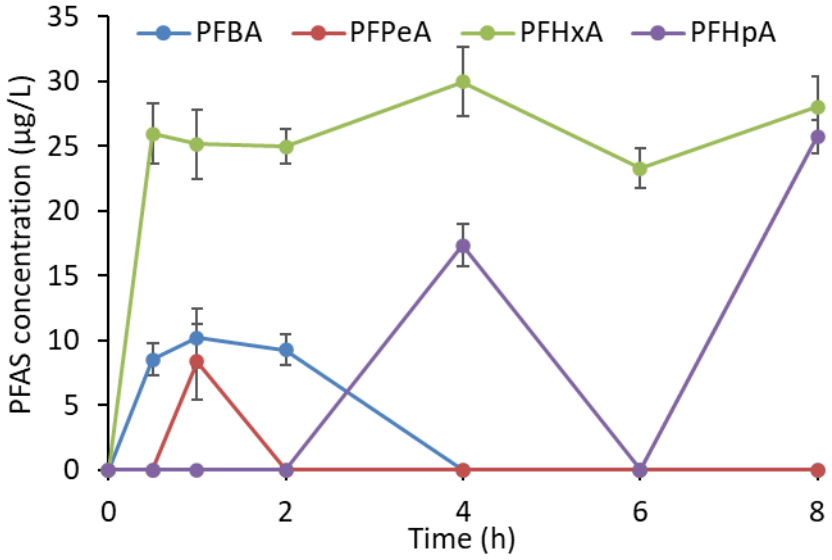

Fig. 4.2 PFAS detected and their variation over time during electrochemical mineralization of FireAde solution in BDD-IV airtight batch reactors at 20 mA/cm^2

PFBA, PFHxA, PFHpA, and PFOA were detected during electrochemical mineralization of the T-Storm solution (Fig. 4.3). The different speciation of PFAA detected during electrochemical mineralization of the T-Storm solution from the FireAde solution (detection of PFOA instead of PFPeA) suggests these two formulas have different compositions. PFHpA had the highest concentration of any detected PFAS at 27 µg/L at eight hours. Similar to electrochemical mineralization of the FireAde solution, PFBA was produced early during the test then removed from the system. A comparable trend was also seen for PFHxA which remained at relatively stable concentration throughout the reaction period (Fig. 4.3). PFHpA showed a linear trend of

production indicating the steady degradation of the precursors that breakdown into PFHpA. PFOA was detected only in the final sample taken at the end of the reaction period indicating that the precursor of PFOA was much more recalcitrant to precursors of other PFAA generated.

4.4.4 PFAA precursor degradation

TOP assay converts PFAA precursors to PFCA using hydroxyl radicals generated by heat-activated persulfate at basic conditions. Therefore, comparing PFAA concentrations in the same sample before and after TOP assay treatment provides indirect information on the quantity of PFAA precursors with unknown structures. Here, TOP assay was used to analyze AFFF solutions before and after electrochemical degradation to assess the total amount of PFAS degraded during electrochemical treatment, counting both PFAA and their precursors.

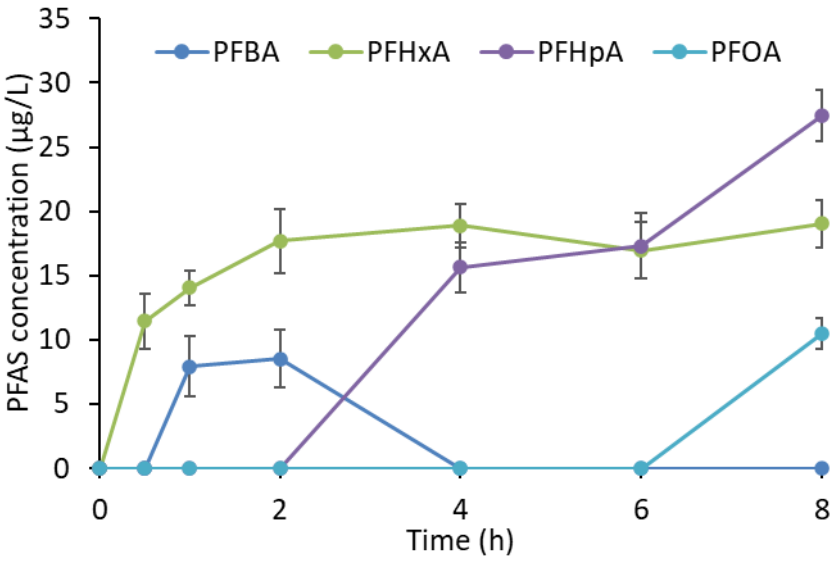

Fig. 4.3 PFAS detected and their variation over time during electrochemical mineralization of T-Storm solution in BDD-IV airtight batch reactors at 20 mA/cm^2

Fig 4.4 shows the targeted and TOP assay results of the initial sample and the samples collected after 8 hours of electrochemical mineralization of the FireAde solution at 20 mA/cm^2. While no

PFCA were detected during targeted analysis in the initial samples, after TOP analysis, PFBA, PFPeA, and PFHxA were detected at concentrations 110, 185, and 345 µg/L, respectively. The appearance of PFCA after TOP assay confirms the presence of PFAA precursors in the FireAde formula.

After 8 hours, targeted analysis identified the presence of PFHxA and PFHpA at 28 and 26 µg/L, respectively. The TOP assay of the same samples detected PFBA, PFPeA, PFHxA, and PFHpA at 26, 43, 116, and 69 µg/L, respectively.

It is interesting to note that PFHpA was detected in the after-treatment sample during targeted analysis and at a higher concentration in the TOP assay. However, PFHpA was not detected during the targeted and TOP assay anlaysis of the before-treatment sample. Three conclusions can be drawn from this observation. The first conlusion is that there was at least one PFAS intermediate between the degradation of PFHpA precursor to form PFHpA. During electrochemical mineralization, the PFHpA precursor degraded to an intermediate PFAS and then to PFHpA. The second conclusion is that TOP assay is unable to oxidize the PFHpA precursor but it could oxidize the PFAS intermediate. This is supported by the absence of PFHpA in the TOP assay of the before-treatment sample and the increased PFHpA concentration detected during TOP assay compared to targeted anlaysis of the after-treatment sample. The third conclusion that can be drawn is that electrochemical mineralization is able to degrade both PFHpA precursor and the PFAS intermediates, supported by the detection of PFHpA in the targeted analysis of the after-treatment sample. Another possibility is that the PFHpA precursor is not oxidizable but reducable during electrochemical treatment forming the PFAS intermediate which is oxidizable to PFHpA.

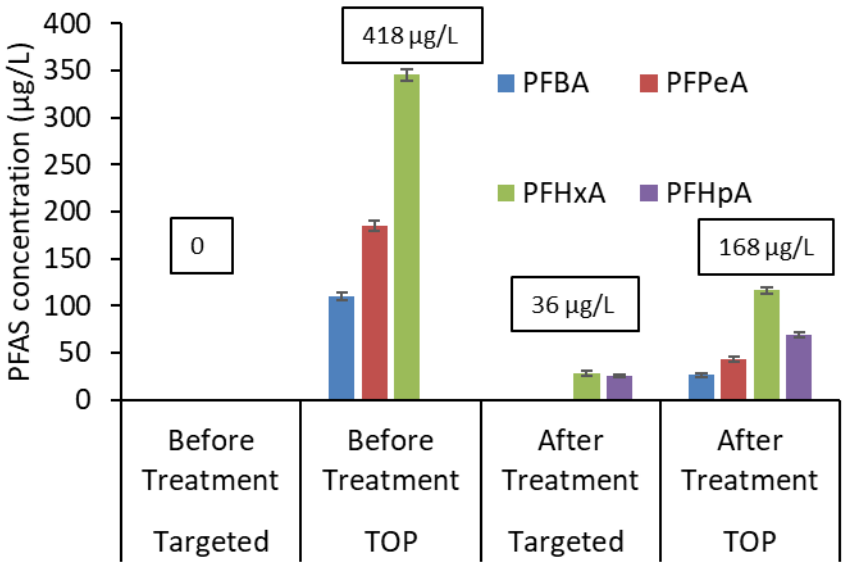

Fig. 4.4 Comparison of Targeted and TOP assay results of reactor samples collected time t=0 and t=8 h during electrochemical mineralization of FireAde solution in BDD-IV airtight batch reactors at 20 mA/cm^2. Values given in the box represent sum fluorine concentration. Experiments were conducted in duplicates.

The absence of PFBA and PFPeA in the targeted analysis while their presence in the TOP assay of after-treatment sample implies that the degradation rate of PFBA and PFPeA were at a higher rate during the electrochemical process than their generation from the degradation of their precursors. This observations further confirms the conclusions made from Fig. 4.2 regarding degradation rate of PFBA and PFPeA. The precursors of PFBA and PFPeA remaining at the end of the reaction period were oxidized during TOP assay resulting in the detection of these short chain PFCA in the TOP assay samples.

Comparing the TOP assay results of the FireAde solution before and after electrochemical mineralization in Fig. 4.4, it is clear that the concentrations of PFBA, PFPeA, and PFHxA reduced. The sum fluorine concentration from the PFAS detected after TOP assay in the initial FireAde solution was 418 µg/L, and it was reduced to 168 µg/L after 8 hours of treatment represented by the concentrations shown in rectangular boxes in Fig. 4.4. Hence there was an overall decrease in

organic fluorine concentration associated with PFAA precursors by 250 µg/L. This conclusion was made possible by the use of TOP assay, as the targeted anlaysis of the before treatment couldn't detect any PFAS and PFAS detected in after treatment sample was minimal.

The lower detection of organic fluorine associated with PFAA precursors cannot be seen as decrease in organic fluorine concentration as only PFAA precursors and PFAA are quantifiable by targeted analysis. It is possible that the PFAA precursors got degraded to unidentfied PFAS during the electrochemical process. This possibility is further supported by the low fluoride concentration of 27 µg/L detected in the reactor solution at the end of the reaction period.

The comparison of targeted and TOP assay analysis of the before and after electrochemical treatment of T-Storm solution is given in Fig. 4.5. Like the observations made during the electrochemical degradation of PFAS in FireAde solution, PFBA and PFPeA were not detected during the targeted analysis of after-treatment sample, however, were present in TOP assay sample. This indicates that the degradation rate of PFBA and PFPeA were much greater than their precursors.

It is interesting to note that PFPeA was not detected during the targeted analysis of samples taken at different times during the electrochemical degradation process including sample taken at the end of the treatment (Fig. 4.3). However, PFPeA was detected in the TOP assay samples of both before and after treatment samples. This further confirms the high degradation rate of PFPeA compared to its precursor.

By comparing the TOP assay results before and after treatment, an overall decrease of 134 µg/L of organic fluorine associated with PFAA and its precursors was estimated. This decrease is just 53% of the decrease achieved in FireAde electrochemical degradation. This suggests that PFAA precursors in T-Storm are more recalcitrant to electrochemical degradation than those in FireAde

or that the other constituents present in T-Storm competed with PFAA precursors for electrochemical degradation. Similar to the FireAde, the lower fluoride generation of 30 µg/L compared to the 134 µg/L decrease in organic fluoride associated with PFAA and its precursors confirms the formation of unidentified PFAS during the electrochemical process.

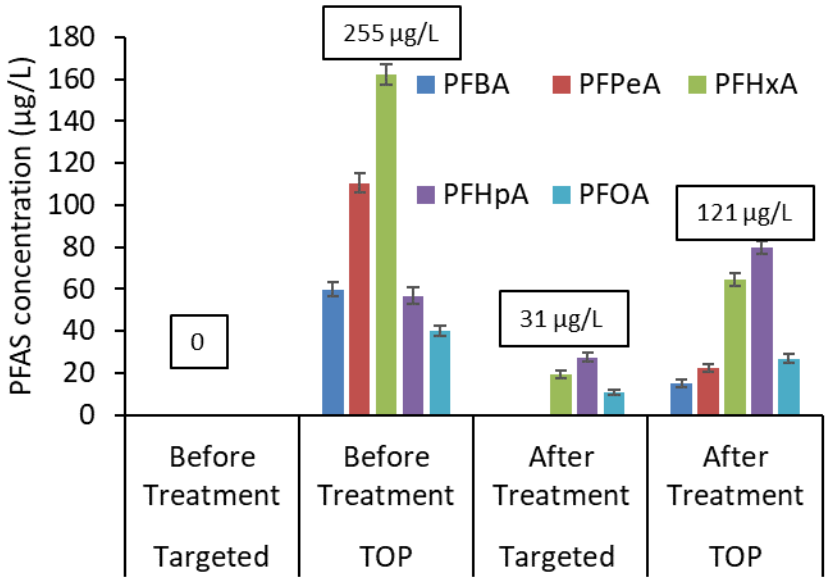

Fig. 4.5 Comparison of Targeted and TOP assay results of reactor samples collected time t=0 and t=8 h during electrochemical mineralization of T-Storm solution in BDD-IV airtight batch reactors at 20 mA/cm^2. The values given in the box represent sum fluorine concentration. Experiments were conducted in duplicates.

Five PFCA, namely PFBA, PFPeA, PFHxA, PFHpA, and PFOA were detected in the TOP assay samples. TOP assay of the sample before treatment had PFBA, PFPeA, PFHxA, PFHpA and PFOA concentrations at 60, 111, 162, 57, and 40 µg/L, respectively. The TOP assay concentrations of samples after treatment reduced to 15, 22, 65, 80, and 27 µg/L, respectively.

4.4.5 Fluorine mass balance based on PFAS and fluoride

Both FireAde and T-Storm were diluted around 1000 times to achieve an organic fluorine concentration of 1 mg/L before electrochemical treatment. Thus, PFAS and fluoride concentrations

were normalized to 1 mg/L to calculate the fluorine mass balance. In addition, since the AFFF formulas contain large amounts of PFAA precursors not captured by targeted analysis, fluorine mass balance was also assessed in samples after the TOP assay.

The mass balance of the FireAde solution based on PFAS and fluoride is given in Fig. 4.6. While no PFAS were detected in the initial solution, the same solution after TOP assay revealed 42% of the organic fluorine content. Note that the organic fluorine content was measured by combusting the AFFF formula and converting all PFAS to fluoride. The discrepancy of fluorine measure by TOP assay and total organic fluorine analysis suggests that the TOP assay did not account for all PFAS in the solution, since some PFAS are not PFAA precursors. After 8 hours of electrochemical treatment, the FireAde solution achieved a fluorine mass balance of 10.5% by targeted analysis and 24% by the TOP assay, with PFHxA as the dominant species in both TOP assay samples and the targeted analysis. The lower fluorine mass detected in the after-treatment TOP assay sample compared to before-treatment indicates the degradation of PFAA precursors and PFCA resulting in the lowering of their concentration.

Lower fluorine mass balance was achieved for the after-treatment sample compared to the before-treatment sample. This larger discrepancy of fluorine measure by TOP assay and total organic fluorine analysis after treatment may be attributed to the unknown PFAS intermediates formed during PFAA degradation. Fluoride in the solution after treatment accounted for only 2.7% (27 µg/L) of the initial fluorine mass, much lower than that observed when PFOA and GenX were treated with the same current density (10-33%). While the PFOA and GenX degradation tests were conducted at similar organic fluorine concentrations (1.03 mg F/L for PFOA and 0.95 mg F/L for GenX), the much lower fluoride production in the AFFF solution tests suggest that other components in AFFF (e.g., organic surfactants) competed with PFAS for electrochemical

treatment capacity and hindered PFAS mineralization. The other possibility is that the PFAS present in the AFFF formulations tested are recalcitrant to electrochemical treatment.

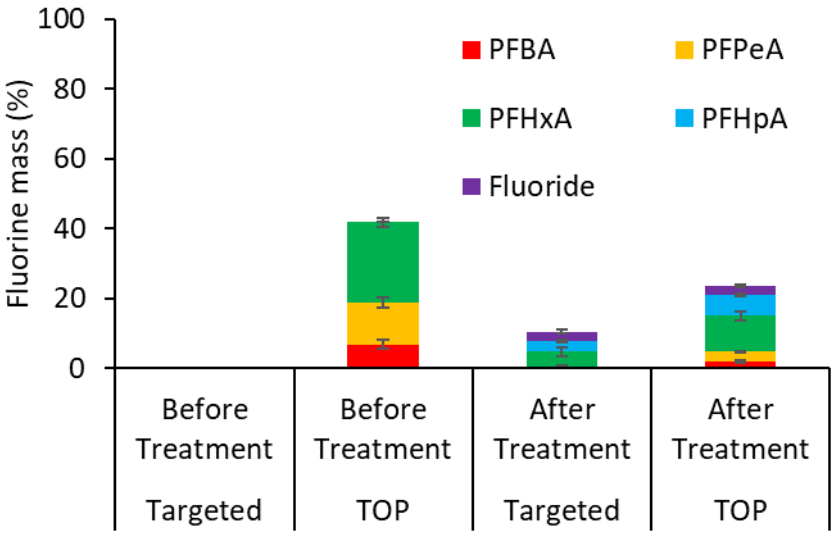

Fig. 4.6 Fluorine mass balance based on PFAS and fluoride targeted and TOP assay samples from electrochemical mineralization of FireAde solution in BDD-IV airtight batch reactors at 20 mA/cm^2. Experiments were conducted in duplicates.

Fig. 4.7 shows the mass balance of the T-Storm solution based on PFAS and fluoride. Unlike FireAde, PFOA was detected in the TOP assays and the targeted analysis of the solution after electrochemical mineralization. The TOP assay of the solution before and after electrochemical mineralization achieved a fluorine mass balance of 28% and 19%, respectively, again suggesting the formation of unknown PFAS intermediates during PFAA degradation.

Similar to the FireAde test results, the TOP assay provided better mass balance than targeted analysis for the same sample, and fluoride generated during the electrochemical treatment accounted for only 3% of the initial fluorine mass.

The lower fluorine mass detected in the T-Storm sample indicates that there were less PFAA precursors present in the T-Storm solution compared to FireAde. Comparison of the TOP assay

results of FireAde and T-Storm shows that quantifiable organic fluorine decreased from 42% to 21% for FireAde whereas T-Storm showed a decrease from 28% to 16%. Hence FireAde showed a decrease of 21% in quantifiable organic fluorine while T-Storm showed just 12%. The lower decrease in organic fluorine in T-Storm can be either due to the recalcitrance of PFAS present in the T-Storm formulation or due to other organic constituents present in T-Storm competing for electrochemical energy.

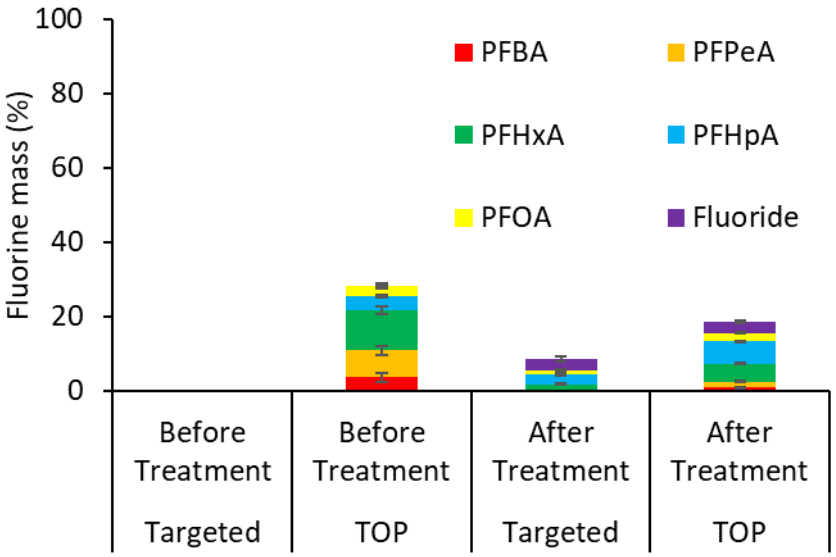

Fig. 4.7 Fluorine mass balance based on PFAS and fluoride in targeted and TOP assay samples from electrochemical mineralization of T-Storm solution in BDD-IV airtight batch reactors at 20 mA/cm^2. Experiments were conducted in duplicates.

4.4.6 Fluorine mass balance based on AOF and fluoride

The normalized AOF and fluoride based mass balance of before and after electrochemical treatment samples of FireAde and T-Storm is given in Fig. 4.8. The normalization was done based on the initial organic fluorine content of 1 mg/L of FireAde and T-Storm solutions due to poor recovery observed for the before treatment samples.

While the before-treatment samples of FireAde and T-Storm showed fluorine mass balance of 17% and 10% respectively, after-treatment samples showed a fluorine mass balance of 17% and 12% respectively. The poor fluorine mass balance observed for both FireAde and T-Storm solutions indicate that the PFAS present in both AFFF solutions had poor sorbability towards the carbon used for AOF analysis or that other organic constituents present in the AFFF formulations competed with PFAS for adsorption sites or both.

In the case of both AFFF formulations, the difference in fluorine mass between the before and after treatment samples were negligible. The comparison on just the AOF present in the reactor solution of FireAde and T-Storm shows a decrease of 86% and 82% respectively indicating that electrochemical degradation occurred. However, the distribution of fluorine mass balance between reactor solution, rinse solution and absorption solution give a clearer picture. Majority of the organic fluorine present in the after-treatment sample, around 7-10% of the initial fluorine mass, was seen in the rinse solution which underwent TOF analysis (Fig. 4.8). This is because, unlike AOF, TOF is not affected by hydrophobicity and type of charge of the PFAS compounds present. Hence TOF was able to quantify all the organic fluorine present in the sample whereas AOF had poor recovery due to the less sorbable nature of the PFAS present or due to other organic constituents competing for adsorption sites. Since the high salt concentration present in the AFFF solutions make it unfeasible for TOF analysis, the use of extractable organic fluorine (EOF) as described in Han et al. is recommended for a better fluorine mass balance (Han et al. 2021).

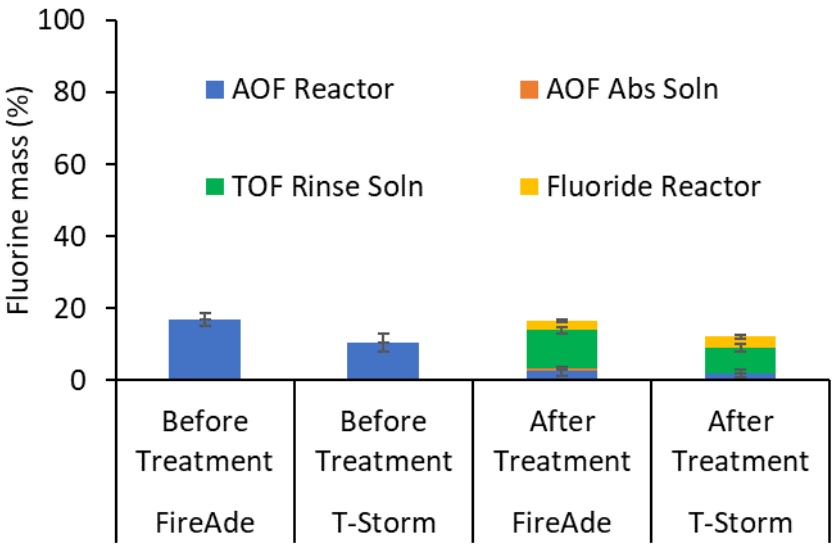

Fig. 4.8 Fluorine mass balance based on AOF and fluoride after treatment samples of electrochemical mineralization of FireAde and T-Storm solution in BDD-IV airtight batch reactors at 20 mA/cm^2. Experiments were conducted in duplicates.

The organic fluorine was detected only in the absorption solution of FireAde reactors that too in negligible amounts. For AFFF electrochemical study, 1M NaOH was used as the absorption solution with the aim to quantify fluoride accurately. However, as inferred from the batch studies comparing different absorption solutions during electrochemical mineralization of GenX, 1M NaOH is not effecient at organic fluorine capture. This could be the reason for the limited amount of organic fluorine in the absorption solution. Since no fluoride was detected in the absorption solution, use of methanol as the absorption solution would have been a better choice.

Comparing the two mass balances, one based on TOP assay and the other on AOF analysis, it can be observed that TOP assay based mass balance showed upto 42% and 28% respectively for FireAde and T-Storm whereas the AOF based mass balance showed upto just 17% and 12% respectively (Fig. 4.6, 4.7, 4.8). The results indicate the advantage of using TOP assay for mass balance of AFFF solutions over AOF based. This observation in contrast to what was observed

during elecrochemical study of GenX and PFOA is either due to the low sorbability of the PFAS present or due to the competion for adsorption sites from other organic constituents present in the AFFF formulations or both.

4.5 Conclusions

- Electrochemical process caused degradation of PFAA precursors
- The degradation rate of PFBA and PFPeA dominated their production rate as the electrochemical treatment progressed, however for PFHxA both rates were similar while for PFHpA the production rate was higher than the degradation rate
- The presence of PFOA during electrochemical mineralization of T-Storm solution while its absence in FireAde degradation indicates the different composition of the two AFFF formulations
- There is at least one PFAS intermediate between PFHpA and its precursor during electrochemical degradation of FireAde solution proven by the absence of PFHpA in the before-treatment TOP sample while its present in the targeted and TOP assay results of after-treatment samples
- Unknown PFAS were formed during electrochemical degradation of FireAde and T-Storm solution shown by the large discrepancy between fluorine mass balance between before and after treatment samples
- Around 3% fluoride generation was observed during the electrochemical mineralization of FireAde and T-Storm solutions

- The low fluoride generation can be attributed to the recalcitrance of PFAS present in the AFFF formulations or to the competition from other organic constituents present in the AFFF formulations for electrochemical energy
- PFAA precursors present in T-Storm is more recalcitrant to electrochemical degradation as indicated by the lower PFAA precursor degradation observed compared to FireAde. The other possibility is that the other organic constituents present in the T-Storm formulation posed a greater competition for electrochemical energy compared to those in FireAde
- TOP assay based fluorine mass balance achieved upto 42% and 28% for FireAde and T-Storm respectively. Whereas AOF based fluorine mass balance attained just 17% and 2% for FireAde and T-Storm respectively. Hence TOP assay based mass balance was superior to AOF based for the AFFF formulations tested
- Poor AOF based mass balance for AFFF formulations tested is attributed to the less sorbability of PFAS present or due to competition from other organic constituents for adsorption sites resulting in poor PFAS recovery

5. Conclusion

5.1 Overall conclusions

i. Aerosol-based PFOA losses can be significant during electrochemical degradation and might lead to over-estimation of PFOA degradation efficiency. Many previous studies have shown high PFAS degradation but not complete fluorine mass balance. The missing fluorine might be PFOA escaping as aerosol-based losses. If that is the case, the high PFOA degradation reported by those studies might be overestimated

ii. Fluorine mass balance based on AOF is superior to PFAS based due to the formers ability to quantify unknown PFAS

iii. Capturing and recirculating aerosol-based PFAS will significantly improve PFAS degradation as shown by the study comparing electrochemical mineralization of GenX using continuous reactor with recirculation and airtight batch reactor

iv. GenX is more recalcitrant to electrochemical oxidation than PFOA as shown by the higher PFOA degradation achieved at lower current density compared to GenX

v. The ideal absorption solution will be 1M NaOH in series with methanol. Use of 1M NaOH ensures maximum fluoride capture while methanol maximizes organic fluorine capture

vi. Since AFFF formulations contain PFAA precursors, incorporating TOP assay into electrochemical mineralization of AFFF formulations could give a clearer picture on organic fluorine remaining in the solution compared to fluorine mass balance based on AOF or targeted PFAS

vii. Electrochemical degradation of AFFF formulations performed poorly compared to PFOA and GenX due to competition from other organic components present in the AFFF formulations or the recalcitrance of the PFAS present

5.2 Novel contributions

- Demonstrated that AOF based fluorine mass balance could provide better fluorine mass balance compared to PFAS based which uses targeted analysis and requires standards to be available for quantification.
- Confirmed the presence and quantified the amount of organic fluorine related to unknown PFAS as potential degradation byproducts generated during electrochemical oxidation of PFAS
- Confirmed the aerosol-based transport of organic fluorine during electrochemical oxidation by capturing and quantifying PFAS and degradation byproducts in absorption solution and quantifying it using targeted and AOF analysis
- Demonstrated the advantage of using continuous reactor with recirculation for electrochemical oxidation of PFAS by achieving significantly higher PFAS degradation compared to completely mixed reactors
- Demonstrated that methanol is best as absorption solution for organic fluorine capture while 1M NaOH solution is best for fluoride capture

5.3 Environmental Implications

Destructive technologies are gaining attention as a permanent solution for remediating PFAS contamination in surface and groundwater. However, the low efficiency of destructive treatments

at environmentally relevant PFAS concentrations and the failure to attain complete fluorine mass balance during PFAS degradation make it is hard to justify the safety and practicality of such treatment practices. This thesis will be a milestone in scientific understanding of the electrochemical oxidation of PFOA, GenX and PFASs in AFFF. The knowledge from this research serves as a guide for future electrochemical research by providing optimal reactor design and suitable analyses. Particularly, results from this study demonstrated the significance of PFAS loss in aerosol forms generated during the electrochemical process and possible solutions to avoid such loss by capturing and recirculating aerosols to achieve high PFAS degradation and complete fluorine mass balance.

5.4 Suggestions for future work

- PFR with its high anode area to volume ratio is a promising reactor for electrochemical degradation of PFAS. However, it has to be redesigned to have separate outlets of the PFAS solution and evolved gases.
- Since methanol is best for organic fluorine capture, and 1M NaOH is best for fluoride capture, future electrochemical oxidation studies should explore the use of these solutions is series to achieve highest possible capture of fluoride and organic fluorine
- Exploring the effectiveness EOF over AOF analysis for quantifying organic fluorine in AFFF electrochemical oxidation experiments is recommended
- Electrochemical studies need to be conducted in natural waters either by using PFAS contaminated or PFAS spiked groundwater and surface water
- Electrochemical chemical reduction of GenX using electrochemical reactors with separated catholyte and anolyte needs to be investigated

6. Bibliography

Backe, W. J., Day, T. C., and Field, J. A. (2013). "Zwitterionic, cationic, and anionic fluorinated chemicals in aqueous film forming foam formulations and groundwater from U.S. military bases by nonaqueous large-volume injection HPLC-MS/MS." *Environmental Science and Technology*, 47(10), 5226–5234.

Baldaguez Medina, P., Cotty, S., Kim, K., Elbert, J., and Su, X. (2021). "Emerging investigator series: electrochemically-mediated remediation of GenX using redox-copolymers." *Environmental Science: Water Research & Technology*, Royal Society of Chemistry.

Bao, Y., Deng, S., Jiang, X., Qu, Y., He, Y., Liu, L., Chai, Q., Mumtaz, M., Huang, J., Cagnetta, G., and Yu, G. (2018). "Degradation of PFOA Substitute - GenX (HFPO-DA ammonium salt)： Oxidation with UV/Persulfate or Reduction with UV/Sulfite?" *Environmental Science & Technology*, acs.est.8b02172.

Calafat, A. M., Wong, L. Y., Kuklenyik, Z., Reidy, J. A., and Needham, L. L. (2007). "Polyfluoroalkyl chemicals in the U.S. population: Data from the national health and nutrition examination survey (NHANES) 2003-2004 and comparisons with NHANES 1999-2000." *Environmental Health Perspectives*, 115(11), 1596–1602.

Cao, X., Wang, C., Lu, Y., Zhang, M., Khan, K., Song, S., Wang, P., and Wang, C. (2019). "Occurrence, sources and health risk of polyfluoroalkyl substances (PFASs) in soil, water and sediment from a drinking water source area." *Ecotoxicology and Environmental Safety*, Elsevier Inc., 174(February), 208–217.

Chen, M. J., Lo, S. L., Lee, Y. C., and Huang, C. C. (2015). "Photocatalytic decomposition of perfluorooctanoic acid by transition-metal modified titanium dioxide." *Journal of Hazardous Materials*, 288, 168–175.

Chen, S., Jiao, X. C., Gai, N., Li, X. J., Wang, X. C., Lu, G. H., Piao, H. T., Rao, Z., and Yang, Y. L. (2016). "Perfluorinated compounds in soil, surface water, and groundwater from rural areas in eastern China." *Environmental Pollution*, Elsevier Ltd, 211, 124–131.

Cheng, W., and Ng, C. A. (2018). "Predicting Relative Protein Affinity of Novel Per- and Polyfluoroalkyl Substances (PFASs) by An Efficient Molecular Dynamics Approach." *Environmental Science and Technology*, 52(14), 7972–7980.

Costanza, J., Arshadi, M., Abriola, L. M., and Pennell, K. D. (2019). "Accumulation of PFOA and PFOS at the Air–Water Interface." *Environmental Science & Technology Letters*, rapid-communication, American Chemical Society, 6, 487–491.

Crone, B. C., Speth, T. F., Wahman, D. G., Smith, S. J., Abulikemu, G., Kleiner, E. J., and Pressman, J. G. (2019). "Occurrence of per- and polyfluoroalkyl substances (PFAS) in source water and their treatment in drinking water." *Critical Reviews in Environmental Science and Technology*, Taylor & Francis, 49(24), 2359–2396.

Darwin, R. L. (2004). *Estimated inventory of Aqueous Film Forming Foam (AFFF) in the United States*.

Darwin, R. L. (2011). *Estimated quntities of PFOS based Aqueous Film Forming Foam (AFFF)*.

Dauchy, X., Boiteux, V., Bach, C., Rosin, C., and Munoz, J. F. (2017a). "Per- and polyfluoroalkyl substances in firefighting foam concentrates and water samples collected near sites impacted by the use of these foams." *Chemosphere*, Elsevier Ltd, 183, 53–61.

Dauchy, X., Boiteux, V., Bach, C., Rosin, C., and Munoz, J. F. (2017b). "Per- and polyfluoroalkyl substances in firefighting foam concentrates and water samples collected near sites impacted by the use of these foams." *Chemosphere*, Elsevier Ltd, 183, 53–61.

Department of Defense. (2017). *Aqueous Film Forming Foam Report to Congress*.
Emmett, E. A., Shofer, F. S., Zhang, H., Freeman, D., Desai, C., and Shaw, L. M. (2006). "Community Exposure to Perfluorooctanoate: Relationships Between Serum Concentrations and Exposure Sources." *Journal of Occupational and Environmenta Medicine*, 48(8), 759–770.
European Food Safety Authority. (2008). "Perfluorooctane sulfonate (PFOS), perfluorooctanoic acid (PFOA) and their salts - Scientific opinion of the Panel on Contaminants in the Food chain." *EFSA Journal*, 653, 1–131.
Gayen, P., and Chaplin, B. P. (2017). "Fluorination of Boron-Doped Diamond Film Electrodes for Minimization of Perchlorate Formation." *ACS Applied Materials and Interfaces*, 9(33), 27638–27648.
Gebbink, W. A., and Leeuwen, S. P. J. Van. (2020). "Environmental contamination and human exposure to PFASs near a fl uorochemical production plant : Review of historic and current PFOA and GenX contamination in the Netherlands." *Environment International*, Elsevier, 137(October 2019), 105583.
Geng, P., Su, J., Miles, C., Comninellis, C., and Chen, G. (2015). "Highly-ordered magnéli Ti4O7 nanotube arrays as effective anodic material for electro-oxidation." *Electrochimica Acta*, Elsevier Ltd, 153, 316–324.
Giesy, J. P., and Kannan, K. (2002). "Peer Reviewed: Perfluorochemical Surfactants in the Environment." *Environmental Science & Technology*, 36(7), 146A-152A.
Gomez-Ruiz, B., Diban, N., and Urtiaga, A. (2019). "Comparison of microcrystalline and ultrananocrystalline boron doped diamond anodes: Influence on perfluorooctanoic acid electrolysis." *Separation and Purification Technology*, 208(March 2018), 169–177.
Gomez-Ruiz, B., Gómez-Lavín, S., Diban, N., Boiteux, V., Colin, A., Dauchy, X., and Urtiaga, A. (2017). "Efficient electrochemical degradation of poly- and perfluoroalkyl substances (PFASs) from the effluents of an industrial wastewater treatment plant." *Chemical Engineering Journal*, Elsevier B.V., 322, 196–204.
Gomis, M. I., Vestergren, R., Borg, D., and Cousins, I. T. (2018). "Comparing the toxic potency in vivo of long-chain perfluoroalkyl acids and fluorinated alternatives." *Environment International*, 113(January), 1–9.
Gorri, D., and Urtiaga, A. (2017). "Ef fi cient treatment of per fl uorohexanoic acid by nano fi ltration followed by electrochemical degradation of the NF concentrate Alvaro." 112, 147–156.
Han, Y., Pulikkal, V. F., and Sun, M. (2021). "Comprehensive Validation of the Adsorbable Organic Fluorine Analysis and Performance Comparison of Current Methods for Total Per- and Polyfluoroalkyl Substances in Water Samples." *ACS ES&T Water*, 1(6), 1474–1482.
Hepburn, E., Madden, C., Szabo, D., Coggan, T. L., Clarke, B., and Currell, M. (2019). "Contamination of groundwater with per- and polyfluoroalkyl substances (PFAS) from legacy landfills in an urban re-development precinct." *Environmental Pollution*, Elsevier Ltd, 248, 101–113.
Heydebreck, F., Tang, J., Xie, Z., and Ebinghaus, R. (2015). "Alternative and Legacy Perfluoroalkyl Substances: Differences between European and Chinese River/Estuary Systems." *Environmental Science and Technology*, 49(14), 8386–8395.
Houtz, E. F., Higgins, C. P., Field, J. A., and Sedlak, D. L. (2013). "Persistence of perfluoroalkyl acid precursors in AFFF-impacted groundwater and soil." *Environmental Science and Technology*, 47(15), 8187–8195.

Houtz, E. F., and Sedlak, D. L. (2012). “Oxidative conversion as a means of detecting precursors to perfluoroalkyl acids in urban runoff.” *Environmental Science and Technology*, 46(17), 9342–9349.

Hu, X. C., Andrews, D. Q., Lindstrom, A. B., Bruton, T. A., Schaider, L. A., Grandjean, P., Lohmann, R., Carignan, C. C., Blum, A., Balan, S. A., Higgins, C. P., and Sunderland, E. M. (2016). “Detection of Poly- and Perfluoroalkyl Substances (PFASs) in U.S. Drinking Water Linked to Industrial Sites, Military Fire Training Areas, and Wastewater Treatment Plants.” *Environmental Science and Technology Letters*, 3(10), 344–350.

ITRC. (2018). “Environmental Fate and Transport for Per-and Polyfluoroalkyl Substances continued.”

Jawando, W., Gayen, P., and Chaplin, B. P. (2015). “The effects of surface oxidation and fluorination of boron-doped diamond anodes on perchlorate formation and organic compound oxidation.” *Electrochimica Acta*, Elsevier Ltd, 174, 1067–1078.

Joerss, H., Schramm, T. R., Sun, L., Guo, C., Tang, J., and Ebinghaus, R. (2020). “Per- and polyfluoroalkyl substances in Chinese and German river water – Point source- and country-specific fingerprints including unknown precursors.” *Environmental Pollution*, 267.

Kormann, C., Bahnemann, D. W., and Hoffmann, M. R. (1991). “Photolysis of chloroform and other organic molecules in aqueous titanium dioxide suspensions.” *Environmental Science & Technology*, 25(3), 494–500.

Kudo, N., and Kawashima, Y. (2003). “Toxicity and toxicokinetics of perfluorooctanoic acid in humans and animals.” *The Journal of toxicological sciences*, 28(2), 49–57.

Kutsuna, S., and Hisao, H. (2007). “Rate constants for aqueous-phase reactions of SO4- with C2F5COO- and C3F7COO- at 298K.” *Turkish Journal of Chemistry*, 31(5), 493–499.

Lau, C., Anitole, K., Hodes, C., Lai, D., Pfahles-Hutchens, A., and Seed, J. (2007). “Perfluoroalkyl acids: A review of monitoring and toxicological findings.” *Toxicological Sciences*, 99(2), 366–394.

Li, F., Zhang, C., Qu, Y., Chen, J., Chen, L., Liu, Y., and Zhou, Q. (2010). “Quantitative characterization of short- and long-chain perfluorinated acids in solid matrices in Shanghai, China.” *Science of the Total Environment*, Elsevier B.V., 408(3), 617–623.

Li, R., Cui, W., Liu, L., Song, T., Cui, Z., and Ma, Q. (2015). “ Electrochemical degradation of perfluorooctanoic acid (PFOA) by Yb-doped Ti/SnO 2 –Sb/PbO 2 anodes and determination of the optimal conditions .” *RSC Advances*, 5(103), 84856–84864.

Liang, S., David, R., Jr, P., Lin, H., Chiang, S. D., and Huang, Q. J. (2018). “Electrochemical oxidation of PFOA and PFOS in concentrated waste streams.” *Remediation*, 28(2), 127–134.

Lin, H., Niu, J., Ding, S., and Zhang, L. (2012). “Electrochemical degradation of perfluorooctanoic acid (PFOA) by Ti/SnO 2-Sb, Ti/SnO 2-Sb/PbO 2 and Ti/SnO 2-Sb/MnO 2 anodes.” *Water Research*, 46(7), 2281–2289.

Lin, H., Niu, J., Liang, S., Wang, C., Wang, Y., Jin, F., Luo, Q., and Huang, Q. (2018). “Development of Macroporous Magnéli Phase Ti 4 O 7 Ceramic Materials : As an Efficient Anode for Mineralization of Poly- and Perfluoroalkyl Substances.” *Chemical Engineering Journal*.

Ma, Q., Liu, L., Cui, W., Li, R., Song, T., and Cui, Z. (2015). “Electrochemical degradation of perfluorooctanoic acid (PFOA) by Yb-doped Ti/SnO_2 –Sb/PbO_2 anodes and determination of the optimal conditions.” *RSC Adv.*, 5(103), 84856–84864.

Moody, C. A., and Field, J. A. (1999). “Determination of perfluorocarboxylates in groundwater

impacted by fire- fighting activity." *Environmental Science and Technology*, 33(16), 2800–2806.
Moody, C. A., and Field, J. A. (2000). "Perfluorinated surfactants and the environmental implications of their use in fire-fighting foams." *Environmental Science and Technology*, 34(18), 3864–3870.
Moody, C. A., Hebert, G. N., Strauss, S. H., and Field, J. A. (2003). "Occurrence and persistence of perfluorooctanesulfonate and other perfluorinated surfactants in groundwater at a fire-training area at Wurtsmith Air Force Base, Michigan, USA." *Journal of environmental monitoring*, 5(2), 341–345.
Mueller, R., and Yingling, V. (2017). *History and Use of Per- and Polyfluoroalkyl Substances (PFAS). Disponible a https://pfas-1.itrcweb.org, Visitat: 16/08/2019*.
Mueller, R., and Yingling, V. (2018). *Aqueous Film-Forming Foam (AFFF). Interstate Technology Regulatory Council Sheets*.
Niu, J., Lin, H., Gong, C., and Sun, X. (2013). "Theoretical and experimental insights into the electrochemical mineralization mechanism of perfluorooctanoic acid." *Environmental Science and Technology*, 47(24), 14341–14349.
Olvera-Vargas, H., Wang, Z., Xu, J., and Lefebvre, O. (2022). "Synergistic degradation of GenX (hexafluoropropylene oxide dimer acid) by pairing graphene-coated Ni-foam and boron doped diamond electrodes." *Chemical Engineering Journal*, Elsevier B.V., 430(P1), 132686.
Pica, N. E., Funkhouser, J., Yin, Y., Zhang, Z., Ceres, D. M., Tong, T., and Blotevogel, J. (2019a). "Electrochemical Oxidation of Hexafluoropropylene Oxide Dimer Acid (GenX): Mechanistic Insights and Efficient Treatment Train with Nanofiltration." *Environmental Science and Technology*, 53(21), 12602–12609.
Pica, N. E., Funkhouser, J., Yin, Y., Zhang, Z., Ceres, D. M., Tong, T., and Blotevogel, J. (2019b). "Electrochemical Oxidation of Hexa fl uoropropylene Oxide Dimer Acid (GenX): Mechanistic Insights and E ffi cient Treatment Train with Nano fi ltration." (October).
Prevedouros, K., Cousins, I. T., Buck, R. C., and Korzeniowski, S. H. (2006). "Sources, fate and transport of perfluorocarboxylates." *Environmental Science and Technology*, 40(1), 32–44.
Quiñones, O., and Snyder, S. A. (2009). "Occurrence of perfluoroalkyl carboxylates and sulfonates in drinking water utilities and related waters from the United States." *Environmental Science and Technology*, 43(24), 9089–9095.
Rodriguez-Freire, L., Balachandran, R., Sierra-Alvarez, R., and Keswani, M. (2015). "Effect of sound frequency and initial concentration on the sonochemical degradation of perfluorooctane sulfonate (PFOS)." *Journal of Hazardous Materials*, Elsevier B.V., 300, 662–669.
Schaefer, C. E., Andaya, C., Burant, A., Condee, C. W., Urtiaga, A., Strathmann, T. J., and Higgins, C. P. (2017). "Electrochemical treatment of perfluorooctanoic acid and perfluorooctane sulfonate: insights into mechanisms and application to groundwater treatment." *Chemical Engineering Journal*, Elsevier B.V., 317, 424–432.
Schaefer, C. E., Andaya, C., Urtiaga, A., Mckenzie, E. R., and Higgins, C. P. (2015a). "Electrochemical treatment of perfluorooctanoic acid (PFOA) and perfluorooctane sulfonic acid (PFOS) in groundwater impacted by aqueous film forming foams (AFFFs)." *Journal of Hazardous Materials*, Elsevier B.V., 295, 170–175.
Schaefer, C. E., Andaya, C., Urtiaga, A., McKenzie, E. R., and Higgins, C. P. (2015b). "Electrochemical treatment of perfluorooctanoic acid (PFOA) and perfluorooctane sulfonic

acid (PFOS) in groundwater impacted by aqueous film forming foams (AFFFs)." *Journal of Hazardous Materials*, Elsevier B.V., 295, 170–175.

Schaefer, C. E., Choyke, S., Ferguson, P. L., Andaya, C., Burant, A., Maizel, A., Strathmann, T. J., and Higgins, C. P. (2018). "Electrochemical Transformations of Perfluoroalkyl Acid (PFAA) Precursors and PFAAs in Groundwater Impacted with Aqueous Film Forming Foams." *Environmental Science and Technology*, research-article, American Chemical Society, 52(18), 10689–10697.

Shi, H., Wang, Y., Li, C., Pierce, R., Gao, S., and Huang, Q. (2019). "Degraation of Perfluorooctanesulfonate by Reactive Electrochemical Membrane Compose of Magnéli Phase Titanium Suboxie." *Environmental Science and Technology*, 53(24), 14528–14537.

Song, X., Vestergren, R., Shi, Y., Huang, J., and Cai, Y. (2018). "Emissions, Transport, and Fate of Emerging Per- and Polyfluoroalkyl Substances from One of the Major Fluoropolymer Manufacturing Facilities in China." *Environmental Science and Technology*, research-article, American Chemical Society, 52, 9694–9703.

Stratton, G. R., Dai, F., Bellona, C. L., Holsen, T. M., Dickenson, E. R. V., and Mededovic Thagard, S. (2017). "Plasma-Based Water Treatment: Efficient Transformation of Perfluoroalkyl Substances in Prepared Solutions and Contaminated Groundwater." *Environmental Science and Technology*, 51(3), 1643–1648.

Strynar, M., Dagnino, S., McMahen, R., Liang, S., Lindstrom, A., Andersen, E., McMillan, L., Thurman, M., Ferrer, I., and Ball, C. (2015). "Identification of Novel Perfluoroalkyl Ether Carboxylic Acids (PFECAs) and Sulfonic Acids (PFESAs) in Natural Waters Using Accurate Mass Time-of-Flight Mass Spectrometry (TOFMS)." *Environmental Science and Technology*, 49(19), 11622–11630.

Sun, M., Arevalo, E., Strynar, M., Lindstrom, A., Richardson, M., Kearns, B., Pickett, A., Smith, C., and Knappe, D. R. U. (2016a). "Legacy and Emerging Perfluoroalkyl Substances Are Important Drinking Water Contaminants in the Cape Fear River Watershed of North Carolina." *Environmental Science and Technology Letters*, 3(12), 415–419.

Sun, M., Arevalo, E., Strynar, M., Lindstrom, A., Richardson, M., Kearns, B., Pickett, A., Smith, C., and Knappe, D. R. U. (2016b). "Legacy and Emerging Perfluoroalkyl Substances Are Important Drinking Water Contaminants in the Cape Fear River Watershed of North Carolina." *Environmental Science and Technology Letters*, 3(12), 415–419.

Suresh Babu, D., Mol, J. M. C., and Buijnsters, J. G. (2022). "Experimental insights into anodic oxidation of hexafluoropropylene oxide dimer acid (GenX) on boron-doped diamond anodes." *Chemosphere*, Elsevier Ltd, 288(P1), 132417.

Trautmann, A. M., Schell, H., Schmidt, K. R., Mangold, K. M., and Tiehm, A. (2015). "Electrochemical degradation of perfluoroalkyl and polyfluoroalkyl substances (PFASs) in groundwater." *Water Science and Technology*, 71(10), 1569–1575.

Trojanowicz, M., Bojanowska-Czajka, A., Bartosiewicz, I., and Kulisa, K. (2018). "Advanced Oxidation/Reduction Processes treatment for aqueous perfluorooctanoate (PFOA) and perfluorooctanesulfonate (PFOS) – A review of recent advances." *Chemical Engineering Journal*, Elsevier, 336(October 2017), 170–199.

USEPA. (2012). "Emerging Contaminants – Perfluorooctane Sulfonate (PFOS) and Perfluorooctanoic Acid (PFOA) At a Glance." <https://nepis.epa.gov/Exe/ZyPDF.cgi/P100EIVC.PDF?Dockey=P100EIVC.PDF>.

USEPA. (2014). *EPA ' s Summary Tables for 2014 Company Progress Reports*.

USEPA. (2016a). *Drinking Water Health Advisory for Perfluorooctanoic Acid (PFOA)*.

USEPA. (2016b). *Drinking Water Health Advisory for Perfluorooctane Sulfonate (PFOS)*.
USEPA. (2016c). *Drinking Water Health Advisory for Perfluorooctanoic Acid (PFOA) – Drinking Water Health Advisory for Perfluorooctanoic Acid (PFOA)*.
USEPA. (2016d). "FACT SHEET PFOA &PFOS Drinking Water Health Advisories." <https://www.epa.gov/sites/production/files/2016-05/documents/drinkingwaterhealthadvisories_pfoa_pfos_5_19_16.final_.1.pdf>.
USEPA. (2017a). *Technical Fact Sheet - Perfluorooctane Sulfonate (PFOS) and Perfluorooctanoic Acid (PFOA)*.
USEPA. (2017b). *The Third Unregulated Contaminant Monitoring Rule (UCMR 3): Data Summary, January 2017*.
Vector Corrosion Technologies. (2012). "Discrete Cathodic Protection Anodes for Reinforced Concrete Structures and Steel Framed Buildings." <https://www.vector-corrosion.com/uploads/content/7000-2012Apr30-Ebonex-Data-Sheet.pdf?force_download>.
Wagner, A., Raue, B., Brauch, H.-J., Worch, E., and Lange, F. T. (2013). "Determination of adsorbable organic fluorine from aqueous environmental samples by adsorption to polystyrene-divinylbenzene based activated carbon and combustion ion chromatography." *Journal of Chromatography A*, 1295, 82–89.
Wang, P., Lu, Y., Wang, T., Meng, J., Li, Q., Zhu, Z., Sun, Y., Wang, R., and Giesy, J. P. (2016). "Shifts in production of perfluoroalkyl acids affect emissions and concentrations in the environment of the Xiaoqing River Basin, China." *Journal of Hazardous Materials*, Elsevier B.V., 307, 55–63.
Wang, Z., Cousins, I. T., Scheringer, M., and Hungerbühler, K. (2013). "Fluorinated alternatives to long-chain perfluoroalkyl carboxylic acids (PFCAs), perfluoroalkane sulfonic acids (PFSAs) and their potential precursors." *Environment International*, Elsevier Ltd, 60(2013), 242–248.
Xiao, F., Simcik, M. F., Halbach, T. R., and Gulliver, J. S. (2015). "Perfluorooctane sulfonate (PFOS) and perfluorooctanoate (PFOA) in soils and groundwater of a U.S. metropolitan area: Migration and implications for human exposure." *Water Research*, Elsevier Ltd, 72, 64–74.
Xiao, H., Lv, B., Zhao, G., Wang, Y., Li, M., and Li, D. (2011). "Hydrothermally enhanced electrochemical oxidation of high concentration refractory perfluorooctanoic acid." *Journal of Physical Chemistry A*, 115(47), 13836–13841.
Xu, B., Liu, S., Zhou, J. L., Zheng, C., Weifeng, J., Chen, B., Zhang, T., and Qiu, W. (2021). "PFAS and their substitutes in groundwater: Occurrence, transformation and remediation." *Journal of Hazardous Materials*, Elsevier B.V., 412, 125159.
Xu, Z., Yu, Y., Liu, H., and Niu, J. (2016). "Highly efficient and stable Zr-doped nanocrystalline PbO2 electrode for mineralization of perfluorooctanoic acid in a sequential treatment system." *The Science of the total environment*, 579, 1600–1607.
Yang, B., Jiang, C., Yu, G., Zhuo, Q., Deng, S., Wu, J., and Zhang, H. (2015). "Highly efficient electrochemical degradation of perfluorooctanoic acid (PFOA) by F-doped Ti/SnO2 electrode." *Journal of Hazardous Materials*, Elsevier B.V., 299, 417–424.
Yang, B., Wang, J., Jiang, C., Li, J., Yu, G., Deng, S., Lu, S., Zhang, P., Zhu, C., and Zhuo, Q. (2017). "Electrochemical mineralization of perfluorooctane sulfonate by novel F and Sb co-doped Ti/SnO 2 electrode containing Sn-Sb interlayer." *Chemical Engineering Journal*, Elsevier B.V., 316, 296–304.

Yang, L. H., Yang, W. J., Lv, S. H., Zhu, T. T., Adeel Sharif, H. M., Yang, C., Du, J., and Lin, H. (2022). “Is HFPO-DA (GenX) a suitable substitute for PFOA? A comprehensive degradation comparison of PFOA and GenX via electrooxidation.” *Environmental Research*, Elsevier Inc., 204(PA), 111995.

Yu, G., Zhuo, Q., Jiang, C., Yang, B., Deng, S., Zhang, H., and Wu, J. (2015). “Highly efficient electrochemical degradation of perfluorooctanoic acid (PFOA) by F-doped Ti/SnO2 electrode.” *Journal of Hazardous Materials*, Elsevier B.V., 299, 417–424.

Zhao, H., Gao, J., Zhao, G., Fan, J., Wang, Y., and Wang, Y. (2013). “Fabrication of novel SnO2-Sb/carbon aerogel electrode for ultrasonic electrochemical oxidation of perfluorooctanoate with high catalytic efficiency.” *Applied Catalysis B: Environmental*, Elsevier B.V., 136–137, 278–286.

Zhuo, Q., Deng, S., Yang, B., Huang, J., and Yu, G. (2011). “Efficient Electrochemical Oxidation of Perfluorooctanoate Using a Ti / SnO 2 -Sb-Bi Anode.” *Environmental Science & Technology*, 45(7), 2973–2979.

Zhuo, Q., Li, X., Yan, F., Yang, B., Deng, S., Huang, J., and Yu, G. (2014). “Electrochemical oxidation of 1H,1H,2H,2H-perfluorooctane sulfonic acid (6:2 FTS) on DSA electrode: Operating parameters and mechanism.” *Journal of Environmental Sciences (China)*, Elsevier B.V., 26(8), 1733–1739.

Zhuo, Q., Luo, M., Guo, Q., Yu, G., Deng, S., Xu, Z., Yang, B., and Liang, X. (2016). “Electrochemical Oxidation of Environmentally Persistent Perfluorooctane Sulfonate by a Novel Lead Dioxide Anode.” *Electrochimica Acta*, Elsevier Ltd, 213, 358–367.

Zhuo, Q., Xiang, Q., Yi, H., Zhang, Z., Yang, B., Cui, K., Bing, X., Xu, Z., Liang, X., Guo, Q., and Yang, R. (2017). “Electrochemical oxidation of PFOA in aqueous solution using highly hydrophobic modi fi ed PbO 2 electrodes.” *Journal of Electroanalytical Chemistry*, Elsevier, 801(July), 235–243.